ATTITUDE CONTROL OF RIGID BODIES WITH TIME-DELAYED MEASUREMENTS

JOÃO VÍTOR CAVALCANTI VILELA

DISSERTAÇÃO DE MESTRADO EM ENGENHARIA ELÉTRICA
DEPARTAMENTO DE ENGENHARIA ELÉTRICA

FACULDADE DE TECNOLOGIA

UNIVERSIDADE DE BRASÍLIA

UNIVERSIDADE DE BRASÍLIA
FACULDADE DE TECNOLOGIA
DEPARTAMENTO DE ENGENHARIA ELÉTRICA

ATTITUDE CONTROL OF RIGID BODIES WITH TIME-DELAYED MEASUREMENTS

JOÃO VÍTOR CAVALCANTI VILELA

DISSERTAÇÃO DE MESTRADO SUBMETIDA AO DEPARTAMENTO DE ENGENHARIA ELÉTRICA DA FACULDADE DE TECNOLOGIA DA UNIVERSIDADE DE BRASÍLIA COMO PARTE DOS REQUISITOS NECESSÁRIOS PARA A OBTENÇÃO DO GRAU DE MESTRE EM ENGENHARIA ELÉTRICA.

APROVADA POR:

____

Prof. João Yoshiyuki Ishihara, Department of Electrical Engineering/ University of Brasilia
(Orientador)

____

Prof. Renato Alves Borges, Deptartment of Electrical Engineering/ University of Brasilia
Presidente

____

Prof. Bruno Vilhena Adorno, Department of Electrical Engineering/ Federal University of Minas Gerais
Examinador Externo

____

Prof. Eduardo Stockler Tognetti, Department of Electrical Engineering/ University of Brasilia
Examinador Interno

BRASÍLIA, 14 DE JUNHO DE 2016.

UNIVERSIDADE DE BRASÍLIA
FACULDADE DE TECNOLOGIA
DEPARTAMENTO DE ENGENHARIA ELÉTRICA

ATTITUDE CONTROL OF RIGID BODIES WITH TIME - DELAYS

JOÃO VITOR CAVALCANTI VILELA

DISSERTAÇÃO DE MESTRADO SUBMETIDA AO DEPARTAMENTO DE ENGENHARIA ELÉTRICA DA FACULDADE DE TECNOLOGIA DA UNIVERSIDADE DE BRASÍLIA, COMO PARTE DOS REQUISITOS NECESSÁRIOS PARA A OBTENÇÃO DO GRAU DE MESTRE.

APROVADA POR:

RENATO ALVES BORGES, Dr., ENE/UNB
(PRESIDENTE)

EDUARDO STOCKLER TOGNETTI, Dr., ENE/UNB
(EXAMINADOR INTERNO)

BRUNO VILHENA ADORNO, Dr., UFMG
(EXAMINADOR EXTERNO)

Brasília, 14 de junho de 2016.

FICHA CATALOGRÁFICA

CAVALCANTI VILELA, JOÃO
Attitude Control of Rigid Bodies withTime-delayed Measurements [Distrito Federal] 2016.
xi, 94p., 210 x 297 mm (ENE/FT/UnB, Mestre, Engenharia Elétrica, 2016).
DISSERTAÇÃO DE MESTRADO – Universidade de Brasília, Faculdade de Tecnologia.
Departamento de Engenharia Elétrica

1. Controle de Atitude	2. Sistemas com Atraso
3. LMI	4. Controle Cinemático e Dinâmico
I. ENE/FT/UnB	II. Título (série)

REFERÊNCIA BIBLIOGRÁFICA

CAVALCANTI, J. (2016). Attitude Control of Rigid Bodies withTime-delayed Measurements, DISSERTAÇÃO DE MESTRADO em Engenharia Elétrica, Publicação PGEAENE.DM-628/2016, Departamento de Engenharia Elétrica, Universidade de Brasília, Brasília, DF, 94p.

____

João Vítor Cavalcanti Vilela
Departamento de Eng. Elétrica (ENE) - FT
Universidade de Brasília (UnB)
Campus Darcy Ribeiro
CEP 70919-970 - Brasília - DF - Brasil

Aos meus pais

AGRADECIMENTOS

Aos que me ajudaram neste trabalho, gostaria de agradecer profundamente ao Prof. Ishihara e ao quasiDr. Figueredo. Ao primeiro, obrigado pela grande oportunidade, pelo cuidado e incentivo, e por ter me ensinado bastante sobre o que é, e como fazer pesquisa. Nunca esquecerei de tudo que ele fez por mim. Ao segundo, obrigado pela solicitude, pelo companheirismo e pelas discussões. Muitas vezes foi como um irmão mais velho, pelos conselhos e apoio que me ajudaram a crescer muito; agora o considero também como um amigo. Espero que possamos continuar a trabalhar juntos e que mantenhamos contato. De qualquer forma, sempre lembrarei com afeto dos anos em que estivemos juntos. Aos que estão comigo fora do trabalho, obrigado aos meus pais. Estes que sempre foram pacientes e tolerantes comigo, e que me deram suporte e apoio para que eu pudesse seguir meus instintos e alcançar meus objetivos. Os dois juntos formam uma pessoa extraordinária com quem eu ainda tenho muito a aprender.

RESUMO

ATTITUDE CONTROL OF RIGID BODIES WITH TIME-DELAYED MEASUREMENTS

Autor: João Vítor Cavalcanti Vilela

Orientador: Prof. João Yoshiyuki Ishihara, Department of Electrical Engineering/ University of Brasilia

Programa de Pós-graduação em Engenharia Elétrica

Brasília, 14 de junho de 2016

Desenvolver condições de estabilidade e projeto de controladores para controle de atitude de corpos rígidos sujeitos a atrasos no tempo é o objetivo desta dissertação. O modelo utilizado, escrito na forma de equação diferencial atrasada, advém das equações cinemática e dinâmica do corpo rígido modificadas considerando atrasos temporais. Estes atrasos podem representar latências dos sensores e atuadores, além de tempo de processamento de dados (e.g., cômputo dos sinais de controle) e de transmissão de dados quando os elementos do sistema de controle estão conectados por redes comunicação. Em particular, são supostos atrasos desconhecidos e variantes no tempo, o que lhes confere generalidade maior do que os casos abordados até então na literatura, onde os poucos trabalhos que abordaram o problema aprensentam resultados dependentes do valor exato do atraso ou o assumem constante, o que na prática dificilmente é verificado. As condições obtidas, escritas na forma de teoremas, são baseadas em sua maioria na teoria de Lyapunov-Krasovskii. Outro aspecto que diferencia este trabalho em relação aos demais é que os teoremas são formulados como desigualdades matriciais lineares (LMIs, em inglês). A formulação por LMIs é vantajosa não só pelas excelentes propriedades computacionais das LMIs (resolução em tempo polinomial), mas também porque as condições são escritas com variáveis, reduzindo o conservadorismo dos resultados e permitindo a automação do processo de verificação de estabilidade e projeto de controladores, o que também é uma contribuição desta dissertação. Além disso, os controladores possuem performance garantida segundo o critério H_∞, isto é, além de estabilidade, este tipo de controlador tem um nível mínimo de atenuação de perturbações assegurado.

ABSTRACT

ATTITUDE CONTROL OF RIGID BODIES WITH TIME-DELAYED MEASUREMENTS

Author: João Vítor Cavalcanti Vilela

Supervisor: Prof. João Yoshiyuki Ishihara, Department of Electrical Engineering/ University of Brasilia

Electrical Engineering Graduation Program

Brasília, 14th June 2016

Developing stability and controller design conditions for rigid body attitude control subjected to time delays is the goal of this dissertation. The rigid body model, written in form of functional differential equation, stems from the kinematic and dynamic rigid body equations, modified to take time delays into account. Such time delays may represent sensor and actuator latency, processing time (e.g., computing control signals) and transmission lags when the control system elements are connected by communication networks. In particular, time delays are considered unknown and time-varying, which makes them generalizations of previous results in literature, where the scarce works to tackle the problem present results dependent on the exact time delay value, which is hardly verified in practice. The proposed conditions, written as theorems, are mostly based on Lyapunov-Krasovskii theory. Another aspect that sets this work apart is that theorems are formulated as linear matrix inequalities (LMIs). LMI formulation is advantageous not only for its excellent computational properties (polynomial time solving), but also for the conditions are written with variables, which reduces results' conservatism e enables automating stability verification and controller design, which is a contribution of this work as well. In addition, controllers attain guaranteed performance according to H_∞ criterion, that is, besides stability, this kind of controller presents a known minimum level of perturbation attenuation.

CONTENTS

List of Figures

List of Tables

SYMBOLS LIST

Latin Symbols

$\mathcal{B}$	Body frame
$\mathcal{I}$	Inertial frame
J	Matrix of inertia with respect to $\mathcal{B}$
$\boldsymbol{q}$	Quaternion
d_1	Attitude measurement time-delay
d_2	Angular velocity measurement time-delay
$\mathbb{R}$	Real numbers field
$\mathbb{R}_{\geq 0}$	Real nonnegative numbers
$\mathbb{R}^n$	n-dimensional real vectors
$\mathbb{R}^{n \times n}$	n-by-n real matrices
$\mathbb{S}^n$	symmetric n-by-n real matrices
$so\left(n\right)$	skew-symmetric n-by-n real matrices

Greek Symbols

$\boldsymbol{\omega}$	Angular velocity
$\dot{\boldsymbol{\omega}}$	Angular acceleration
η	Quaternion scalar part
$\boldsymbol{\zeta}$	Quaternion vector part
τ_i	d_i time-delay lower bound
μ_i	d_i time-delay average delay bound
ν_i	d_i time-delay upper bound

Acronyms

TDS	Time-Delay Systems
RTDS	Retarded Time-Delay Systems
NTDS	Neutral Time-Delay Systems
FDE	Functional Differential Equation
RFDE	Retarded Functional Differential Equation
NCS	Networked Control Systems
LKF	Lyapunov-Krasovskii Functional
LMI	Linear Matrix Inequality
PAM	Piecewise Analysis Method
DFA	Delay-Fractioning Analysis
CA	Convex Analysis

NOTATION

In this dissertation, vectors are represented by boldfaced lowercase letters, whereas boldfaced uppercase letters denote matrices. Sets and spaces are, in general, represented by uppercase calligraphic letters.

1 RESUMO EXTENDIDO

Satélites de telecomunicações precisam apontar suas antenas em direção à Terra para transmitir dados, painéis solares montados em veículos espaciais têm de alinhar-se ortogonalmente ao Sol para gerar energia e braços robóticos necessitam aproximar-se de objetos com determinadas orientações para coletá-los. Estas são apenas algumas dentre uma infinidade de problemas de engenharia que dependem fundamentalmente da orientação de corpos rígidos, e ressaltam a importância do problema chamado *Controle de Atitude*.

Sistemas dinâmicos submetidos a atrasos no tempo também constituem uma área de pesquisa importante, tanto pelo apelo teórico como pelo prático. Estes sistemas são caracterizados por equações funcionais diferenciais [1], fundamentalmente distintas de equações diferenciais ordinárias [2, 3], empregadas em sistemas dinâmicos típicos, o que torna diversos critérios de análise de estabilidade inválidos [4, 5]. Isto requer que o problema seja analisado através de outras ferramentas, já que, em geral, o efeito de atrasos em sistemas de controle é complexo, podendo desestabilizar sistemas estáveis e *vice versa* [2, 3]. Em relação ao controle de atitude, os efeitos são majoritariamente indesejados, incluindo comportamento oscilatório [6], deterioração de performance [7], e instabilidade [8]. Assim, nesta dissertação as demonstrações baseam-se, em geral, na teoria de Lyapunov-Krasovskii [9, 2, 3], uma extensão natural do (segundo) método de Lyapunov, onde os resultados dependem de funcionais relacionados à energia do sistema considerando o estado $\boldsymbol{x}_t$ do sistema atrasado. Tipicamente, isto leva à verificação de desigualdades, que muitas vezes podem ser formuladas como problemas de desiguldade lineares de matrizes (LMIs, em inglês) [10]. Estas desigualdades podem ser facilmente resolvidas devido a características computacionais muito favoráveis, resultado da convexidade do problema.

Atrasos no tempo são comuns em sistemas dinâmicos, com exemplos em biologia, química, economia e mecânica [9, 11, 2, 3]. Em particular, sensores e atuadores sempre introduzem atrasos no tempo, independente de quão pequenos são [12], pois toda interação física propaga-se com velocidade finita. Os computadores e redes de comunicação utilizados no cômputo da lei de controle e transmissão de dados em sistemas de controle também são fontes de atrasos temporais [13, 9, 11, 2, 3].

Sistemas de controle de atitude não são isentos de atrasos no tempo; tanto sensores como atuadores podem induzir atrasos no tempo. Sistemas de propulsão à jato, por exemplo, sofrem com atrasos eletromecânicos nos circuitos valvuláres e fluxo propulsor [14]. Sensores embarcados de baixo custo também podem introduzir atrasos. Magnetômetros, por exemplo, precisam ser desligados na presença de torques magnéticos, postergando o acesso do controlador a medições de atitude [15]. Sensores de estrela [16] e GPS [17, 18] também podem causar atrasos.

As não-linearidades oriundas da cinemática e dinâmica de corpos rígidos tornam controle de atitude um problema complexo, principalmente quando são considerados atrasos no tempo. O termo giroscópico, que caracteriza a não-linearidade dinâmica, é particularmente problemático, e três abordagens são tipicamente empregadas para tratá-lo. A primeira consiste numa espécie de linearização, onde um termo, baseado na matriz de inércia do corpo rígido compensa a não-linearidade dinâmica, é acrescido ao controlador [19]. No entanto, a determinação dos parâmetros do modelo (matriz de inércia) pode ser difícil, e como não existem resultados baseados em modelo que sejam robustos a incertezas, isto pode comprometer a performance e estabilidade do sistema. Esta limitação é tratada por controladores adaptativos, que estimam parâmetros de modelo em tempo real, dispensando informação prévia sobre o modelo. Em [15, 20], esta estratégia é utilizada no contexto de controle de trajetória considerando apenas medições de atitude atrasadas. Além disto, os resultados obtidos são dependentes do valor exato do atraso, considerado constante, e uma parametrização baseada em matrizes de rotação é utilzada, o que requer mais parâmetros e é mais custosa do ponto de vista computacional quando comparada com quatérnios. A terceira forma de tratar não-linearidades consiste em provar resultados utilizando controladores que independam explicitamente de informação sobre o modelo. No primeiro trabalho a considerar controle de atitude com atraso, [8] prova estabilidade exponencial utilizando parâmetros de Rodrigues (que apresentam singularidades), e considerando atrasos constantes. Os resultados dependem da atitude inicial do corpo, do valor exato dos atrasos, e de informações do modelo (apesar do controlador não utilizá-la diretamente). Parâmetros de Rodrigues modificados, também vítimas de problemas com singularidades, são utilizados por [21], que prova estabilidade exponencial considerando estados medidos com atrasos desconhecidos, mas constantes. No entanto, os resultados dependem da orientação inicial. O problema de singularidades e dependência de orientação inicial é resolvido em [22], através da parametrização por quatérnios. Apenas uma cota para a norma da matriz de inércia é necessária para provar os resultados baseados em controladores proporcionais derivativos, mas dependem do valor exato do atraso, considerado constante. Em seguida, [23] extende [22] ao considerar controladores independentes de medições de velocidade.

Neste trabalho, são desenvolvidos critérios de estabilidade e performance para o problema de controle de atitude. A abordagem distingue-se das anteriores no sentido de que as condições são escritas na forma de LMIs, o que permite automatizar o projeto de controladores, algo inédito na área, além de produzir resultados menos conservadores. Além disto, são considerados controladores com performance garantida no que diz respeito a rejeição de perturbações (controle H_∞), outra novidade neste campo. Outrossim, os atrasos são supostos variantes no tempo e desconhecidos, e no caso dinâmico, diferentes para atitude e velocidade. Estas são generalizações das hipóteses anteriores, onde em geral são apenas atrasos constantes, muitas vezes conhecidos são tratados.

2 INTRODUCTION

2.1 MOTIVATION AND BACKGROUND

Telecommunication satellites must point their antennas toward Earth to transmit data, solar panels mounted on spacecraft need to face the Sun to generate power and robotic arms have to approach objects with particular orientations to pick them up. These represent only a few among a myriad of engineering problems where the orientation of a certain object is key, and shed light on the relevance of the so-called *Attitude Control Problem*.

2.1.1 Attitude Control

The attitude of an object represents its orientation relative to a certain reference frame, and attitude control is concerned with steering the object to a, possibly time-varying, desired orientation. For example, consider the Atacama Large Millimeter/submillimeter Array (ALMA), an astronomical interferometer of radio telescopes on a plateau at five thousand meters altitude in the Atacama desert of northern Chile. ALMA was conceived to study star birth during early universe and consists of sixty six radio telescopes, partly depicted in Figure 2.1, observing at millimeter and submillimeter wavelengths (0.3 to 9.6 millimeters). In order to provide detailed images of 0.1" angular precision, the telescopes must meet extremely tight attitude error requirements, especially considering the reference frame in this case is moving: Earth is rotating and translating with respect to the Stars.

Figure 2.1: Four ALMA antennas.

The International Space Station (ISS) is a low Earth orbit artificial satellite that has been progessively assembled since 1998, and is intended to be a microgravity and space environment research laboratory. The experiments span a wide variety of scientifical fields, including astronomy, meteorology, and physics. In order to conduct these experiments, a complex set of instruments and equipment is required, such as the Alpha Magnetic Spectrometer (AMS), which is designed to study antimatter. The detectors placed in AMS, however, can only detect particles that enter it at certain orientations ("top to bottom"), which makes attitude control crucial to AMS operation. Attitude control was also vital for AMS to make its way to ISS: in order to be installed, the AMS needed to be removed from a shuttle cargo using a robotic arm and handed off to ISS's own robotic arm. Likewise, robotic arms are constantly used by ISS to perform several other tasks, such as deploying cube satellites, as illustrated by Figure 2.2. These represent only a few among multiple scenarios of equipment in ISS that rely on attitude control to operate.

Figure 2.2: Cube satellites being deployed by ISS.

Attitude control is also crucial to an activity society already takes for granted: safe long-distance commercial air transportation. Throughout last century, major technological breakthroughs boosted the range of early aircraft models, enabling flights lasting several hours long. The increase in flight hours, however, came at the price of further pilot fatigue. As a means to assist pilots by performing some of their tasks during flights, the autopilot was introduced in 1912 by Sperry Corporation. Autopilots control aircraft trajectory, eliminating the need of continuous manual control by a human operator. These systems allow pilots to supervise higher-level aspects of flying aircraft, such as weather, systems and trajectory, making flights less stressful, less demanding and, consequently, safer. In fact, modern autopilot systems are even capable of executing automated landing under the supervision of a pilot. This feature is currently available on many major airports runways, especially those susceptible to severe adverse weather.

Autopilots typically use inertial guidance systems to assess aircraft's position and attitude, which are used to control orientation. The degree of autopilot control can be categorized into three types, and the larger and more complex the aircraft, the higher the level of required control. Single-axis autopilots, also called "wing levelers", control aircraft in the *roll axis,* shown in Figure 2.3. Two-axis consist in single-axis autopilots that also control the *pitch axis*, and three-axis autopilots are two-axis autopilots that additionally control the *yaw axis*, also represented in Figure 2.3. Typically, large commercial aircraft employ three-axis autopilots to automate most phases of flights (e.g., cruise,

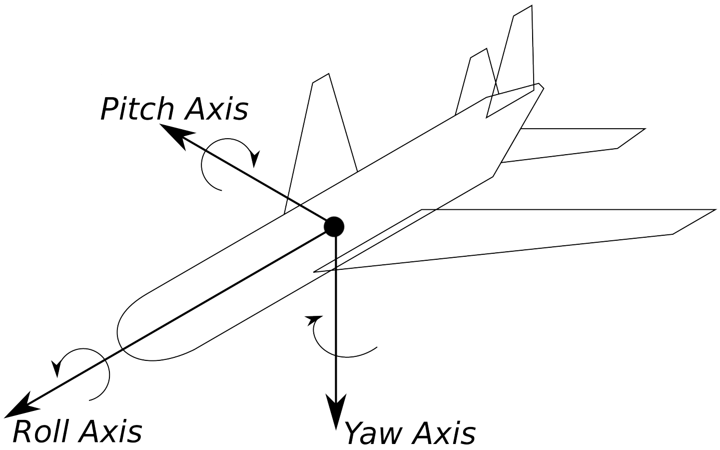

Figure 2.3: Autopilots regulate aircraft pitch, roll and yaw angles.

where aircraft must maintain a certain altitude).

The previous example introduced an intuitive attitude parameterization based on roll, pitch and yaw angles. These are, in fact, a special case of a formal and more general parameterization named *Euler Angles* [24]. Formal representation of attitude is an interesting problem in its own sake, and has been the subject of research for more than a century [25], leading to almost a dozen of sound different approaches. Each of these presents idiosyncrasies that make unique compromises between general qualities. For example, attitudes require at least a three-element parameterization, called *minimum parameterizations* [24]. Nevertheless, minimum parameterizations suffer from continuity issues [26] that hinder representation at certain attitudes. Similar trade-offs have to be made regarding other aspects of representations, such as computational burden and singularities.

In addition to particular technical aspects of each representation, from the dynamics stand-point the attitude control problem is also a challenging one due to nonlinearities, typically dealt with using three strategies [19]. Model-based control is the first one, where the rigid body's matrix of inertia is used directly cancel out the problematic terms, which is discussed in the context of delay-free trajectory tracking by the classic work of [19]. In practice, however, it can be difficult to obtain model parameters, and robustness is only proved for the delay-free case. The second strategy avoids this issue with an adaptative scheme, where the feedforward stems from the estimated matrix inertia. Although no model information is needed, performance can be deteriorated [19]. In the delayed case, [15, 20] also treated adaptative tracking, but considered only attitude measurements were subjected to constant time delays. In addition, results depend on the exact time delay value (i.e., the delay is known) and were obtained using a vector form of rotation matrices, which require more parameters and are more expensive from the computational standpoint compared to quaternions. The third approach is to prove results without explicit model information. In [8], the first work to deal with attitude control with time delays, exponential stability is proved considering constant delays. Another inconvenience is that results are dependent on initial attitude, the exact delay value, and model information. Moreover, Rodrigues Parameters (RP) are used, which present singularities. The proposed controller, which does not use velocity measurements, does have a feedforward term, but its purpose is not to eliminate nonlinearities, and it's chosen zero for stabilizing the origin. Modified Rodrigues Parameters were chosen by [21] to prove exponential stability considering state measurements subjected to unknown constant delays. Nevertheless, sufficient conditions depend on initial orientations. The singularity issue has been eliminated by [22], who used quaternion parameterization to prove asymptotic stability. No model information is necessary, and results are proved assuming simple Proportional Derivative (PD) controllers, but the stability conditions do depend on the delay value, considered constant. This work was extended by [23], which considers velocity-free controllers.

2.1.2 Time-delay Systems

Dynamical systems that are subjected to delays are an important research area. The first investigations can be traced back to the time of the Bernoulli brothers and Euler in the eighteenth century, whereas Bellman and Myshkis started systematical study at the 1940s [27]. Instead of ordinary differential equations (ODEs), the so-called *Time-delay Systems*[1] (TDSs) are characterized by infinite-dimensional *Functional Differential Equations* (FDEs) [1] because of the very nature of their solutions [1, 2, 12]. This makes several classical stability analysis criteria not applicable [5, 3].

Time-delays are pervasive in dynamical systems, existing examples in several fields ranging from biology, chemistry and economics to mechanics [1, 9, 11, 2]. In particular, sensor and actuator devices always introduce time delays, regardless of how small these are [3]. Indeed, the so-called latency, is a broad phenomenon that affects sensors and actuators and is consequence of the fact that any physical interaction propagates with limited velocity. Since these devices typically employ some kind of transducer, which cannot transfer energy immediately due to latency, time-delays are introduced. Also, most modern control systems rely on digital computers to calculate control signals [4, 3], which cannot perform such calculations instantly. More recently, general multipurpose communication networks have gained popularity in control systems, in which they are used to connect its elements, such as sensors and controllers. Introducing communication networks gives these systems an edge over traditional feedback architectures, where the components are typically connected through point-to-point cables. Some of the advantages are reduced costs and weight, simpler installation and maintenance, and remote control [28, 11]. The so-called *Networked Control Systems* (NCS) [13, 9, 11, 2, 3], however, suffer from undesirable effects caused by the networks, namely time-varying delays and packet dropouts. Thus, despite common hypothesis such as states being instantly available for feedback and actuators immediately acting upon processes, real-world control systems can all be considered TDSs [3], as depicted in Figure 2.4.

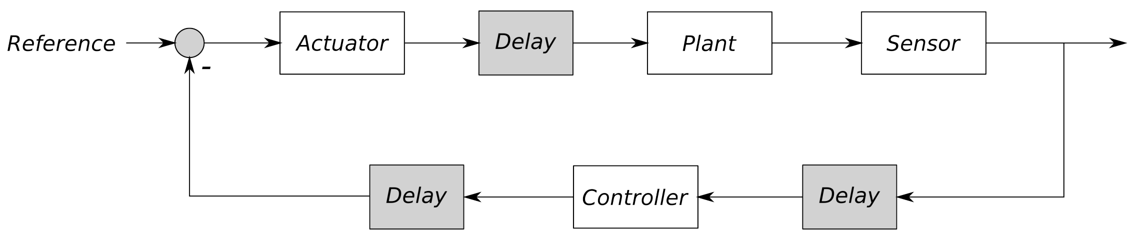

Figure 2.4: Feedback system delays.

Attitude control systems are no exception, both sensors and actuators can induce time-delays.

[1] Alternative nomenclatures include systems with dead-time or affect effect, hereditary systems, equations with deviating argument or differential-difference equations.

Thrust profile of gas jet control systems, which are affected by electromechanical delays in valve circuits and propellant flow [14], are an example of actuator capable of causing delays. Low-cost onboard attitude sensors can also be responsible for introducing delays. For example, magnetometers. In the presence of magnetic torques they must be turned off, delaying controller access to attitude measurements [15]. Low-rate sensors might contribute with delays as well. Star trackers, for instance, may need up to ten seconds to identify stars [16]. Global Positioning System (GPS) also causes sensing delays due to data latency and momentary outages, while evaluating satellite position in orbit [17, 18].

The impact of time-delays on control systems behavior is involved [9, 2, 3]. Stable systems can become unstable, and, conversely, unstable systems can be stabilized by time-delays [9, 12]. Sometimes both scenarios are simultaneously possible, depending on the exact value of the delay [3]. Regarding the TDSs that are dealt with in this dissertation, the effects are mostly harmful. For example, closed-loop performance can be damaged [7], reducing a system's robustness to disturbances. Even worse, delays can cause oscillations [6] and actual instability [8]. The stability and performance analysis of these systems is nontrivial, especially because of the combination of nonlinearities with time-delays. Indeed, TDSs are infinite-dimensional systems, and the corresponding *characteristic quasipolynomial* [3] has, therefore, infinite solutions (poles). This immediately discards some classical analysis methods, such as root locus [5], and force others to be adapted, e.g., the *Nyquist criterion* [5, 3]. The issue is aggravated by nonlinearities, which make several classical analysis methods useless.

The (second or direct) Lyapunov method, on the other hand, is an efficient and standard approach to study stability of dynamical systems [29]. *Grosso modo*, it consists in finding energy-like positive definite functionals/functions V that are coupled with the systems dynamics and whose derivative is negative definite, i.e., V decays with time [29]. In the context of TDSs, two flavors of Lyapunov-like techniques are prevalent: the *Krasovskii* method of Lyapunov *functionals* [30, 9, 11, 2, 3] and the *Razumikhin* method of Lyapunov *functions* [13, 2, 3]. Krasovskii's is a natural step from Lyapunov's second method, since it is based on an analogous process of finding energy-like functions, except that these are functions of the TDS state, $\boldsymbol{x}_t$, which completely differs from ordinary control systems modeled by ODEs [3]. Razumikhin's method, on the other hand, does not explore functions of $\boldsymbol{x}_t$, and, in general, leads to more conservative results.

As in standard Lyapunov analysis, assessing stability comes down to verifying inequalities [10, 29, 2]. In the case of linear TDSs, this translates to Linear Matrix Inequalities (LMIs) conditions [10]. Whenever the stability of a TDS, or dynamical system, in general, can be stated as LMI conditions, due to convexity and nice numerical algorithms, the problem can be considered solved [10, 3]. The effort is then concentrated in tweaking Lyapunov terms to benefit from general mathematical inequalities and identities in order to obtain less conservative results [31, 32, 33, 34, 35, 36, 37, 38].

2.2 CHALLENGES AND PROBLEM STATEMENT

The presence of sensing and actuating time-delays reinvigorates many of the challenges which have already been solved or partly solved in the context of attitude control. In particular, the interaction of time-delays with nonlinearities of rigid body kinematics and dynamics is entangled and make many available analysis and design techniques impractical or not directly applicable. This is also true regarding TDS literature, which is more developed for linear systems than it is for nonlinear ones. Moreover, the techniques which can be adapted are still widely unknown to a considerable part of attitude control community. This leads to results that cannot be readily implemented, verified or optimized. In this sense, the issues addressed in this dissertation can be segmented into the subproblems below.

1. **[PROB1]** Time-delays is an undeveloped field in attitude control literature. Nevertheless, evidence shows sensors and actuator technologies introduce time-delays in many practical applications. Overlooking the effects of these delays on closed-loop behavior can be disastrous, culminating in poor performance or even unstable operation.

2. **[PROB2]** The nonlinearities associated with rigid body kinematics and dynamics have, so far, led to nonlinear stability conditions which cannot be easily implemented or that are computationally inefficient to verify. In addition, the analysis techniques from TDS are seldom invoked, which can potentially make results more conservative.

3. **[PROB3]** The few results in attitude control literature that address robustness to disturbances do not provide conditions to design the controllers, neither works allow to actually quantify the impact disturbances have on closed-loop performance.

2.3 GOALS AND OBJECTIVES

In light of the paucity of results and relevance of the problem depicted above, this dissertation addresses the issues of attitude control problem subjected to time-delays, disturbances and attitude control despite lack of model information. The main goals are presented in the following.

1. **[GO1] Obtain LMI attitude stability conditions**

   State stability conditions in the form of LMI using state-of-the-art TDS analysis techniques. In particular, adapt linear TDS methods to exploit kinematics and dynamics nonlinearities. Stability conditions may be model-dependent or model-independent. In practice, exact parameter models (inertia J) are difficult to identify. Hence, model-independent conditions will be favored. This addresses **[PROB1]** and **[PROB2]**.

2. **[GO2] Determine LMI controller design conditions for attitude control**

   Establish LMI conditions to enable numerical controller design. More specifically, these conditions should allow casting design as an optimization problem, where the LMIs are constraints of the problem. Moreover, results should warrant disturbance rejection performance quantitatively. By doing this, **[PROB3]** is encompassed.

3. **[GO3] Develop attitude tracking controllers**

   Rigid bodies are often required to follow desired trajectories, instead of resting at equilibrium orientations. Thus, it is important to establish results that guarantee precise trajectory tracking.

2.4 RESEARCH APPROACH AND CONTRIBUTIONS

The strategy to obtain the stability and design criteria that address the outlined problems is to modify classical rigid body kinematics and dynamics equations by adding time-delays, and use Lyapunov-Krasovskii arguments to prove the results. This research started with the extension of state-of-the-art linear TDS techniques that are suited to proportional controllers, to the more general case of dynamical controllers. Although the results, which produced two IEEE international conference papers [39, 40], were not directly applied to the specific problem of attitude control, much of the acquaintance with TDS techniques was gained during that period.

The transition to the attitude control problem occurred naturally by, to the best of the author knowledge, deriving the first controller design conditions that have guaranteed disturbance rejection performance. Proposing a new technique to exploit kinematic nonlinearities, it was possible to adapt efficient TDS techniques and obtain the results, which are described in Section 5.1, and also culminated in an IEEE international conference paper [7]. The same technique was used to address dynamical trajectory tracking with attitude measurement delays. Subsection 5.2.1 describes the outcomes of this study.

The final research stage was focused on solving the more general case of dynamical stabilization with input delays. The stability criterion obtained is detailed in Subsection 5.2.2, and for the first time considers distinct attitude and velocity time-varying delays. The criterion also introduces LMI conditions, which distinguish the theorem from previous results, and is also responsible for reducing the analysis conservatism. Furthermore, conditions are liable to relaxations that can be used to design stabilizing controllers, which to best of the author knowledge is a completely unexplored problem.

3 RIGID BODY KINEMATICS AND DYNAMICS

The attitude, or the orientation, of a rigid body can be represented through various mathematical descriptions [24]. Since most engineering applications require calculations, storage and manipulation of the objects that represent the attitude by some kind of computer, the choice of a particular description is based on a compromise that favors certain aspects. Among such aspects, the following list ranks the most relevant

1. Range and smoothness

   Attitudes can be globally continuously represented by a single set of parameters.

2. Computational burden

   The amount of operations (sums and multiplications) necessary to make calculations involving the objects that represent attitude; The number of required parameters to store these objects, which translates into memory usage.

3. Physical intuitiveness and algebraic complexity

   Representation parameters have physical meaning; The complexity of a representation's conceptual foundations.

Taking the above criteria into account, quaternions are chosen to represent attitude. The interested reader is referred to [24] for more details on quaternions and many other attitude representation approaches.

3.1 FRAMES AND RIGID MOTION

The orientation of an object is not absolute. It changes depending on the observer's perspective. For example, consider the attitude of satellite represented in Figure 3.1. If the observer is located on Earth, the satellite is pointing at a different direction than the one observed by someone on the moon. In fact, even two distinct observers on Earth or the moon can perceive different orientations of the satellite. Thus, in order to provide an unambiguous description of attitude, a reference must be adopted, and the orientation described relative to that reference.

Formally, a reference is defined by a *coordinate system*, which consists in a *dextral orthonormal basis* of the three-dimensional vector space $\mathbb{R}^3$ [14, 41, 42, 24]. A coordinate system is denoted by $\mathcal{E}$, representing a basis $\{\boldsymbol{e}_1, \boldsymbol{e}_2, \boldsymbol{e}_3\}$ of orthonormal three-dimensional vectors, and is also called a ***frame***. The *attitude* or *orientation*, represents the coordinates of another coordinate system with respect to a frame. In order to avoid ambiguity, a coordinate system must be arbitrated and attached to the object, so that attitude can be precisely described as the coordinates of the object's coordinate system with respect to the reference frame. The coordinate system that is attached to the object is called the ***body frame***, denoted by $\mathcal{B}$. A reference frame that does not present relative motion to the object is said to be an ***inertial frame***, represented by $\mathcal{I}$.

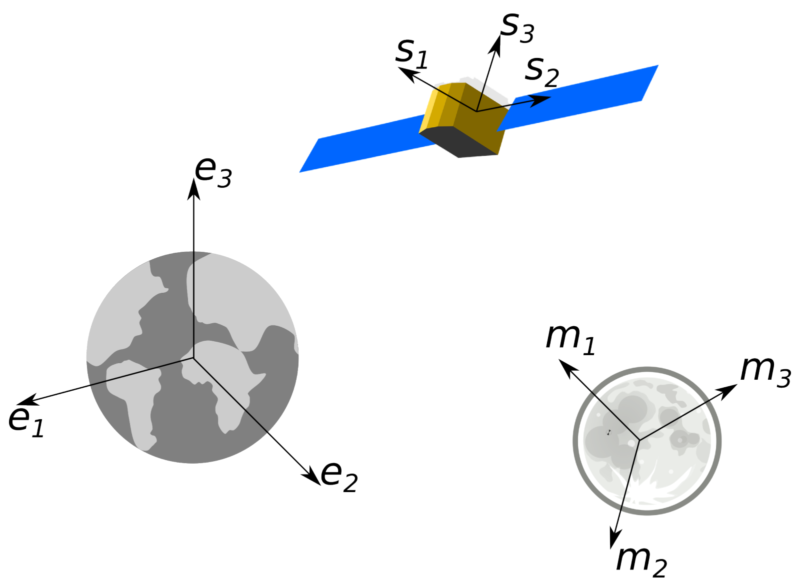

Figure 3.1: Different reference frames.

In general, the rotating motion of a particle $\boldsymbol{p}$ can be described by its body frame coordinates at each instant of time relative to an inertial frame, attached to another particle $\boldsymbol{o}$. Then, adopting a determined attitude representation method, the orientation of $\boldsymbol{p}$ relative to $\boldsymbol{o}$ is described by the coordinates of $\mathcal{B}$ relative to $\mathcal{I}$. Analogously, this approach can be used to describe the collective motion of a group of particles. In this sense, the notion of an undeformable body is introduced. A collection of particles which preserves the distances between any two particles throughout time, despite body motions and external forces, is called a ***rigid body*** [42, 43]. More formally, given a set $\mathcal{P}$ representing a set of particles $\{\boldsymbol{p}_1, \boldsymbol{p}_2, \ldots\}$, if any two particles $\boldsymbol{p}_i$ and $\boldsymbol{p}_j$ have their relative coordinates expressed by maps $\boldsymbol{p}_i : \mathbb{R}_{\geq 0} \to \mathbb{R}^3$ and $\boldsymbol{p}_i : \mathbb{R}_{\geq 0} \to \mathbb{R}^3$, then

$$\|\boldsymbol{p}_i(t) - \boldsymbol{p}_j(t)\| = \|\boldsymbol{p}_i(0) - \boldsymbol{p}_j(0)\|$$

holds for all t greater than or equal to zero.

Analogously, a ***rigid motion***[1] of a particle set $\mathcal{P}$ is a movement of the particles of $\mathcal{P}$, such that distances between any two of them are preserved throughout time [43]. Although real bodies, such as spacecraft, are not actually rigid [42, 6, 14], since the goal of this dissertation is to address the interaction between time-delays and body dynamics from a more abstract point of view, rigid body attitude and motion are considered. Indeed, the analysis of rigid body attitudes involves only three degrees of freedom, in contrast with accurate structural analysis [42], which is outside the scope of this work.

Although the definition of inertial and body frames allows the unambiguous characterization of a rigid body's attitude, the representation of the coordinates can be done following different approaches

[1] More specifically, the kind of motion called ***rigid transformations [43]*** is of interest, since it does not allow reflections. Formally, a mapping $r : \mathbb{R}^3 \to \mathbb{R}^3$ is a rigid transformation if distances and the cross-product are preserved, i.e.,

1. $\|r(p_1) - r(p_2)\| = \|p_1 - p_2\|, \forall p_1, p_2 \in \mathbb{R}^3$.
2. $r(p_1 \times p_2) = r(p_1) \times r(p_2), \forall p_1, p_2 \in \mathbb{R}^3$.

From the definition of rotation matrices, it can be seen that rotations are rigid transformations.

and conventions. Attitude representation, therefore, comprises the parameterization of such coordinates. Rotation matrices, Euler angles, and Angle/Axis are only some of the possible choices [42, 24]. Quaternions, however, standout among them, and constitute a good balance between analytical and computational aspects of representations.

3.2 QUATERNIONS

It is well-established one-to-one minimum representations of attitude without singularities do not exist. In fact, the minimum continuous global one-to-one parametrization of rotations requires five elements [26]. Nevertheless, by adding a fourth parameter, a continuous two-to-one representation can be obtained. In 1843, Hamilton introduced four-dimensional hypercomplex numbers that can be used to represent attitudes [25]. These hypercomplex numbers are called ***Quaternions***, and noted by $\mathbb{H}$. In this dissertation, the adopted convention is described in the following. Let $\mathbf{i}, \mathbf{j}, \mathbf{k}$ be imaginary numbers such that

$$\mathbf{i}^2 = \mathbf{j}^2 = \mathbf{k}^2 = \mathbf{ijk} = -1, \tag{3.1}$$

which implies

$$\mathbf{ij} = -\mathbf{ji} = \mathbf{k}, \mathbf{jk} = -\mathbf{kj} = \mathbf{i}, \mathbf{ki} = -\mathbf{ik} = \mathbf{j}. \tag{3.2}$$

A quaternion q can be written as

$$\boldsymbol{q} = q_0 + q_1\mathbf{i} + q_2\mathbf{j} + q_3\mathbf{k},$$

with real numbers q_0, q_1, q_2, q_3. Quaternions also admit a more compact vector form [24]

$$\boldsymbol{q} = \begin{bmatrix} q_0 & q_1 & q_2 & q_3 \end{bmatrix}^T.$$

In fact, it is more convenient to split the quaternion into two components: the *scalar part* η accounting for q_0 and the *vector part* $\boldsymbol{\zeta}$ representing $\begin{bmatrix} q_1 & q_2 & q_3 \end{bmatrix}^T$. Thus, $\boldsymbol{q}$ can be compactly repesented as

$$\boldsymbol{q} = \begin{bmatrix} \eta & \boldsymbol{\zeta}^T \end{bmatrix}^T. \tag{3.3}$$

Expression (3.3) defines the quaternion representation convention that will be adopted in this dissertation. A quaternion with zero vector part $\boldsymbol{\zeta}$, is called a *real quaternion* or *scalar quaternion.* On the other hand, if η is zero, $\boldsymbol{q}$ is a *vector quaternion* or *pure quaternion.* Pure quaternions can represent points and translations (vectors) [44]. Indeed, a pure quaternion $\boldsymbol{p}$ given by $\begin{bmatrix} 0 & \boldsymbol{\zeta}_p^T \end{bmatrix}^T$, with $\boldsymbol{\zeta}_p$ equal to $\begin{bmatrix} p_x & p_y & p_z \end{bmatrix}^T$, represents a point or a translation $\boldsymbol{p}_v$ equal to $\boldsymbol{\zeta}_p$.

Now, considering map

$$\begin{aligned} [\cdot]_\times &: \mathbb{R}^3 \to \mathfrak{o}(3) \\ \boldsymbol{x} \mapsto [\boldsymbol{x}]_\times &:= \begin{bmatrix} 0 & -x_3 & x_2 \\ x_3 & 0 & -x_1 \\ -x_2 & x_1 & 0 \end{bmatrix}, \end{aligned}$$

and since

$$\alpha \boldsymbol{q} = \begin{bmatrix} \alpha\eta & \alpha\boldsymbol{\zeta}^T \end{bmatrix}^T,$$

for any given scalar α, the following operations, which are consistent with (3.1)-(3.2), are defined.

Definition 3.2.1. Quaternion Operations

Let $\alpha, \beta \in \mathbb{R}$, $\boldsymbol{q}_1 = \begin{bmatrix} \eta_1 & \boldsymbol{\zeta}_1^T \end{bmatrix}^T$, $\boldsymbol{q}_2 = \begin{bmatrix} \eta_2 & \boldsymbol{\zeta}_2^T \end{bmatrix}^T \in \mathbb{H}$.

1. The *quaternion addition and subtraction*, denoted by "$\pm$", is defined as

$$\alpha \boldsymbol{q}_1 \pm \beta \boldsymbol{q}_2 = \begin{bmatrix} \alpha\eta_1 \pm \beta\eta_2 & (\alpha\boldsymbol{\zeta}_1 \pm \beta\boldsymbol{\zeta}_2)^T \end{bmatrix}^T. \tag{3.4}$$

2. The *quaternion multiplication*, noted as "$\otimes$", is defined as

$$\boldsymbol{q}_1 \otimes \boldsymbol{q}_2 = \begin{bmatrix} \eta_1\eta_2 - \boldsymbol{\zeta}_1^T\boldsymbol{\zeta}_2 \\ \eta_1\boldsymbol{\zeta}_2 + \eta_2\boldsymbol{\zeta}_1 + [\boldsymbol{\zeta}_1]_\times \boldsymbol{\zeta}_2 \end{bmatrix}. \tag{3.5}$$

3. The *quaternion conjugation* of a quaternion is designated by a "$\overline{\cdot}$" and defined as

$$\overline{\boldsymbol{q}}_1 = \begin{bmatrix} \eta_1 & -\boldsymbol{\zeta}_1^T \end{bmatrix}^T. \tag{3.6}$$

Combining operations (3.5) and (3.6), it is possible to define a norm [41], that is the same as l_2 Euclidean norm.

Definition 3.2.2. The norm $\|\cdot\|$ of a quaternion $\boldsymbol{q}$ is defined as

$$\|\boldsymbol{q}\| = (\boldsymbol{q} \otimes \overline{\boldsymbol{q}})^{\frac{1}{2}} = \left(\eta^2 + \boldsymbol{\zeta}^T\boldsymbol{\zeta}\right)^{\frac{1}{2}}. \tag{3.7}$$

Note that $(\mathbb{H}, +)$ forms a group which is isomorphic[2] to $\left(\mathbb{R}^4, +\right)$ [24]. In addition, it follows that $(\mathbb{H}, +, \cdot)$ is a division ring [24]. Indeed, even though (3.5) is distributive, it is not commutative. Moreover, given a nonzero quaternion $\boldsymbol{q}$, its multiplicative inverse $\boldsymbol{q}^{-1}$ is given by $\frac{1}{\|\boldsymbol{q}\|}\overline{\boldsymbol{q}}$.

In particular, the four-dimensional unit-sphere is an important subset of $\mathbb{R}^4$,

$$\mathcal{S}^3 = \left\{\boldsymbol{q} \in \mathbb{R}^4 | \ \|\boldsymbol{q}\| = 1\right\}. \tag{3.8}$$

Indeed, because of the $\mathbb{R}^4$-$\mathbb{H}$ isomorphism, $\mathcal{S}^3$ is isomorphic to an $\mathbb{H}$ subset, called ***Unit Quaternions***–also *Euler-Rodrigues symmetric parameters* or simply *Euler symmetric parameters* [24]. Unit quaternions form a group under multiplication: given two unit quaternions, q_1 and q_2, $q_1 \otimes q_2$ also belongs to $\mathcal{S}^3$; $\mathbf{1}$ is the identity element, given by $\begin{bmatrix} 1 & \mathbf{0} \end{bmatrix}^T$ in $\mathcal{S}^3$; and the inverse element of any unit quaternion can be readily obtained by conjugation, since

$$\boldsymbol{q} \otimes \overline{\boldsymbol{q}} = \begin{bmatrix} \eta^2 - \boldsymbol{\zeta}^T(-\boldsymbol{\zeta}) \\ -\eta(-\boldsymbol{\zeta}) + \eta(-\boldsymbol{\zeta}) + [\zeta]_\times \boldsymbol{\zeta} \end{bmatrix} = \begin{bmatrix} \|\boldsymbol{q}\|^2 \\ \mathbf{0} \end{bmatrix} = \mathbf{1}.$$

[2] To see this, consider the mapping $q_0 + q_1\mathbf{i} + q_2\mathbf{j} + q_3\mathbf{k} \mapsto \begin{bmatrix} q_0 & q_1 & q_2 & q_3 \end{bmatrix}^T$

From this point on, the quaternion multiplication symbol "⊗" will be omitted in order to simplify notation. Quaternions provide a two-to-one parametrization of $SO(3)$ [26, 24], a group that characterizes three-dimensional rotations. This can be seen considering the map $\mathcal{R} : \mathcal{S}^3 \to SO(3)$, such that

$$\mathcal{R}(\boldsymbol{q}) = \mathbf{I} + 2\eta [\boldsymbol{\zeta}]_\times + 2 [\boldsymbol{\zeta}]_\times^2 . \quad (3.9)$$

The map $\mathcal{R}$ is called the *Rodrigues formula*, and from (3.9) it can be seen that $\mathcal{R}(\boldsymbol{q}) = \mathcal{R}(-\boldsymbol{q})$, i.e., $\mathcal{R}$ is two-to-one. Explicitly, considering quaternion $\boldsymbol{q}$, given by $\begin{bmatrix} \eta & \zeta_1 & \zeta_2 & \zeta_3 \end{bmatrix}^T$, then

$$\mathcal{R}(\boldsymbol{q}) = \begin{bmatrix} \zeta_1^2 - \zeta_2^2 - \zeta_3^2 + \eta^2 & 2(\eta\zeta_1 + \zeta_2\zeta_3) & 2(\eta\zeta_2 - \zeta_1\zeta_3) \\ 2(\eta\zeta_1 - \zeta_2\zeta_3) & -\zeta_1^2 + \zeta_2^2 - \zeta_3^2 + \eta^2 & 2(\zeta_1\zeta_2 + \eta\zeta_3) \\ 2(\eta\zeta_2 + \zeta_1\zeta_3) & 2(\zeta_1\zeta_2 - \eta\zeta_3) & -\zeta_1^2 - \zeta_2^2 + \zeta_3^2 + \eta^2 \end{bmatrix} . \quad (3.10)$$

Conversely, given a rotation matrix R, the corresponding quaternion $\begin{bmatrix} \eta & \zeta_1 & \zeta_2 & \zeta_3 \end{bmatrix}^T$ can be obtained. Indeed, from (3.10), it follows that

$$\zeta_3 = \pm\frac{1}{2}\sqrt{1 + Tr(R)}. \quad (3.11)$$

If ζ_3 is nonzero, then

$$\eta = \tfrac{1}{4\zeta_3}(R_{23} - R_{32}), \quad \zeta_1 = \tfrac{1}{4\zeta_3}(R_{31} - R_{13}), \quad \zeta_2 = \tfrac{1}{4\zeta_3}(R_{12} - R_{21}).$$

On the other hand, if ζ_3 is zero, then a nonzero element of the remaining three can be used to obtain the others. Note that, since $\boldsymbol{q}$ is unit-norm, there always exist at least one such element. The ambiguity of the sign in (3.11) reflects the double-covering of $SO(3)$ by quaternions.

From (3.5) and (3.9), it follows that, given three unit quaternions $\boldsymbol{q}_1, \boldsymbol{q}_2, \boldsymbol{q}_3$ such that

$$\boldsymbol{q}_3 = \boldsymbol{q}_2\boldsymbol{q}_1,$$

then

$$\mathcal{R}(\boldsymbol{q}_3) = \mathcal{R}(\boldsymbol{q}_2)\,\mathcal{R}(\boldsymbol{q}_1).$$

Therefore, successive rotations can be represented by the product of the corresponding quaternions. A quaternion can also be directly obtained from a rotation expressed in Axis/Angle form $(\mathbf{n}, \theta)$ (depicted in Figure 3.2), as

$$\eta = \cos\left(\tfrac{\theta}{2}\right), \quad \boldsymbol{\zeta} = \sin\left(\tfrac{\theta}{2}\right)\mathbf{n}. \quad (3.12)$$

3.2.1 Comparison between representations

Quaternions are compared individually with three classical representations in order to point out the advantages of adopting this representation regarding the criteria mentioned at the beginning of the chapter. Even though other representations are omitted (Rodrigues, Modified Rodrigues, Cayley-Klein parameters, see [24]), similar arguments could be used to argue in favor of quaternions.

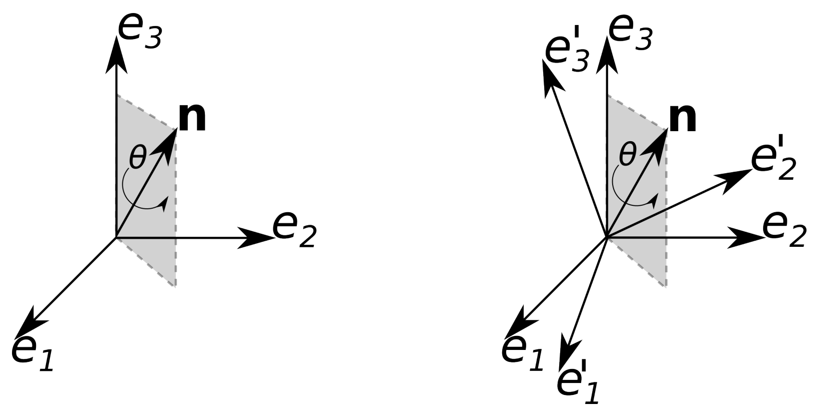

Figure 3.2: Rotation by an angle θ about axis $\boldsymbol{n}$.

Rotation Matrices *versus* Quaternions

Since the mathematical tools concerning rotation matrices involve basically linear algebra, rotation matrices tend to be more intuitive to work with initially. For the same reason, there already exist a breadth of available algorithms and programming libraries capable of handling rotation matrices.

Nevertheless, compared to rotation matrices, quaternions are a more economical parametrization, requiring four elements, instead of nine. Even though both allow the composition of rotations to be obtained through group multiplication, the one involving quaternions is significantly lighter, since sixteen multiplications are necessary, instead of twenty seven. In addition, there are less constraints in the quaternion case: only one unit-norm constraint, rather than six constraints [24]. Moreover, this constraint is considerably less expensive from the computational standpoint than orthogonalization algorithms [24].

Euler Angles *versus* Quaternions

The most appealing arguments in favor of Euler angles are that they are a minimal representation, which require one less parameter than quaternions, and that they are conceptually more intuitive and easy to grasp, since the parameters have direct physical meaning.

On the other hand, the extra parameter spares the quaternions from singularities, which ultimately require two sets of Euler angles to be overcome, therefore eliminating the advantage of needing less parameters. In addition, if the singularities are avoided, this implies switching the dynamic system's differential equations, which falls into the realm of hybrid systems, and would require more sophisticated stability analysis tools [45]. Moreover, successive rotations can be readily combined using quaternions, in contrast to the Euler angle setting [24].

Quaternions *versus* Axis/Angle

Quaternion parameters do not have an explicit physical significance, but they are closely related to axis/angle's. In this sense, the little gain in intuitiveness provided by the latter representation does not justify its adoption, since axis/angle suffers from infinite possible choices of angles (multiples of

2π) that force them to be constrained. This causes discontinuities around 0 and 2π and, consequently, a similar problem regarding hybrid systems occur. In addition, rotations of zero degrees do not admit valid axis. Moreover, successive axis/angle rotations are significantly harder to combine than quaternion ones [24].

3.3 KINEMATIC AND DYNAMIC EQUATIONS

The previous sections introduced a formal approach to represent the orientation of a rigid body with respect to a fixed reference. In particular, rigid motion was defined as a mapping that preserves distances throughout time. This section will be concerned with establishing the equations that govern the way the orientation of a rigid body evolves with time.

Kinematic equations

Kinematics[3] is a classical mechanics subfield whose object of study is the motion of particles disregarding their masses and the forces causing motion [42, 43]. More specifically, Kinematics employs geometrical arguments to describe the way a particle's position, velocity, acceleration and all higher-order derivatives evolve in time given initial conditions. In this work, in particular, the relationship between attitude and angular velocity will be explored.

Consider two frames $\mathcal{B}$ and $\mathcal{I}$. Let $\boldsymbol{q}$ be a unit quaternion that represents the attitude of $\mathcal{B}$ relative to $\mathcal{I}$ and suppose $\boldsymbol{q}$ is subjected to a small rotation $\Delta\boldsymbol{\theta}$, represented by unit quaternion $\Delta\boldsymbol{q}$, such that it can be approximated by its Taylor expansion

$$\boldsymbol{\Delta q} = \begin{bmatrix} \cos 0 \\ (\sin 0)\,\mathbf{n} \end{bmatrix} + \frac{1}{2}\begin{bmatrix} -\sin 0 \\ (\cos 0)\,\Delta\boldsymbol{\theta} \end{bmatrix} + O\left(\|\Delta\boldsymbol{\theta}\|^2\right) = \begin{bmatrix} 1 \\ \frac{1}{2}\Delta\boldsymbol{\theta} \end{bmatrix} + O\left(\|\Delta\boldsymbol{\theta}\|^2\right). \tag{3.13}$$

Let $\boldsymbol{\omega}$ denote the vector $\lim_{t\to 0}\Delta\boldsymbol{\theta}$. Then, rotated quaternion $\boldsymbol{q}\,(t+\Delta t)$ is such that

$$\begin{aligned}\frac{d}{dt}\boldsymbol{q}\,(t) = \lim_{\Delta t\to 0}\frac{\boldsymbol{q}\,(t+\Delta t)-\boldsymbol{q}\,(t)}{\Delta t} = \lim_{\Delta t\to 0}\frac{\boldsymbol{q}\boldsymbol{\Delta q}-\boldsymbol{q}}{\Delta t} &= \lim_{\Delta t\to 0}\frac{\boldsymbol{q}\left(\begin{bmatrix} 1 \\ \frac{1}{2}\Delta\boldsymbol{\theta}\end{bmatrix} - \begin{bmatrix} 1 \\ \mathbf{0}\end{bmatrix}\right)}{\Delta t} \\ &= \frac{1}{2}\boldsymbol{q}\begin{bmatrix} 0 \\ \boldsymbol{\omega}\end{bmatrix},\end{aligned}$$

and the kinematic equation of the quaternion in vector notation is given by

$$\dot{\boldsymbol{q}}\,(t) = \frac{1}{2}\begin{bmatrix} -\boldsymbol{\zeta}^T \\ \eta\mathbf{I} + [\boldsymbol{\zeta}]_\times \end{bmatrix}\boldsymbol{\omega}. \tag{3.14}$$

Alternatively, (3.14) can be obtained using algebraic [46] and topological [26] arguments. Note that, since $\Delta\boldsymbol{q}$ corresponds to a small rotation with respect to $\mathcal{B}$, the vector $\Delta\boldsymbol{\theta}$ represents the angular velocity observed at $\mathcal{B}$. For example, consider Figure 3.1, with $\mathcal{I}$ represented by $\{\boldsymbol{e}_1, \boldsymbol{e}_2, \boldsymbol{e}_3\}$, and $\mathcal{B}$ collocated at the satellite's center of mass, denoted by $\{\boldsymbol{b}_1, \boldsymbol{b}_2, \boldsymbol{b}_3\}$. Then, $\boldsymbol{\omega}$ corresponds to local measurements made by, for example, an onboard accelerometer.

[3]The term was introduced by Ampère (*cinématique*), and derives from the Greek word *kinein* ("to move").

Dynamic equations

Relying solely on the kinematic description of a rigid body to control its attitude presupposes that angular velocities can be considered as control inputs, i.e., the relationship between velocities and torques is transparent for the purposes of control. In many cases, however, it is not possible to ignore this relationship, especially if the input torques are subjected to time-delays. Thus, the *Dynamics* of a rigid body, which is precisely the description of how angular velocities and torques are related, must be taken into account. For more on dynamics, the reader is referred to [14, 42, 6, 43].

Let R be map from $\mathbb{R}_{\geq 0}$ into $SO(3)$, that corresponds to the attitude of body frame $\mathcal{B}$ with respect to an inertial frame $\mathcal{I}$. Since $R(t)$ is orthogonal, it follows that

$$R(t)\,R(t)^T = \mathbf{I}, \tag{3.15}$$

for all $t \geq 0$. Differentiating (3.15) yields

$$\frac{dR}{dt}R(t)^T + R(t)\,\frac{dR^T}{dt} = 0,$$

which means that

$$\frac{dR}{dt}R(t)^T = -R(t)\,\frac{dR^T}{dt} = -\left(\frac{dR}{dt}R(t)^T\right)^T, \tag{3.16}$$

that is, $R(t)\,\frac{dR}{dt}^T$ defines a skew-symmetric matrix. Because $[\cdot]_\times$ is bijective (Section I.1), for each t, there exists a vector $\boldsymbol{\omega}_0(t)$ in $\mathbb{R}^3$ and $[\boldsymbol{\omega}_0(t)]_\times$ in $\mathbb{SK}^3$, where $\boldsymbol{\omega}_0(t)$ is the *angular velocity* expressed in the inertial frame. Then, substituting $[\boldsymbol{\omega}_0(t)]_\times$ for $R(t)\,\frac{dR}{dt}^T$ in (3.16) gives

$$\dot{R}(t) = [\boldsymbol{\omega}_0(t)]_\times\,R(t), \tag{3.17}$$

that is, the rigid body angular velocity expressed in $\mathcal{I}$. The angular velocity can also be expressed in the body frame, as

$$\boldsymbol{\omega}(t) = R(t)^T\,\boldsymbol{\omega}_0(t). \tag{3.18}$$

Now, Newton's second law gives that the change in angular momentum equals the net torque applied to the rigid body, that is

$$\frac{d}{dt}\left(R(t)\,JR(t)^T\,\boldsymbol{\omega}_0(t)\right) = \frac{d}{dt}\left(R(t)\,J\boldsymbol{\omega}(t)\right) = \tau_0, \tag{3.19}$$

where J represents the (constant) inertia matrix of the rigid body with respect to $\mathcal{B}$, and τ_0 represents the net input torque expressed in $\mathcal{I}$. Note that in (3.19), the change in angular momentum, is expressed in $\mathcal{I}$. Thus, (3.17) yields

$$\begin{aligned}\frac{d}{dt}\left(R(t)\,J\boldsymbol{\omega}(t)\right) &= \dot{R}(t)\,J\boldsymbol{\omega}(t) + R(t)\,J\dot{\boldsymbol{\omega}}(t)\\ &= [\boldsymbol{\omega}_0(t)]_\times\,R(t)\,J\boldsymbol{\omega}(t) + R(t)\,J\dot{\boldsymbol{\omega}}(t),\end{aligned} \tag{3.20}$$

Then, considering the angular momentum expressed in $\mathcal{B}$, and $[\cdot]_\times$ property (I.4), (3.20) yields

$$\tau = R(t)^T\left([\boldsymbol{\omega}_0(t)]_\times\,R(t)\,J\boldsymbol{\omega}(t) + R(t)\,J\dot{\boldsymbol{\omega}}(t)\right)$$

$$= \left[R\left(t\right)^T \boldsymbol{\omega}_0\left(t\right)\right]_\times J\boldsymbol{\omega}\left(t\right) + J\dot{\boldsymbol{\omega}}\left(t\right). \tag{3.21}$$

Thus, assuming the control input $u\left(t\right)$ is an input torque, (3.21) gives

$$J\dot{\boldsymbol{\omega}}\left(t\right) = -\left[\boldsymbol{\omega}\left(t\right)\right]_\times J\boldsymbol{\omega}\left(t\right) + u\left(t\right), \tag{3.22}$$

which is the *dynamics equation* of the rigid body expressed in $\mathcal{B}$. The nonlinear vector map $\left[\boldsymbol{\omega}\left(t\right)\right]_\times J\boldsymbol{\omega}\left(t\right)$, called *gyroscopic term* is the source of many technical challenges in attitude control. Indeed, not only it is nonlinear, but also quadratic-like, which means it can only be bounded by quadratic terms.

The motivation to express dynamics in the body frame are twofold. First, since $\mathcal{B}$ is attached to the rigid body, J can be assumed constant, which simplifies the final expression. This choice is also convenient from the control standpoint, since the velocity information that is available to controller is measured locally, i.e., $\boldsymbol{\omega}\left(t\right)$, instead of $\boldsymbol{\omega}_0\left(t\right)$. Note, however, that since $\mathcal{I}$ is inertial, when $\boldsymbol{\omega}\left(t\right)$ tends to zero, so does $\boldsymbol{\omega}_0\left(t\right)$, which is what (3.18) is expressing. Thus, because velocity control will concern steering the rigid body to rest, there is no advantage in considering dynamics expressed in the inertial frame.

4 TIME-DELAY SYSTEMS FUNDAMENTALS

This chapter provides the fundamentals of *Time-Delay Systems* (TDSs) that will support the arguments used to prove stability and design conditions to be established in the remainder of the chapter. For complete references, the reader is referred to the excellent works of [28, 13, 11, 2, 3]. Otherwise, the reader who is already familiar with TDSs may skip this section entirely, and move forward to Section 5.1.

4.1 PRELIMINARIES

Time-delays are a widespread phenomenon among dynamical systems. Control systems, in particular, are routinely subjected to delays, mostly because of the time required to acquire data, compute control signals and actuate on the systems [28, 2, 3]. Also, modern control systems typically operate on sampling-based control feedback loops, which, because of its elements' latency, introduce sampling delays. Even though this is typically addressed using discrete control strategies [4], these systems are amenable to the more general framework of TDS [11]. More recently, multipurpose communication networks have experienced a surge in popularity among control systems due to benefits they provide. Namely, *reduced weight and costs, increased flexibility, maintainance and installation ease, and remote control* [28, 11]. Time-varying communication delays and package dropouts, however, are only two of the countereffects that are caused by such networks, and can seriously degrade a control system's peformance and stability [28, 11, 3]. Thus, actuators, sensors, controllers and field networks are all responsible for introducing delays, that allow feedback control systems to be all considered under the more general framework of TDS.

Contrary to dynamical systems, which are described by *Ordinary Differential Equations* (ODEs), TDSs are characterized by *Functional Differential Equations* (FDEs) [13, 47, 3]. For example, consider the simple TDS described by

$$\dot{x}(t) = -x(t-d), \quad x(t) \in \mathbb{R}, \quad d > 0, \quad t \geq 0 \ . \tag{4.1}$$

The solutions of (4.1) for time t in $[0, d]$ require the definition of $x(t-d)$ for t in $[0, d]$, which leads to the *initial value function*

$$x(s) = \phi(s), s \in [-d, 0],$$

rather than an *initial value* $x(0)$, which would be the case for a typical ODE. The solutions can then be found via the *step method* by Bellman [27]. The method starts by finding a solution to (4.1) for t in $[0, d]$ by solving

$$t \in [0, d], \quad \dot{x}(t) = -\phi(t-d), \quad x(0) = \phi(0),$$

and procedure is repeated to find solutions for t in $[d, 2d], [2d, 3d]$, etc. Thus, in TDSs, states are actually *functions*

$$x_t : [-d, 0] \to \mathbb{R}$$

$$x(t) \mapsto x_t(\theta) = x(t+\theta), \theta \in [-d, 0],$$

which means the domain of TDSs' states is *infinite-dimensional*.

Time-delay systems can be divided into two categories: *retarded TDSs (RTDSs)* and *neutral TDSs (NTDSs)*. The former are characterized by delayed states only, whereas the latter have delayed higher-order state derivatives. For instance,

$$\ddot{x}(t) = a\dot{x}(t-d_2) + bx(t-d_1), x(t) \in \mathbb{R},$$

is an RTDS, contrary to

$$\dot{x}(t) = a\dot{x}(t-d) + bx(t), x(t) \in \mathbb{R},$$

which is an NTDS. The closed-loop kinematics and dynamics systems subjected to time-delays considered in this dissertation all fall into the RTDS case.

The general form of an RTDSs is

$$\dot{\boldsymbol{x}}(t) = f(t, \boldsymbol{x}_t),$$

where $\boldsymbol{x}(t)$ is a vector in $\mathbb{R}^n$, $\dot{\boldsymbol{x}}(t)$ is the right-hand derivative of $\boldsymbol{x}(t)$, and $f : \mathbb{R} \times \boldsymbol{C}[-d, 0] \to \mathbb{R}^n$, where $\boldsymbol{C}[-d, 0]$ denotes the function space of continuous function with compact support $[-d, 0]$. The initial function $\phi : [-d, 0] \to \mathbb{R}^n$ is assumed to be in $\boldsymbol{C}[-d, 0]$, and initial conditions are given by

$$\boldsymbol{x}(t_0+\theta) = \boldsymbol{x}_{t_0}(\theta) = \phi(\theta), \theta \in [-d, 0].$$

The interaction between time-delays and dynamical systems is involved. The presence of delays can manipulate the solutions of dynamical system, compromising once stable systems. For example, consider NTDS

$$\dot{x}(t) - a\dot{x}(t-d) = ax(t-d) - x(t), x(t) \in \mathbb{R},$$

with a greater than one. If d is zero, the system is exponentially stable, with solutions e^{-t}. When d is positive, however, the situation is quite different. The solutions, in this case, can be found via the roots of characteristic equation

$$(s+1)\left(1 - ae^{-ds}\right) = 0,$$

which are given by -1, and

$$s_n = \frac{1}{d}(\ln a + 2n\pi i), n \in \mathbb{Z}.$$

Thus, since the positive real part of s_n, $\frac{1}{d}\ln a$, is positive, solutions $e^{s_n t}$ are unbounded, and the system is unstable. This shows that even an arbitrarily small delay in the feedback loop are capable of completely transforming the nature of solutions. In particular, this means controllers that are based on derivative terms, such as Proportional-Integral-Derivative (PID) and Proportional-Derivative (PD) controllers, are extremely vulnerable to feedback delays.

Time-delays are also dangerous in the case of *Retarded Functional Differential Equations* (RFDEs). For instance, the system

$$\dot{x}(t) = -x(t-d), x(t) \in \mathbb{R}$$

is asymptotically stable for d in $\left[0, \frac{\pi}{2}\right)$, but unstable for h greater than $\frac{\pi}{2}$. Indeed, consider the system's characteristic equation

$$s + e^{-ds} = 0,$$

and assume solutions of form $a + bi$. It follows that

$$a + bi + e^{-ad-bdi} = a + bi + e^{-ad} \left(\cos bd - i \sin bd\right) = 0,$$

which implies

$$a = -e^{-ad} \cos bd, \quad b = e^{-ad} \sin bd \ .$$

For a to be positive, $\cos bd$ must be negative. If d belongs to $\left[0, \frac{\pi}{2}\right)$, b must be greater than one in module. This, however, contradicts the fact that both $\left|e^{-ad}\right|$ and $|\sin bd|$ are less than or equal to one. Thus, the system does not admit solutions with positive real parts, and it is stable. Nevertheless, if d is greater than $\frac{\pi}{2}$, then there exist solutions with positive real parts, which means the system is unstable.

Sometimes, though, time-delays are benefitial to stability: the system

$$\ddot{x}\left(t\right) + x\left(t\right) - x\left(t-d\right) = 0$$

is unstable for d equal to zero, but asymptotically stable when d equals one (consider the approximation $\dot{x}\left(t\right) \simeq \left[x\left(t\right) - x\left(t-d\right)\right]/d$) [3]. This illustrates how time-delays can alter the behavior of dynamical systems in unexpected manners.

The previous examples showed the effects of time-delays on closed-loop systems are nontrivial, and surprinsing, sometimes. The analysis of these effects relied on the examination of the systems' characteristic equations, which are more complicated in the case of TDSs, since they are infinite-dimensional. This approach, however, was only possible because the systems analyzed were linear, which have simpler Laplace transforms. In the general case of nonlinear systems, transforms become intractable and the resort is not available anymore. Thus, the behavior of TDSs need to be analyzed using a more systematic and general approach.

4.2 LYAPUNOV-KRASOVSKII THEORY

The infinite-dimensional nature of TDSs automatically discard several of classical analysis methods such as root locus [4, 5]. Other classical tools, e.g., Nyquist criterion, need to be adapted, and still, might only be available to linear systems.

Lyapunov's *direct method* (also called the second method of Lyapunov) is an efficient approach to analyze stability and performance of feedback systems. Introduced by Aleksandr Lyapunov [48] in 1890, the direct method to analyze a dynamical system consists in finding an energy-like function whose dynamics are coupled with the system's by means of the differential equation describing the dynamical system, and proving that function decays, i.e., it dissipates the "energy". Roughly speaking, this implies the original system's states tend to an equilibrium point, which is said to be stable.

First, consider a dynamical systems without delays

$$\dot{\boldsymbol{x}}\left(t\right) = f\left(\boldsymbol{x}\left(t\right)\right), \tag{4.2}$$

where $f : U \to \mathbb{R}^n$ is a locally Lipschitz map from an open set U contained in $\mathbb{R}^n$ into $\mathbb{R}^n$, and suppose there exists $\bar{\boldsymbol{x}}$ in U, such that $f(\bar{\boldsymbol{x}})$ equals $\bar{\boldsymbol{x}}$, which under these circumstances is called an *equilibrium point*. Without loss of generality, $\bar{\boldsymbol{x}}$ is considered zero. Indeed, if $\bar{\boldsymbol{x}}$ is different from zero, a change of variables $\boldsymbol{y}(t) = \boldsymbol{x}(t) - \bar{\boldsymbol{x}}$ results in

$$\dot{\boldsymbol{y}}(t) = \dot{\boldsymbol{x}}(t) = f(\boldsymbol{x}(t)) = f(\boldsymbol{y}(t) + \bar{\boldsymbol{x}}).$$

Then, defining

$$g(\boldsymbol{y}(t)) := f(\boldsymbol{y}(t) + \bar{\boldsymbol{x}}),$$

the equilibrium of $\bar{x}$ can be analyzed via the zero equilibrium point of $g(\boldsymbol{y}(t))$.

Definition 4.2.1. Given positive real number ϵ, the equilibrium point $\bar{\boldsymbol{x}}(t_0) = 0$ of (4.2) is *stable* if there exist $\delta(t_0, \epsilon)$, also positive real number, such that

$$\|\boldsymbol{x}(t_0)\| < \delta(t_0, \epsilon) \Rightarrow \|\boldsymbol{x}(t)\| < \epsilon, \forall t \geq t_0.$$

If, for any ϵ, there exist $\delta(t_0)$ (not dependent on ϵ) and $T(\delta, \epsilon)$ such that

$$\|\boldsymbol{x}(t_0)\| < \delta \Rightarrow \|\boldsymbol{x}(t)\| < \epsilon, \forall t \geq T(\delta, \epsilon) + t_0,$$

then $\bar{\boldsymbol{x}}$ is *asymptotically stable*. If $\bar{\boldsymbol{x}}$ is not stable, it said to be *unstable*.

If δ do not depend on t_0, then $\bar{\boldsymbol{x}}$ is said to be globally stable (globally asymptotically stable).

The distinction between a stable and an asymptotic stable point $\bar{\boldsymbol{x}}$ is that the former implies system's trajectories are guaranteed to stay within a certain neighborhood of $\bar{\boldsymbol{x}}$, whereas the latter ensures trajectories actually converge to the origin. The Lyapunov Theorem provides sufficient conditions to prove the origin is stable or asymptotically stable. The conditions are based on the construction of an energy-like function which is always nonnegative, decreases with time, and is coupled with the system's dynamics via its differential equation. Nonnegative and nonpositive functions receive special names.

Definition 4.2.2. Consider a function $f : U \to \mathbb{R}$, where U is an open set in $\mathbb{R}^n$ which contains the origin. If

$$f(\mathbf{0}) = 0, \quad f(\boldsymbol{x}) > 0, \forall \boldsymbol{x} \in U \backslash \{\mathbf{0}\},$$

then f is said to be a *positive definite*. Otherwise, if

$$f(\mathbf{0}) = 0, \quad f(\boldsymbol{x}) < 0, \forall \boldsymbol{x} \in U \backslash \{\mathbf{0}\},$$

then f is called *negative definite*.

Theorem 4.2.3. *Lyapunov Theorem[29]*

Let $\bar{\boldsymbol{x}} = 0$ be an equilibrium point for (4.2)*, that belongs to U, which is contained in $\mathbb{R}^n$. Let $V : U \to \mathbb{R}^n$ be continuously differentiable positive definite function such that*

$$\dot{V}(\boldsymbol{x}(t)) = \frac{\partial V}{\partial \boldsymbol{x}} f(\boldsymbol{x}) \leq 0, \boldsymbol{x}(t) \in U.$$

Then, the origin is a stable equilibrium point. If $\dot{V}(\boldsymbol{x}(t))$ is negative definite, then the origin is asymptotically stable.

Lyapunov's method is a standard and powerful approach to study stability of feedback systems. It is not, however, directly applicable to TDSs, for it is not adapted to the infinite-dimensional nature of solutions time-delays imply. The energy functions are dependent on current states (i.e., $\boldsymbol{x}(t)$) only, instead of regarding states throughout the entire delay window $[-d, 0]$, which makes the criterion inconclusive when delays are present. For example, consider

$$\dot{x}(t) = ax(t) + bx(t-d), d > 0, t \geq 0, \tag{4.3}$$

with $x(t)$ in $\mathbb{R}$. A natural choice as Lyapunov function V for linear systems, such as (4.3), is x^2. Then, the time derivative along the solutions of (4.3) gives

$$\dot{V}(x(t)) = 2x(t)\dot{x}(t) = 2x(t)[ax(t) + bx(t-d)] = 2ax(t)^2 + 2bx(t)x(t-d).$$

If b equals zero, then a negative suffices to prove (4.3) is asymptotically stable using Lyapunov's Theorem. Nevertheless, when b differs from zero, even if a is negative, not much can be said about the sign of $2bx(t)x(t-d)$, regardless of the sign of b. The system is not stable (or unstable). Thus, the method needs to be modified to prove anything about TDS.

This new requirement implies the concepts of stability, which are not suited to TDS, should also be adapted. Similarly to the nondelayed case, trivial solutions (i.e., equilibrium points at the origin) are the focus of stability investigations. Again, this represents no loss of generality, since stability of nontrivial solutions $y(t)$ can still be analyzed by changing variables

$$z(t) = x(t) - y(t),$$

and applying the subsection's methods to

$$\dot{z}(t) = f(t, z_t + y_t) - f(t, y_t),$$

with trivial solution $z(t)$ equal to zero.

Consider the general retarded differential equation

$$\dot{\boldsymbol{x}}(t) = f(t, \boldsymbol{x}_t), t \geq t_0, \tag{4.4}$$

where $f : \mathbb{R} \times \boldsymbol{C}[-d, 0] \to \mathbb{R}^n$ is continuous in both arguments, and $f(t, \mathbf{0})$ equals zero, which guarantees (4.4) admits a trivial solution.

Definition 4.2.4. The trivial solution of TDS (4.4) is said to be stable if for any $\epsilon > 0$ and $t_0 \geq 0$ there exists a positive $\delta(\epsilon, t_0)$ such that for every initial function $\varphi \in \boldsymbol{C}([-\nu, -\tau], \mathbb{R}^n)$, if $\|\varphi\|_{\boldsymbol{C}}$ less than $\delta(\epsilon, t_0)$ implies

$$\|\boldsymbol{x}(t)\| < \epsilon, t \geq t_0.$$

Definition 4.2.5. The trivial solution of TDS (4.4) is said to be asymptotically stable if it is stable and there exists positive scalar $\delta(t_0)$, $t_0 \geq 0$, such that for any positive scalar η there exists $T(\delta(t_0), \eta)$ such that $\|\boldsymbol{x}_{t_0}\|_{\boldsymbol{C}}$ less than $\delta(t_0)$ implies

$$\|\boldsymbol{x}(t)\| < \eta, t \geq t_0 + T(\delta_a, \eta).$$

Remark 4.2.6. If δ in Definitions 4.2.4 and 4.2.5 is independent of t_0, i.e., $\delta = \delta(\epsilon)$, then the trivial solution is uniformly stable and uniformly asymptotically stable (in t_0), respectively.

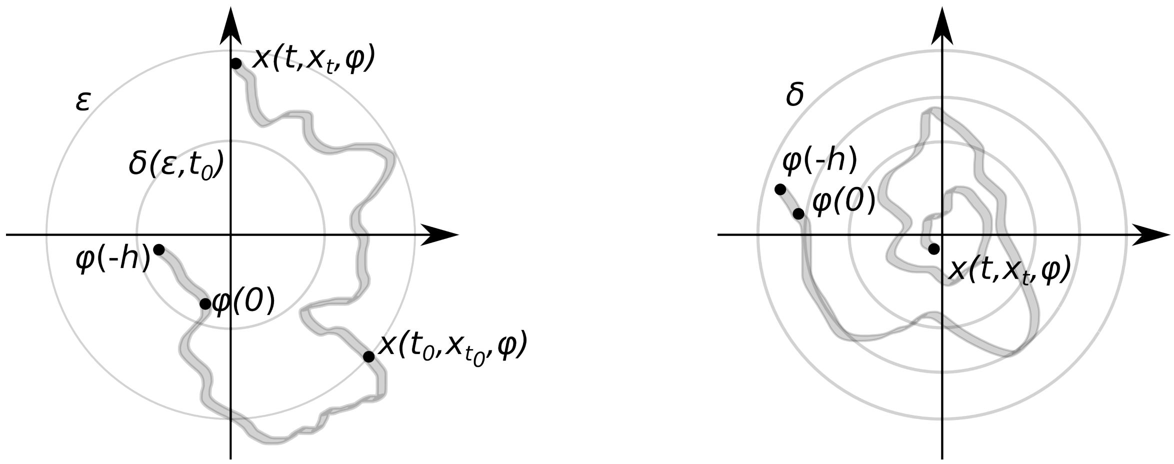

(a) Stable origin: solutions remain bounded.

(b) Asymptotically stable origin: solutions converge to the origin.

Figure 4.1: Stability Notions.

Definition 4.2.7. *The system is stable (asymptotically stable) if the trivial solution is stable (asymptotically stable).*

Similarly to nondelayed dynamical systems, asymptotic stability guarantees that for initial conditions functions sufficiently close to the origin, the solution of general RFDE (4.4) converges to the trivial solution, as illustrated in Figure 4.1b. On the other hand, stability only ensures solutions remain bounded with time, as in Figure 4.1a, not necessarily decreasing in norm.

Lyapunov's Theorem has two main TDS versions. *Krasovskii* method, like Lyapunov's, consists in finding a positive definite function V, with negative definite derivative $\dot{V}$ along the trajectories of the system being analyzed. The function, however, stems not from $x(t)$, but from the proper TDS state x_t. Thus, finding Lyapunov-Krasovskii Functionals (LKF) is a smooth transition from someone used to applying Lyapunov's method. On the other hand, *Razumikhin* method [3] is based on finding positive definite functions V of $x(t)$ with negative definite derivatives $\dot{V}$, but also guaranteeing that $V(x(t))$ upper bounds $V(x(t+\theta))$ for the whole delay interval $[-d, 0]$.

Since Krasovskii's method is more natural for considering delay information, and generally leads to less conservative stability and performance conditions, the proofs throughout the dissertation will be mostly based on LKF functionals.

Theorem 4.2.8. *Lyapunov-Krasovskii Theorem [2, 3]*

Suppose $f : \mathbb{R} \times \boldsymbol{C}[-\nu, -\tau] \to \mathbb{R}^n$ *maps* $\mathbb{R}\times$*(bounded sets in* $\boldsymbol{C}[-\nu, -\tau]$*) into bounded sets of* $\mathbb{R}^n$ *and that* $u, v, w : \mathbb{R}_{\geq 0} \to \mathbb{R}_{\geq 0}$ *are continuous nondecreasing functions,* u *and* v *positive definite. The trivial solution of general RFDE* (4.4) *is uniformly stable if there exists a continuously differentiable functional* $V : \mathbb{R} \times \boldsymbol{C}[-\nu, -\tau] \to \mathbb{R}_{\geq 0}$*, positive definite*

$$u(\|\varphi(0)\|) \leq V(t, \varphi) \leq v(\|\varphi\|_{\boldsymbol{C}}),$$

such that its derivative along (4.4) *is non-positive, that is*

$$\dot{V}(t, \varphi) = \frac{\partial}{\partial x} V(t, \varphi) f(t, x_t) \leq -w(\|\varphi(0)\|).$$

If w is positive definite, then the trivial solution is uniformly asymptotically stable.

In addition, if $\lim_{s\to\infty} u(s) = \infty$, then the trivial solution is globally uniformly asymptotically stable.

4.3 LINEAR MATRIX INEQUALITIES

Lyapunov's and Lyapunov-like methods, such as Krasovskii's, are based on building positive and negative functionals. This means that verifying Lyapunov-based stability and performance conditions always comes down to checking inequalities. For example, consider linear dynamical system

$$\dot{\boldsymbol{x}}(t) = A\boldsymbol{x}(t), t \geq 0, \tag{4.5}$$

with $\boldsymbol{x}(t)$ in $\mathbb{R}^n$. Assume Lyapunov functional candidate $x(t)^T Px(t)$, P in $\mathbb{R}^{n\times n}$. If V is positive definite and

$$\begin{aligned}\dot{V}(\boldsymbol{x}(t)) &= \dot{\boldsymbol{x}}(t)^T P\boldsymbol{x}(t) + \boldsymbol{x}(t)^T P\dot{\boldsymbol{x}}(t)\\ &= \boldsymbol{x}(t)^T A^T P\boldsymbol{x}(t) + \boldsymbol{x}(t)^T AP\boldsymbol{x}(t)\\ &= \boldsymbol{x}(t)^T \left(A^T P + PA\right)\boldsymbol{x}(t) < 0,\end{aligned} \tag{4.6}$$

holds, then (4.5) is asymptotically stable. Similarly to inequality (4.6), which is the notorious Lyapunov inequality [48], many Lyapunov functionals are built based on matrices and result in conditions involving matrices. In this sense, analogously to functions, positive and negative matrices can also be defined.

Definition 4.3.1. Let P be a real symmetric matrix in $\mathbb{S}^n$. Then, if

$$\boldsymbol{x}^T P\boldsymbol{x} > 0, \forall \boldsymbol{x} \in \mathbb{R}^n \backslash \{\boldsymbol{0}\},$$

holds, P is said to be a *positive definite matrix*. Otherwise, if

$$\boldsymbol{x}^T P\boldsymbol{x} < 0, \forall \boldsymbol{x} \in \mathbb{R}^n \backslash \{\boldsymbol{0}\},$$

holds, then P is said to be a *negative definite matrix*.

From Definition 4.3.1, it follows that if P is positive definite, then so is V, and (4.6) is satisfied if $A^T P + PA$ is negative definite, proving (4.5) is asymptotically stable.

Likewise, the stability and performance of many other control systems can be stated in terms of the "sign" of matrices. Indeed, the so-called *Linear Matrix Inequalities* (LMIs) are pervasive in control theory, especially due to desirable computational properties [10]. This can be traced back to the 1980s, with the realization LMIs can be cast as convex opmization problems [49], which ignited the development of powerful solving methods, called interior point algorithms [10]. These methods, which were pioneered by authors such as Nesterov and Nemirovskii [50], are available in many programming packages such as *SeDuMi* [51] and *SPDT3* [52]. Combined with a programming interface, as, for instance, YALMIP [53], this makes the whole process of programming and verifying LMIs extremely fast.

LMIs have further advantageous properties from the control standpoint. Consider general-form LMI

$$F(\boldsymbol{x}) = F_0 + \Sigma_{i=1}^{n} \boldsymbol{x}_i F_i \geq 0, \tag{4.7}$$

where F_i are given matrices in $\mathbb{R}^{n\times n}$ and $\boldsymbol{x}_i$ are vectors in $\mathbb{R}^n$ (or matrices in $\mathbb{R}^{n\times n}$) that represent the decision variables of the problem. The set defined by $\{\boldsymbol{x} \in \mathbb{R}^n | F(\boldsymbol{x}) \geq 0\}$ is a convex set that defines a convex restriction in $\boldsymbol{x}$. Thus, multiple LMIs can be stacked to form a single LMI that fulfills several conditions, i.e., LMIs can be used to cast multiobjective control problems. In addition, multiobjective conditions can also be used as constraints in minimization problems of the form $\min\left\{\boldsymbol{c}^T\boldsymbol{x}\right\}$ subjected to $F(\boldsymbol{x}) \geq 0$, as in (4.7). This allows the design of controllers that ensure stability, but also satisfy some performance criterion.

4.4 TDS ANALYSIS TECHNIQUES

Lyapunov-Krasovskii Theorem provides sufficient conditions to analyze stability and performance of a TDS. It does not, however, tell how to. Several examples have been given, that show the exact value of the delay can have enourmous impact on a TDS's behavior, and shows they carry essential information about the feedback system. In general, the more an LKF functional exploits delay information, the less conservative the suficient conditions are. For this reason, delays can and should be used to analyze TDSs, and the few following techniques are efficient ways to do that. For that, consider a general TDS (4.4) with continuous time-varying delay

$$\begin{aligned} d : \mathbb{R}_{\geq 0} &\rightarrow [\tau, \nu] \\ t &\mapsto d(t) \end{aligned} \tag{4.8}$$

4.4.1 Piecewise Analysis

Although the time-delay function takes values in the whole interval $[\tau, \nu]$, it cannot take all its values at once. This suggests only parts of the interval are actually valid at each instant of time. Hence, considering LKF candidates "specialized" in each of the subintervals, less conservative analysis is possible. This "divide and conquer" approach is called *Piecewise Analysis Method* (PAM) [54, 55, 56, 36] and consists in segmenting the total delay interval into an arbitrary number of disjoint subintervals which cover $[\tau, \nu]$. For the sake of simplicity, consider two subintervals of the same length

$$[\tau, \nu] = [\tau, \mu] \cup (\mu, \nu],$$

where

$$\mu = \frac{\tau + \nu}{2} \tag{4.9}$$

represents the mid-point of the total interval, as shown in Figure 4.2.

Given these two subintervals, let $\chi : [\tau, \nu] \rightarrow \{0, 1\}$ be defined as

$$\chi(s) : \begin{cases} 0, & s \in [\tau, \mu] \\ 1, & s \in (\mu, \nu] \end{cases}, \tag{4.10}$$

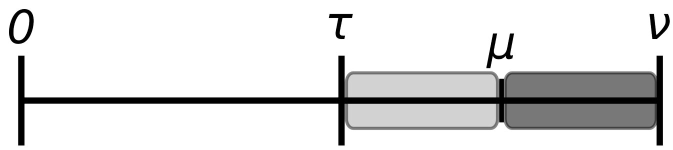

Figure 4.2: Piecewise analysis with two subintervals.

which is known as the *indicator function*. This allows an LKF candidate containing explicit delay information to be rewritten considering χ and the corresponding delay interval. Hence, instead of a monolithic V which guarantees stability for the whole delay interval, the LKF candidate might be built as a sum of different terms that take care of a determined delay subinterval. These extra degrees-of-freedom result in a less conservative analysis.

4.4.2 Delay Fractioning Analysis

The so-called *Delay Fractioning Analysis* (DFA) [37, 57] is conceptually similar to piecewise analysis, but, rather than dividing the interval in that the delay function can actually take values, the interval $[0, \tau]$ is subdivided into smaller ones, resulting in LKF terms dedicated to each subinterval. Once more, the extra degrees of freedom grant less conservative results. The technique is particularly interesting in the case $\tau \to \nu$, since the effectiveness of piecewise analysis is compromised because of the nearly constant delay, which "shrinks" the smaller subintervals, and make the specialist conditions more similar. Specifically, this can be done by adding terms to V containing auxiliary states

$$\boldsymbol{x}\left(t - k\frac{\tau}{n}\right), 0 \leq k \leq n,$$

where k and n are integers, and the latter represents the amount of subintervals in that $[0, \tau]$ is subdivided. For example, Figure 4.3 shows the case where n equals two, and the grey boxes represent the subintervals considered.

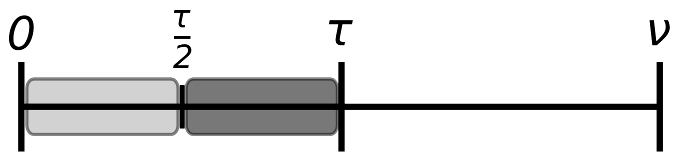

Figure 4.3: Delay-fractioning with two subintervals, $n = 2$.

4.4.3 Convex Analysis

In agreement with the previous two techniques, convex analysis also seeks to reduce the constraints over stability conditions by specializing in particular delay cases. Nevertheless, the strategy differs from the others in that it focus on the compactness of delay interval, instead of the interval's values.

Consider the function

$$\begin{aligned} \mathbb{D} : [\tau, \nu] &\to [0, 1] \\ d(t) &\mapsto \frac{d(t) - \tau}{\nu - \tau} \end{aligned}$$

The delay function d (4.8) is, by definition, continuous with compact interval domain $[\tau, \nu]$. Thus, new function $\mathbb{D}$ is continuous, and defined on a compact interval. Consequently, it reaches a maximum and a minimum value [58]. In particular, if $\mathbb{D}$ satisfies a certain property, called convexity [10], then $\mathbb{D}$ reaches its extrema at the limits of the interval[1] $[\tau, \nu]$.

Definition. Let X be a convex set contained in a vector space and f a real-valued function of X, $f : X \rightarrow \mathbb{R}$. If, for any $\boldsymbol{x}_1, \boldsymbol{x}_2$ in X and $t \in [0, 1]$

$$f\left(t\boldsymbol{x}_1 + (1-t)\,\boldsymbol{x}_2\right) \leq tf\left(\boldsymbol{x}_1\right) + (1-t)\,f\left(\boldsymbol{x}_2\right),$$

then f is called *convex function*. If the inequality is strict, f is *strictly convex*.

By inspection, it can be verified $\mathbb{D}$ is convex with respect to $d\,(t)$. Hence, if the derivative of an LKF can be bounded by a function of $\mathbb{D}$, it will be convex with respect to $d\,(t)$. Therefore, this convex function that bounds $\dot{V}$ also reaches its maximum at the extrema of the delay interval, and if negativity is verified at both of the interval limits, then $\dot{V}$ is negative definite. This approach is called *Convex Analysis* (CA) [59, 34]. In contrast with the two previous techniques, convex analysis exploits the exact value of $d\,(t)$. The goal is to obtain stability conditions that are convex with respect to $d\,(t)$, and verify feasibility only at the extrema of delay function. This also gives more freedom to the LMI variables, since they need to satisfy only two inequalities per convex set. The technique is particularly effective when combined with tools such as Jensen's Inequality (II.0.3), which avoids replacing $d\,(t)$ for its worst case value, reducing analysis conservatism [36].

[1] This follows trivially from the definition of $d\,(t)$: since it belongs to the interval $[\tau, \nu]$, $\mathbb{D}$ reaches its maximum of one and minimum of zero at ν and τ, respectively.

5 ATTITUDE CONTROL WITH DELAYED MEASUREMENTS

Attitude control consists in steering a rigid body to a, possibly time-varying, desired orientation, according to some reference frame. Considering the attitude of the rigid body a dynamical system described by kinematics and dynamics equations (3.14) and (3.22), this translates to assessing the equilibrium of certain attitudes.

In the delay-free case, the attitude control problem has been developed for several decades [19], and is still a prolific research topic [15, 60, 8, 61, 62, 45, 22, 63, 64, 65, 66]. This can be partially explained by the extensive range of applications that consist in attitude control problems, such as rigid aircraft and spacecraft systems [60, 61, 67], multiagent coordination [60, 61, 68], among others [69]. In the delay-free case, it is well-established that Proportional-Derivative (PD) [19, 15], and even velocity-free controllers [8, 23] are enough to stabilize the system. When feedback delays are present, however, this does not hold true. The problem is particularly challenging because of nonlinearities introduced by kinematics and dynamics. For this reason, many of the techniques used to study linear time-delay systems [13, 2, 3] are not suited to or not directly applicable to the attitude control problem subjected to feedback delays. Among the scarce results, [8] first proposed a velocity-free solution to the particular case where time-delays are constant and precisely known. Assuming similar delay settings, [15] tackled the problem using modified Rodrigues parameters (MRP). The authors of [21] extended this to the case with large unknown constant delays, but results are dependent on attitude initial conditions. In [22], the problem was solved using singularity-free quaternion representation, and then expanded to the velocity-free case in [23].

5.1 KINEMATIC ATTITUDE CONTROL

In some rigid bodies, low-level controllers are responsible for controlling input torques, which might not available to the attitude controller (e.g., robotic arms [43, 69]). If this low-level controller is fast enough, rigid body dynamics might be considered transparent, and angular velocities considered control inputs. This is the *kinematic attitude control* problem, which serves as a good starting point to the more general problem where rigid body dynamics is taken into account.

5.1.1 Kinematic Stabilization

Kinematic stabilization is the first step taken in this dissertation towards dynamic attitude control. Rigid body kinematics is considered subjected to time-delays affecting attitude measurements, or actuation. More precisely, (3.14) is slightly modified to become

$$\dot{\boldsymbol{q}}(t) = \begin{bmatrix} \dot{\eta}(t) \\ \dot{\boldsymbol{\zeta}}(t) \end{bmatrix} = \frac{1}{2} \begin{bmatrix} -\boldsymbol{\zeta}(t)^T \\ \eta(t)\mathbf{I} + [\boldsymbol{\zeta}(t)]_\times \end{bmatrix} \boldsymbol{\omega}(t - d(t)), \tag{5.1}$$

where $d : \mathbb{R}_{\geq 0} \to \mathbb{R}_{\geq 0}$ represents the time-varying delay, and it is deemed bounded by known nonnegative real numbers τ, ν such that

$$0 \leq \tau \leq d(t) \leq \nu, \forall t \geq 0. \tag{5.2}$$

Hereafter, time dependency will be omitted whenever possible in order to simplify notation. From unit-norm constraint quaternion definition (3.8) and from (3.3),

$$|\eta(t)| \leq 1, \|\boldsymbol{\zeta}(t)\| \leq 1, \forall t \geq 0. \tag{5.3}$$

The system's input is driven by a standard proportional controller,

$$\omega(t) = -\kappa\boldsymbol{\zeta}(t) \tag{5.4}$$

with κ a positive real number, which will be shown to be enough to stabilize (5.1).

Proposition 5.1.1. *Let $P \in \mathbb{S}^n$ be a positive definite matrix. Then, for all $\boldsymbol{x} \in \mathbb{R}^n$,*

$$0 < \lambda_{\min}(P)\boldsymbol{x}^T\boldsymbol{x} \leq \boldsymbol{x}^T P\boldsymbol{x} \leq \lambda_{\max}(P)\boldsymbol{x}^T\boldsymbol{x}$$

holds, where $\lambda_{\max}(P)$ and $\lambda_{\min}(P)$ represent the largest and smallest eigenvalues of P.

Proof. Since P is symmetric, it admits diagonal decomposition $Q^T DQ$, with Q orthogonal and D diagonal matrix with $P's$ eigenvalues. Let $\lambda_{\min}(P), \ldots \lambda_i, \ldots, \lambda_{\max}(P)$ be the ordered n eigenvalues of P, which are all real since P is symmetric. Assuming Q is given by $\begin{bmatrix} \boldsymbol{q}_1^T & \cdots & \boldsymbol{q}_n^T \end{bmatrix}^T$, it follows that

$$\boldsymbol{x}^T P\boldsymbol{x} = \boldsymbol{x}^T Q^T DQ\boldsymbol{x} = \Sigma_{i=1}^n \boldsymbol{x}^T\boldsymbol{q}_i^T\lambda_i\boldsymbol{q}_i\boldsymbol{x} \leq \Sigma_{i=1}^n \boldsymbol{x}^T\boldsymbol{q}_i^T\lambda_{\max}(P)\boldsymbol{q}_i\boldsymbol{x} = \lambda_{\max}(P)\boldsymbol{x}^T\boldsymbol{x}.$$

Likewise, since P is positive definite, $\lambda_{\min}(P)$ is positive, and it follows that

$$0 < \lambda_{\min}(P)\boldsymbol{x}^T\boldsymbol{x} = \lambda_{\min}(P)\Sigma_{i=1}^n \boldsymbol{x}^T\boldsymbol{q}_i\boldsymbol{q}_i^T\boldsymbol{x} \leq \Sigma_{i=1}^n \boldsymbol{x}^T\boldsymbol{q}_i\lambda_i\boldsymbol{q}_i^T\boldsymbol{x} = \boldsymbol{x}^T P\boldsymbol{x}.$$

□

Proposition 5.1.2. *Let P be a positive definite matrix in $\mathbb{S}^n$, $\boldsymbol{y}$ a vector in $\mathbb{R}^n$ and ρ a positive real number. Suppose $\boldsymbol{x}$ is a vector in $\mathbb{R}^n$ such that*

$$\boldsymbol{x}^T\boldsymbol{x} \leq \rho\boldsymbol{y}^T\boldsymbol{y}.$$

If ρ satisfies

$$\rho \leq \frac{\lambda_{\min}(P)}{\lambda_{\max}(P)},$$

where $\lambda_{\max}(P)$ and $\lambda_{\min}(P)$ denote the largest and smallest eigenvalues of P, respectively, then

$$\boldsymbol{x}^T P\boldsymbol{x} \leq \boldsymbol{y}^T P\boldsymbol{y}.$$

Proof. Let $\lambda_{\min}(P) \leq \ldots \leq \lambda_{\max}(P)$ be the ordered n eigenvalues of P. Note that $\lambda_{\min}(P)$ is positive because P is positive definite. Assuming

$$\rho \leq \tfrac{\lambda_{\min}(P)}{\lambda_{\max}(P)} \quad \text{and} \quad \boldsymbol{x}^T\boldsymbol{x} \leq \rho \boldsymbol{y}^T\boldsymbol{y},$$

hold, then

$$\rho \boldsymbol{y}^T\boldsymbol{y} \leq \frac{\lambda_{\min}(P)}{\lambda_{\max}(P)}\boldsymbol{y}^T\boldsymbol{y} \Rightarrow \boldsymbol{x}^T\boldsymbol{x} \leq \frac{\lambda_{\min}(P)}{\lambda_{\max}(P)}\boldsymbol{y}^T\boldsymbol{y} \Rightarrow \lambda_{\max}(P)\,\boldsymbol{x}^T\boldsymbol{x} \leq \lambda_{\min}(P)\,\boldsymbol{y}^T\boldsymbol{y}.$$

Therefore, from Proposition 5.1.1, it follows that

$$\boldsymbol{x}^T P\boldsymbol{x} \leq \lambda_{\max}(P)\,\boldsymbol{x}^T\boldsymbol{x} \leq \lambda_{\min}(P)\,\boldsymbol{y}^T\boldsymbol{y} \leq \boldsymbol{y}^T P\boldsymbol{y}.$$

□

Stability of closed-loop system (5.1)-(5.4) will be proven using Lyapunov-Krasovskii arguments, considering LKF candidate

$$V(t) = \sum_{i=1}^{4} V_i(t), \tag{5.5}$$

where

$$\begin{aligned}
V_1(t) &= 2\left[\boldsymbol{\zeta}(t)^T\boldsymbol{\zeta}(t) + (1-\eta(t))^2\right],\\
V_2(t) &= \int_{t-\frac{\tau}{2}}^{t}\begin{bmatrix}\boldsymbol{\zeta}(s)\\ \boldsymbol{\zeta}\left(s-\frac{\tau}{2}\right)\end{bmatrix}^T\begin{bmatrix}Q_{11} & Q_{12}\\ * & Q_{22}\end{bmatrix}\begin{bmatrix}\boldsymbol{\zeta}(s)\\ \boldsymbol{\zeta}\left(s-\frac{\tau}{2}\right)\end{bmatrix}ds\\
&\quad + \int_{t-\mu}^{t-\tau}\begin{bmatrix}\boldsymbol{\zeta}(s)\\ \boldsymbol{\zeta}(s-\mu+\tau)\end{bmatrix}^T\begin{bmatrix}R_{11} & R_{12}\\ * & R_{22}\end{bmatrix}\begin{bmatrix}\boldsymbol{\zeta}(s)\\ \boldsymbol{\zeta}(s-\mu+\tau)\end{bmatrix}ds,\\
V_3(t) &= \int_{-\tau}^{0}\int_{t+\beta}^{t}\tau\dot{\boldsymbol{\zeta}}(s)^T U\boldsymbol{\zeta}(s)\,ds\,d\beta,\\
V_4(t) &= (\mu-\tau)\int_{-\mu}^{-\tau}\int_{t+\beta}^{t}\dot{\boldsymbol{\zeta}}(s)^T S\dot{\boldsymbol{\zeta}}(s)\,ds\,d\beta + (\nu-\mu)\int_{-\nu}^{-\mu}\int_{t+\beta}^{t}\dot{\boldsymbol{\zeta}}(s)^T T\dot{\boldsymbol{\zeta}}(s)\,ds\,d\beta.
\end{aligned}$$

and μ is the mid-interval delay bound given by (4.9). The LKF components of (5.5) are standard in TDS literature, and except for V_1, each of them introduces one of the TDS analysis techniques presented in Section 4.4. V_2 exploits both PAM (4.4.1) and FDA (4.4.2), while V_3 employs PAM (4.4.1) through Jensen's Inequality (Lemma II.0.3). V_4 also exploits PAM, but uses Jensen's Inequality to introduce CA (4.4.3) instead.

Since Lyapunov-Krasovskii theory will be used, V (5.5) must be positive definite. Because V is composed of quadratic terms only, if

$$Q = \begin{bmatrix}Q_{11} & Q_{12}\\ * & Q_{22}\end{bmatrix} > 0, \quad R = \begin{bmatrix}R_{11} & R_{12}\\ * & R_{22}\end{bmatrix} > 0, \quad U > 0, \quad S > 0, \quad T > 0, \tag{5.6}$$

all hold, V is positive definite.

Theorem 5.1.3. *Given nonnegative real numbers τ and ν satisfying* (5.2)*, and real positive LMI parameter α, the closed-loop system* (5.1)-(5.4) *subjected to measurement delay* (5.2) *is asymptotically* *stable if there exist proportional positive gain κ, and symmetric matrices Q, R and diagonal matrices U, S and T satisfying* (5.6)*, and free-weighting matrices $\mathscr{F}_l$ such that*

$$\begin{gathered}\overline{\Omega} + \Omega_l|_{\overline{\mathbb{D}}_l} + \mathscr{F}_l \mathscr{G}_l + \mathscr{G}_l^T \mathscr{F}_l^T < 0; \\ 0 < \kappa \le \sqrt{\alpha};\end{gathered} \tag{5.7}$$

$$\alpha \lambda_{\max}(Z) \le \lambda_{\min}(Z), Z \in \{U, S, T\}; \tag{5.8}$$

hold for all $\overline{\mathbb{D}}_l \in \{0,1\}$ and $l \in \{1,2\}$ where

$$\overline{\Omega} = \begin{bmatrix} \Omega_{11} & Q_{12} & U & \mathbf{0} & \mathbf{0} & -\kappa \mathbf{I} & \mathbf{0} \\ * & \Omega_{22} & -Q_{12} & \mathbf{0} & \mathbf{0} & \mathbf{0} & \mathbf{0} \\ * & * & \Omega_{3,3} & R_{12} & \mathbf{0} & \mathbf{0} & \mathbf{0} \\ * & * & * & \Omega_{44} & -R_{12} & \mathbf{0} & \mathbf{0} \\ * & * & * & * & -R_{22} & \mathbf{0} & \mathbf{0} \\ * & * & * & * & * & \Omega_{66} & \mathbf{0} \\ * & * & * & * & * & * & \mathbf{0} \end{bmatrix}, \tag{5.9}$$

with

$$\begin{aligned}
\Omega_{11} &= Q_{11} - U, & \Omega_{22} &= Q_{22} - Q_{11}, \\
\Omega_{33} &= R_{11} - Q_{22} - U, & \Omega_{44} &= R_{22} - R_{11} \\
\Omega_{66} &= (\mu - \tau)^2 S + (\nu - \tau)^2 T + \tau^2 U, & & \\
\Omega_1|_{\overline{\mathbb{D}}_1} &= -(\mathbb{I}_4 - \mathbb{I}_5)^T T (\mathbb{I}_4 - \mathbb{I}_5) - \mathbb{I}_7^T S \mathbb{I}_7, & \Omega_2|_{\overline{\mathbb{D}}_2} &= -(\mathbb{I}_3 - \mathbb{I}_4)^T S (\mathbb{I}_3 - \mathbb{I}_4) - \mathbb{I}_7^T T \mathbb{I}_7, \quad (5.10) \\
\mathscr{G}_1 &= \begin{bmatrix} \overline{\mathscr{G}}_1 & \mathscr{G}_{1\overline{\mathbb{D}}_1} \end{bmatrix}, & \mathscr{G}_2 &= \begin{bmatrix} \overline{\mathscr{G}}_2 & \mathscr{G}_{2\overline{\mathbb{D}}_2} \end{bmatrix}, \quad (5.11) \\
\overline{\mathscr{G}}_1 &= \begin{bmatrix} 0 & 0 & -I & 0 & 0 & I \\ 0 & 0 & 0 & I & 0 & -I \end{bmatrix}, & \overline{\mathscr{G}}_2 &= \begin{bmatrix} \mathbf{0} & \mathbf{0} & \mathbf{0} & -\mathbf{I} & \mathbf{0} & \mathbf{I} \\ \mathbf{0} & \mathbf{0} & \mathbf{0} & \mathbf{0} & \mathbf{I} & -\mathbf{I} \end{bmatrix} \\
\mathscr{G}_{1\overline{\mathbb{D}}_1} &= \begin{bmatrix} \overline{\mathbb{D}}_1 \mathbf{I} \\ \left(1 - \overline{\mathbb{D}}_1\right) \mathbf{I} \end{bmatrix}, & \mathscr{G}_{2\overline{\mathbb{D}}_2} &= \begin{bmatrix} \overline{\mathbb{D}}_2 \mathbf{I} \\ \left(1 - \overline{\mathbb{D}}_2\right) \mathbf{I} \end{bmatrix},
\end{aligned}$$

where $\mathbb{I}_k \in \mathbb{R}^{3\times 21}, k \in \{1, \ldots, 7\}$ are block entry matrices with seven elements, e.g., $\mathbb{I}_7 = \begin{bmatrix} \mathbf{0}\ \mathbf{0}\ \mathbf{0}\ \mathbf{0}\ \mathbf{0}\ \mathbf{0}\ \mathbf{I} \end{bmatrix}$.

Proof. Suppose LKF variables Q, R, U, S and T satisfy (5.6), which means V is positive definite. It remains to show its derivative, given by $\Sigma_{i=1}^4 \dot{V}_i$, is negative definite along trajectories of $\boldsymbol{q}$, where

$$\dot{V}_1 = 2\frac{d}{dt}\left[\boldsymbol{\zeta}^T \boldsymbol{\zeta} + (1-\eta)^2\right] = -4\dot{\eta} = -2\kappa \boldsymbol{\zeta}^T \boldsymbol{\zeta}(t - d(t)), \tag{5.12}$$

$$\begin{aligned}\dot{V}_2 = &\begin{bmatrix} \boldsymbol{\zeta} \\ \boldsymbol{\zeta}\left(t - \frac{\tau}{2}\right) \end{bmatrix}^T Q \begin{bmatrix} \boldsymbol{\zeta} \\ \boldsymbol{\zeta}\left(t - \frac{\tau}{2}\right) \end{bmatrix} - \begin{bmatrix} \boldsymbol{\zeta}\left(t - \frac{\tau}{2}\right) \\ \boldsymbol{\zeta}(t-\tau) \end{bmatrix}^T Q \begin{bmatrix} \boldsymbol{\zeta}\left(t - \frac{\tau}{2}\right) \\ \boldsymbol{\zeta}(t-\tau) \end{bmatrix} \\ &+ \begin{bmatrix} \boldsymbol{\zeta}(t-\tau) \\ \boldsymbol{\zeta}(t-\mu) \end{bmatrix}^T R \begin{bmatrix} \boldsymbol{\zeta}(t-\tau) \\ \boldsymbol{\zeta}(t-\mu) \end{bmatrix} - \begin{bmatrix} \boldsymbol{\zeta}(t-\mu) \\ \boldsymbol{\zeta}(t-\nu) \end{bmatrix}^T R \begin{bmatrix} \boldsymbol{\zeta}(t-\mu) \\ \boldsymbol{\zeta}(t-\nu) \end{bmatrix},\end{aligned} \tag{5.13}$$

$$\dot{V}_3 = \tau^2 \dot{\boldsymbol{\zeta}}^T U \dot{\boldsymbol{\zeta}} - \tau \int_{t-\tau}^{t} \dot{\boldsymbol{\zeta}}(s)^T U \dot{\boldsymbol{\zeta}}(s)\, ds, \tag{5.14}$$

$$\dot{V}_4 = \dot{V}_{4(0)} + \dot{V}_{4(I)}$$

$$\dot{V}_{4(0)} = (\mu-\tau)^2 \dot{\boldsymbol{\zeta}}^T S \dot{\boldsymbol{\zeta}} + (\nu-\mu)^2 \dot{\boldsymbol{\zeta}}^T T \dot{\boldsymbol{\zeta}}, \tag{5.15}$$

$$\dot{V}_{4(I)} = -(\mu-\tau)\int_{t-\mu}^{t-\tau} \dot{\boldsymbol{\zeta}}(s) S \dot{\boldsymbol{\zeta}}(s)\, ds - (\nu-\mu)\int_{t-\nu}^{t-\mu} \dot{\boldsymbol{\zeta}}(s)^T T \dot{\boldsymbol{\zeta}}(s)\, ds. \tag{5.16}$$

Rather than proving $\dot{V}$ is negative definite for the whole possible delay interval $[\tau, \nu]$, the analysis is broken down in two cases by considering mutually exclusive delay subintervals. Namely, using equal-measure subintervals $[\tau, \mu]$ and $(\mu, \nu]$, indicator function χ (4.10) is invoked to define two delay scenarios

$$\mathbb{S}_1 := \{d(t) \in \mathbb{R} | \chi(d(t)) = 1\}, \quad \mathbb{S}_2 := \{d(t) \in \mathbb{R} | \chi(d(t)) = 0\}, \tag{5.17}$$

such that

$$\dot{V}_4 = \dot{V}_{4(0)} + \dot{V}_{4(\mathbb{S}_1)} + \dot{V}_{4(\mathbb{S}_2)},$$

with

$$\dot{V}_{4(\mathbb{S}_1)}(t) := \chi(d(t))\dot{V}_{4(I)}(t), \quad \dot{V}_{4(\mathbb{S}_2)}(t) := (1-\chi(d(t)))\dot{V}_{4(I)}(t). \tag{5.18}$$

Since d cannot belong to $\mathbb{S}_1$ and $\mathbb{S}_2$ simultaneously, one, and only one of $\dot{V}_{4(\mathbb{S}_1)}$ or $\dot{V}_{4(\mathbb{S}_2)}$ will be different from zero at any given time. Thus, each scenario is addressed individually. For the former, since d belongs to interval $[\tau, \mu]$, $\chi(d(t))$ equals one, and $\dot{V}_{4(\mathbb{S}_1)}(t)$ is rewritten to introduce convex analysis (4.4.3)

$$\dot{V}_{4(\mathbb{S}_1)} = -\chi(d(t))\Bigg\{(\mu-\tau)\left[\int_{t-\mu}^{t-d(t)} \dot{\boldsymbol{\zeta}}(s)^T S\dot{\boldsymbol{\zeta}}(s)\, ds + \int_{t-d(t)}^{t-\tau} \dot{\boldsymbol{\zeta}}(s)^T S\dot{\boldsymbol{\zeta}}(s)\, ds\right]$$
$$+(\nu-\mu)\int_{t-\nu}^{t-\mu} \dot{\boldsymbol{\zeta}}(s)^T T\dot{\boldsymbol{\zeta}}(s)\, ds\Bigg\},$$

which is an inviting expression to Jensen's Inequality (Lemma II.0.3), checking $\dot{V}_4$ such that

$$\dot{V}_4 \leq (\mu-\tau)^2 \dot{\boldsymbol{\zeta}}^T S\dot{\boldsymbol{\zeta}} + (\nu-\mu)^2 \dot{\boldsymbol{\zeta}}^T T\dot{\boldsymbol{\zeta}} - \chi\Big\{\boldsymbol{\xi}_{11}{}^T(\mathbb{D}_1 S)\boldsymbol{\xi}_{11} + \boldsymbol{\xi}_{12}{}^T(1-\mathbb{D}_1)S\boldsymbol{\xi}_{12}$$
$$+[\boldsymbol{\zeta}(t-\mu)-\boldsymbol{\zeta}(t-\nu)]^T T[\boldsymbol{\zeta}(t-\mu)-\boldsymbol{\zeta}(t-\nu)]\Big\}, \tag{5.19}$$

with

$$\boldsymbol{\xi}_{11}(t) := \tfrac{\mu-\tau}{d(t)-\tau}\int_{t-d(t)}^{t-\tau}\dot{\boldsymbol{\zeta}}(s)\, ds, \quad \boldsymbol{\xi}_{12}(t) := \tfrac{\mu-\tau}{\mu-d(t)}\int_{t-\mu}^{t-d(t)}\dot{\boldsymbol{\zeta}}(s)\, ds. \tag{5.20}$$

Expression (5.19) is convex with respect to $d(t)$. Indeed, introducing

$$\mathbb{D}_1(d(t)) := \frac{d(t)-\tau}{\mu-\tau} \in [0,1] \tag{5.21}$$

shows that, and shows $\dot{V}_4$ is bounded by a convex functional with extrema at the edges of $\mathbb{D}_1$, namely 0 and 1.

If closed-loop system (5.1)-(5.4) was linear, the differential equation that governs its state changes could be substituted for $\dot{\boldsymbol{\zeta}}$, and analysis could be carried on. This is not the case, however, because of the nonlinearities introduced by rigid body kinematics. Since the goal is to obtain conditions that can be stated as LMIs, $\dot{\boldsymbol{\zeta}}$ must be taken care of. From quaternion unit-norm constraint (5.3), $[\cdot]_\times$ operator property $\left\|[\boldsymbol{\zeta}]_\times\right\| \leq \|\boldsymbol{\zeta}\|$ (I.6), and triangle inequality, it follows that

$$\left\|\dot{\boldsymbol{\zeta}}\right\| = \left\|\frac{1}{2}\left[\eta(-\kappa\boldsymbol{\zeta}(t-d(t))) + [\boldsymbol{\zeta}]_\times(-\kappa\boldsymbol{\zeta}(t-d(t)))\right]\right\|$$

$$\leq \frac{1}{2}\left[\left\|[\boldsymbol{\zeta}]_\times\left(\kappa\boldsymbol{\zeta}\left(t-d\left(t\right)\right)\right)\right\|+\left\|\eta\kappa\boldsymbol{\zeta}\left(t-d\left(t\right)\right)\right\|\right]$$
$$\leq \frac{1}{2}\left[\left\|\boldsymbol{\zeta}\right\|\left\|\kappa\boldsymbol{\zeta}\left(t-d\left(t\right)\right)\right\|+\left|\eta\right|\left\|\kappa\boldsymbol{\zeta}\left(t-d\left(t\right)\right)\right\|\right]$$
$$\leq \frac{1}{2}\left[\left\|\kappa\boldsymbol{\zeta}\left(t-d\left(t\right)\right)\right\|+\left\|\kappa\boldsymbol{\zeta}\left(t-d\left(t\right)\right)\right\|\right]$$
$$\leq \kappa\left\|\boldsymbol{\zeta}\left(t-d\left(t\right)\right)\right\|, \tag{5.22}$$

which implies

$$\dot{\boldsymbol{\zeta}}^T\dot{\boldsymbol{\zeta}} \leq \kappa^2\boldsymbol{\zeta}\left(t-d\left(t\right)\right)^T\boldsymbol{\zeta}\left(t-d\left(t\right)\right). \tag{5.23}$$

Now, suppose κ and U, S, T satisfy

$$0 < \kappa \leq \sqrt{\alpha},$$
$$\alpha\lambda_{\max}\left(Z\right) \leq \lambda_{\min}\left(Z\right), Z \in \left\{U, S, T\right\}.$$

This implies that

$$\kappa^2 \leq \min\left\{\frac{\lambda_{\min}\left(U\right)}{\lambda_{\max}\left(U\right)}, \frac{\lambda_{\min}\left(S\right)}{\lambda_{\max}\left(S\right)}, \frac{\lambda_{\min}\left(T\right)}{\lambda_{\max}\left(T\right)}\right\}.$$

Using Lemma 5.1.2, (5.23) bound yields

$$\dot{\boldsymbol{\zeta}}^T\dot{\boldsymbol{\zeta}} \leq \boldsymbol{\zeta}\left(t-d\left(t\right)\right)^T X\boldsymbol{\zeta}\left(t-d\left(t\right)\right), X \in \left\{U, S, T\right\}, \tag{5.24}$$

that combined with $\dot{V}_4$ bound (5.19), gives

$$\begin{aligned}\dot{V}_4 \leq{} & \left(\mu-\tau\right)^2\boldsymbol{\zeta}\left(t-d\left(t\right)\right)^T S\boldsymbol{\zeta}\left(t-d\left(t\right)\right)+\left(\nu-\mu\right)^2\boldsymbol{\zeta}\left(t-d\left(t\right)\right)^T T\boldsymbol{\zeta}\left(t-d\left(t\right)\right)\\ & -\chi\left\{\boldsymbol{\xi}_{11}{}^T\left(\mathbb{D}_1 S\right)\boldsymbol{\xi}_{11}+\boldsymbol{\xi}_{12}{}^T\left(1-\mathbb{D}_1\right)S\boldsymbol{\xi}_{12}\right.\\ & \left.+\left[\boldsymbol{\zeta}\left(t-\mu\right)-\boldsymbol{\zeta}\left(t-\nu\right)\right]^T T\left[\boldsymbol{\zeta}\left(t-\mu\right)-\boldsymbol{\zeta}\left(t-\nu\right)\right]\right\}.\end{aligned} \tag{5.25}$$

Similarly, $\left\|\dot{\boldsymbol{\zeta}}\right\|^2$ upper bound (5.24) and Jensen's Inequality check $\dot{V}_3$ (5.14), such that

$$\dot{V}_3 \leq \tau^2\boldsymbol{\zeta}\left(t-d\left(t\right)\right)^T U\boldsymbol{\zeta}\left(t-d\left(t\right)\right)-\left[\int_{t-\tau}^{t}\dot{\boldsymbol{\zeta}}\left(s\right)ds\right]^T U\left[\int_{t-\tau}^{t}\dot{\boldsymbol{\zeta}}\left(s\right)ds\right]. \tag{5.26}$$

Since $\dot{V}_4$ bound (5.25) is convex with respect to $d\left(t\right)$, it attains its maximum at $\mathbb{D}_1$ extrema. When this occurs, $\mathbb{D}_1$ and $1-\mathbb{D}_1$ are mutually exclusive, which means either $\boldsymbol{\xi}_{11}$ or $\boldsymbol{\xi}_{12}$ vanishes from $\dot{V}_4$ bound expression (5.25). Thus, the upper bounds (5.12), (5.13), (5.25) and (5.26) lead to LMIs that can be expressed as

$$\dot{V} \leq \boldsymbol{\vartheta}_{1l}^T\Omega\boldsymbol{\vartheta}_{1l},$$

where

$$\Omega = \overline{\Omega}+\Omega_{1|\overline{\mathbb{D}}_1},$$

with $\overline{\Omega}$ and $\Omega_{1|\overline{\mathbb{D}}_1}$ given by (5.9) and (5.10), respectively, and $\boldsymbol{\vartheta}_{1l}$ given by

$$\boldsymbol{\vartheta}_{1l}\left(t\right) := \left[\begin{array}{ccccccc}\boldsymbol{\zeta}\left(t\right)^T & \boldsymbol{\zeta}\left(t-\frac{\tau}{2}\right)^T & \boldsymbol{\zeta}\left(t-\tau\right)^T & \boldsymbol{\zeta}\left(t-\mu\right)^T & \boldsymbol{\zeta}\left(t-\nu\right)^T & \boldsymbol{\zeta}\left(t-d\left(t\right)\right)^T & \boldsymbol{\xi}_{1l}\left(t\right)^T\end{array}\right]^T,$$

where l belongs to $\{1, 2\}$, depending on which of $\boldsymbol{\xi}_{1l}$ is nonzero.

Let $\mathscr{F}_1$ be a free-weighting matrix, and $\mathscr{G}_1$ be defined as $\left[\overline{\mathscr{G}}_1 \; \hat{\mathscr{G}}_{1\mathbb{D}}\right]$, $\overline{\mathscr{G}}_1$ as in (5.11) and

$$\hat{\mathscr{G}}_{1\mathbb{D}} = \begin{bmatrix} \overline{\mathbb{D}}_1 \mathbf{I} \\ \left(1 - \overline{\mathbb{D}}_1\right) \mathbf{I} \end{bmatrix}, \tag{5.27}$$

with $\overline{\mathbb{D}}_1$ in $\{0, 1\}$. For $\overline{\mathbb{D}}_1$ equal to zero, that means $d(t)$ equals τ. Then,

$$\begin{aligned} \lim_{d(t)\to\tau} \mathscr{G}_1 \boldsymbol{\vartheta}_{1l} &= \lim_{d(t)\to\tau} \begin{bmatrix} -\boldsymbol{\zeta}(t-\tau) + \boldsymbol{\zeta}(t - d(t)) + \mathbf{0}\dot{\boldsymbol{\zeta}}(t - d(t)) \\ \boldsymbol{\zeta}(t-\mu) - \boldsymbol{\zeta}(t - d(t)) + \frac{\mu-\tau}{\mu - d(t)} \int_{t-\mu}^{t-d(t)} \dot{\boldsymbol{\zeta}}(s)\, ds \end{bmatrix} \\ &= \begin{bmatrix} -\boldsymbol{\zeta}(t-\tau) + \boldsymbol{\zeta}(t-\tau) + \mathbf{0}\dot{\boldsymbol{\zeta}}(t - d(t)) \\ \boldsymbol{\zeta}(t-\mu) - \boldsymbol{\zeta}(t-\tau) + (\boldsymbol{\zeta}(t-\tau) - \boldsymbol{\zeta}(t-\mu)) \end{bmatrix} \\ &= \begin{bmatrix} \mathbf{0} \\ \mathbf{0} \end{bmatrix}. \end{aligned}$$

Analogously, when $\overline{\mathbb{D}}_1$ equals one, $\mathscr{G}_1 \boldsymbol{\vartheta}_{1l}$ equals zero, i.e., $\mathscr{G}_1$ and $\boldsymbol{\vartheta}_{1l}$ are orthogonal. Thus, from Finsler's Lemma (Lemma II.0.1), Ω is negative definite if, and only if,

$$\tilde{\Omega} = \Omega + \mathscr{F}_1 \mathscr{G}_1 + \mathscr{G}_1^T \mathscr{F}_1^T < 0.$$

Since $\boldsymbol{\vartheta}_{1l}^T \tilde{\Omega} \boldsymbol{\vartheta}_{1l}$ remains convex with respect to $d(t)$, its extrema coincide with $\mathbb{D}_1$'s, i.e., $\boldsymbol{\vartheta}_{1l}^T \tilde{\Omega} \boldsymbol{\vartheta}_{1l}$ reaches its maximum when $\mathbb{D}_1$ equals zero or one. Thus, if $\tilde{\Omega}$ is negative definite when $\mathbb{D}_1$ equals one and zero, then so is Ω, and $\dot{V}$ is negative definite. Therefore, the closed-loop system is stable considering the first delay scenario. Similar analysis leads to the conclusion that $\dot{V}$ is also negative definite for the second delay scenario $\mathbb{S}_2$. Therefore, if the hypotheses of Theorem 5.1.3 are valid, $\dot{V}$ is negative definite regardless of delay characteristics (first or second interval), and (5.1) is asymptotically stable. □

Although the design of controller gain κ via the conditions from Theorem 5.1.3 requires a predetermined α, since this parameter is a scalar, several searching algorithms (e.g., binary search) can be used to find a feasible α.

5.1.2 H_∞ Kinematic Control

Although Subsection 5.1.1 provided sufficient stability conditions in the form of LMIs, the question remains whether the controllers are resilient to exogenous disturbances. This subsection addresses this issue.

The input angular velocity is assumed to be corrupted by an exogenous disturbance $\boldsymbol{r}_1$, such that

$$\dot{\boldsymbol{q}}(t) = \begin{bmatrix} \dot{\eta}(t) \\ \dot{\boldsymbol{\zeta}}(t) \end{bmatrix} = \frac{1}{2} \begin{bmatrix} -\boldsymbol{\zeta}(t)^T \\ \eta(t)\mathbf{I} + [\boldsymbol{\zeta}(t)]_\times \end{bmatrix} [\boldsymbol{\omega}(t - d(t)) + \boldsymbol{r}_1(t)], \tag{5.28}$$

and the proportional feedback controller structure (5.4) is maintained.

The exact notion of resilience to disturbance is still vague, though. The following definition formalizes the concept with an index that quantifies a controller's ability to reject disturbances.

Definition 5.1.4. For a positive real number γ, disturbance rejection is achieved with H_∞ norm bound γ if the following conditions are met

1. The closed-loop system is asymptotically stable with $\boldsymbol{r}_1 = 0$;
2. Assuming $\boldsymbol{r}_1$ and $\boldsymbol{\zeta}$ belong to $L_2\,[0, +\infty)$, disturbance is attenuated below γ under zero initial conditions, i.e., $\|\boldsymbol{\zeta}\|_2 \leq \gamma\,\|\boldsymbol{r}_1\|_2$.

Similarly to the previous subsection, stability and now, disturbance rejection, are proved using Lyapunov-Krasovskii arguments. Thus, let V be a modified LKF candidate such that

$$V\,(t) = \sum_{i=1}^{4} V_i\,(t)\,, \tag{5.29}$$

where

$$\begin{aligned}
V_1 &= 2\beta\left[\boldsymbol{\zeta}^T\boldsymbol{\zeta} + (1-\eta)^2\right],\\
V_2 &= \int_{t-\frac{\tau}{2}}^{t}\begin{bmatrix}\boldsymbol{\zeta}\,(s)\\ \boldsymbol{\zeta}\left(s-\frac{\tau}{2}\right)\end{bmatrix}^T\begin{bmatrix}Q_{11} & Q_{12}\\ * & Q_{22}\end{bmatrix}\begin{bmatrix}\boldsymbol{\zeta}\,(s)\\ \boldsymbol{\zeta}\left(s-\frac{\tau}{2}\right)\end{bmatrix}ds\\
&+\int_{t-\mu}^{t-\tau}\begin{bmatrix}\boldsymbol{\zeta}\,(s)\\ \boldsymbol{\zeta}\,(s-\mu+\tau)\end{bmatrix}^T\begin{bmatrix}R_{11} & R_{12}\\ * & R_{22}\end{bmatrix}\begin{bmatrix}\boldsymbol{\zeta}\,(s)\\ \boldsymbol{\zeta}\,(s-\mu+\tau)\end{bmatrix}ds,\\
V_3 &= \int_{-\tau}^{0}\int_{t+l}^{t}\dot{\boldsymbol{\zeta}}\,(s)^T\,\mathfrak{u}\dot{\boldsymbol{\zeta}}\,(s)\,dsdl,\\
V_4 &= (\mu-\tau)\int_{-\mu}^{-\tau}\int_{t+l}^{t}\dot{\boldsymbol{\zeta}}\,(s)^T\,\mathfrak{s}\dot{\boldsymbol{\zeta}}\,(s)\,dsdl + (\nu-\mu)\int_{-\nu}^{-\mu}\int_{t+l}^{t}\dot{\boldsymbol{\zeta}}\,(s)^T\,\mathfrak{t}\dot{\boldsymbol{\zeta}}\,(s)\,dsdl.
\end{aligned}$$

The replacement of U, S, T with real number counterparts $\mathfrak{u}, \mathfrak{s}, \mathfrak{t}$ is necessary, since $\left\|\dot{\boldsymbol{\zeta}}\right\|^2$ bound (5.22) can no longer be guaranteed because of $\boldsymbol{r}_1$. The introduction of a new variable β, will also be key to obtaining LMIs liable to controller design. Since V is composed of quadratic terms only, inequalities

$$Q = \begin{bmatrix}Q_{11} & Q_{12}\\ * & Q_{22}\end{bmatrix} > 0,\quad R = \begin{bmatrix}R_{11} & R_{12}\\ * & R_{22}\end{bmatrix} > 0,\quad \beta > 0,\quad \mathfrak{u} > 0,\quad \mathfrak{s} > 0,\quad \mathfrak{t} > 0, \tag{5.30}$$

are sufficient to ensure V is positive definite.

Theorem 5.1.5. *Let τ, ν be nonnegative real numbers checking time-delay d such that* (5.2) *holds. Then, closed-loop system* (5.28)-(5.4) *is asymptotically stable and achieves disturbance rejection with H_∞ norm bound γ if there exist real matrices Q, R and positive real numbers $\beta, \mathfrak{u}, \mathfrak{s}, \mathfrak{t}$ satisfying* (5.30)*, plus real number $\mathfrak{n}$, positive real numbers $\mathfrak{m}$, δ, α, and free-weighting matrices $\mathscr{F}_l$ such that*

$$\overline{\Omega} + \Omega_l|_{\overline{\mathbb{D}}_l} + \mathscr{F}_l\mathscr{G}_l + \mathscr{G}_l^T\mathscr{F}_l^T < 0 \tag{5.31}$$

holds for all $\overline{\mathbb{D}}_l \in \{0,1\}$ *and* $l \in \{1,2\}$, *where*

$$\overline{\Omega}=\begin{bmatrix} \Omega_{11} & Q_{12} & U & \mathbf{0} & \mathbf{0} & -\mathfrak{n}\mathbf{I} & \mathbf{0} & \mathfrak{n}\mathbf{I} \\ * & \Omega_{22} & -Q_{12} & \mathbf{0} & \mathbf{0} & \mathbf{0} & \mathbf{0} & \mathbf{0} \\ * & * & \Omega_{33} & R_{12} & \mathbf{0} & \mathbf{0} & \mathbf{0} & \mathbf{0} \\ * & * & * & \Omega_{44} & -R_{12} & \mathbf{0} & \mathbf{0} & \mathbf{0} \\ * & * & * & * & -R_{22} & \mathbf{0} & \mathbf{0} & \mathbf{0} \\ * & * & * & * & * & \mathfrak{m}\mathbf{I} & \mathbf{0} & -\mathfrak{m}\mathbf{I} \\ * & * & * & * & * & * & \mathbf{0} & \mathbf{0} \\ * & * & * & * & * & * & * & (\mathfrak{m}-\delta)\,\mathbf{I} \end{bmatrix}, \tag{5.32}$$

and

$$\Omega_{11}=Q_{11}-\mathfrak{u}\mathbf{I}+\alpha\mathbf{I}, \qquad \Omega_{22}=Q_{22}-Q_{11},$$

$$\Omega_{33}=R_{11}-Q_{22}-U, \qquad \Omega_{44}=R_{22}-R_{11},$$

$$\Omega_1|_{\overline{\mathbb{D}}_1}=-\mathfrak{t}\left(\mathbb{J}_4-\mathbb{J}_5\right)^T\left(\mathbb{J}_4-\mathbb{J}_5\right)-\mathfrak{s}\mathbb{J}_7^T\mathbb{J}_7, \quad \Omega_2|_{\overline{\mathbb{D}}_2}=-\mathfrak{s}\left(\mathbb{J}_3-\mathbb{J}_4\right)^T\left(\mathbb{J}_3-\mathbb{J}_4\right)-\mathfrak{t}\mathbb{J}_7^T\mathbb{J}_7, \tag{5.33}$$

$$\mathscr{G}_1=\left[\overline{\mathscr{G}}_1\ \mathscr{G}_{1\overline{\mathbb{D}}_1}\ \mathbf{0}\right], \qquad \mathscr{G}_2=\left[\overline{\mathscr{G}}_2\ \mathscr{G}_{2\overline{\mathbb{D}}_2}\ \mathbf{0}\right], \tag{5.34}$$

$$\overline{\mathscr{G}}_1=\begin{bmatrix} \mathbf{0} & \mathbf{0} & -\mathbf{I} & \mathbf{0} & \mathbf{0} & \mathbf{I} \\ \mathbf{0} & \mathbf{0} & \mathbf{0} & \mathbf{I} & \mathbf{0} & -\mathbf{I} \end{bmatrix}, \qquad \overline{\mathscr{G}}_2=\begin{bmatrix} \mathbf{0} & \mathbf{0} & \mathbf{0} & -\mathbf{I} & \mathbf{0} & \mathbf{I} \\ \mathbf{0} & \mathbf{0} & \mathbf{0} & \mathbf{0} & \mathbf{I} & -\mathbf{I} \end{bmatrix},$$

$$\mathscr{G}_{1\overline{\mathbb{D}}_1}=\begin{bmatrix} \overline{\mathbb{D}}_1\mathbf{I} \\ \left(1-\overline{\mathbb{D}}_1\right)\mathbf{I} \end{bmatrix}, \qquad \mathscr{G}_{2\overline{\mathbb{D}}_2}=\begin{bmatrix} \overline{\mathbb{D}}_2\mathbf{I} \\ \left(1-\overline{\mathbb{D}}_2\right)\mathbf{I} \end{bmatrix},$$

and $\mathbb{J}_k \in \mathbb{R}^{3\times 24}, k \in \{1,\dots,8\}$, *are zero block entry matrices except for the* k*-th block, which is the identity* $\mathbf{I}_{3\times 3}$, *e.g.,* $\mathbb{J}_7=\left[\mathbf{0}\ \mathbf{0}\ \mathbf{0}\ \mathbf{0}\ \mathbf{0}\ \mathbf{0}\ \mathbf{I}\ \mathbf{0}\right]$.

Then, if (5.31) *holds, the proportional stabilizing controller gain* κ *is given by*

$$\kappa=2\left\{\frac{\mathfrak{m}}{\left[(\mu-\tau)^2\mathfrak{s}+(\nu-\mu)^2\mathfrak{t}+\tau^2\mathfrak{u}\right]}\right\}^{\frac{1}{2}}$$

with guaranteed performance attenuation given by $\gamma=\kappa^{-1}\sqrt{\delta\alpha^{-1}}$.

Proof. Suppose LKF variables $Q, R, \beta, \mathfrak{u}, \mathfrak{s}, \mathfrak{t}$ satisfy inequalities (5.30). Then, V is positive definite. Thus, asymptotic stability is conditional on $\dot{V}$, given by $\Sigma_{i=1}^4 \dot{V}_i$, being negative definite, where

$$\dot{V}_1=-2\beta\boldsymbol{\zeta}^T\left[\kappa\boldsymbol{\zeta}\left(t-d\left(t\right)\right)-\boldsymbol{r}_1\right], \tag{5.35}$$

$$\dot{V}_2=\begin{bmatrix} \boldsymbol{\zeta} \\ \boldsymbol{\zeta}\left(t-\frac{\tau}{2}\right) \end{bmatrix}^T Q \begin{bmatrix} \boldsymbol{\zeta} \\ \boldsymbol{\zeta}\left(t-\frac{\tau}{2}\right) \end{bmatrix}-\begin{bmatrix} \boldsymbol{\zeta}\left(t-\frac{\tau}{2}\right) \\ \boldsymbol{\zeta}\left(t-\tau\right) \end{bmatrix}^T Q \begin{bmatrix} \boldsymbol{\zeta}\left(t-\frac{\tau}{2}\right) \\ \boldsymbol{\zeta}\left(t-\tau\right) \end{bmatrix}$$
$$+\begin{bmatrix} \boldsymbol{\zeta}\left(t-\tau\right) \\ \boldsymbol{\zeta}\left(t-\mu\right) \end{bmatrix}^T R \begin{bmatrix} \boldsymbol{\zeta}\left(t-\tau\right) \\ \boldsymbol{\zeta}\left(t-\mu\right) \end{bmatrix}-\begin{bmatrix} \boldsymbol{\zeta}\left(t-\mu\right) \\ \boldsymbol{\zeta}\left(t-\nu\right) \end{bmatrix}^T R \begin{bmatrix} \boldsymbol{\zeta}\left(t-\mu\right) \\ \boldsymbol{\zeta}\left(t-\nu\right) \end{bmatrix}, \tag{5.36}$$

$$\dot{V}_3=\tau^2\dot{\boldsymbol{\zeta}}^T\mathfrak{u}\dot{\boldsymbol{\zeta}}-\tau\int_{t-\tau}^{t}\dot{\boldsymbol{\zeta}}\left(s\right)^T\mathfrak{u}\mathbf{I}\dot{\boldsymbol{\zeta}}\left(s\right)ds,$$

$$\dot{V}_4=\dot{V}_{4(0)}+\dot{V}_{4(I)},$$

$$\dot{V}_{4(0)}=\left(\mu-\tau\right)^2\dot{\boldsymbol{\zeta}}^T\mathfrak{s}\dot{\boldsymbol{\zeta}}+\left(\nu-\mu\right)^2\dot{\boldsymbol{\zeta}}^T\mathfrak{t}\dot{\boldsymbol{\zeta}},$$

$$\dot{V}_{4(I)} = -(\mu-\tau)\int_{t-\mu}^{t-\tau}\dot{\boldsymbol{\zeta}}(s)^T \mathfrak{s}\dot{\boldsymbol{\zeta}}(s)\,ds - (\nu-\mu)\int_{t-\nu}^{t-\mu}\dot{\boldsymbol{\zeta}}(s)^T \mathfrak{t}\dot{\boldsymbol{\zeta}}(s)\,ds.$$

Instead of proving $\dot{V}$ is negative definite for the whole admissible delay interval $[\tau,\nu]$, the analysis is split in two cases by considering mutually exclusive delay subintervals. Namely, using equal-measure subintervals $[\tau,\mu]$ and $(\mu,\nu]$, indicator function χ (4.10) allows two delay scenarios to be defined, as in (5.17)

$$\mathbb{S}_1 := \{d(t)\in\mathbb{R}|\chi(d(t))=1\},\quad \mathbb{S}_2 := \{d(t)\in\mathbb{R}|\chi(d(t))=0\},$$

such that

$$\dot{V}_4 = \dot{V}_{4(0)} + \dot{V}_{4(\mathbb{S}_1)} + \dot{V}_{4(\mathbb{S}_2)},$$

with

$$\dot{V}_{4(\mathbb{S}_1)}(t) := \chi(d(t))\,\dot{V}_{4(I)}(t)\,,\dot{V}_{4(\mathbb{S}_2)}(t) := (1-\chi(d(t)))\,\dot{V}_{4(I)}(t)\,.$$

Since d belongs to either one of $\mathbb{S}_1$ and $\mathbb{S}_2$ at a time, only one of $\dot{V}_{4(\mathbb{S}_l)}$ will be different from zero at any given time. Therefore, scenarios are scrutinized separately. For $\mathbb{S}_1$, $\chi(d(t))$ equals one, since d belongs to $[\tau,\mu]$, which allows $\dot{V}_{4(\mathbb{S}_1)}$ to be restated as

$$\dot{V}_{4(\mathbb{S}_1)} = -\chi(d(t))\left\{(\mu-\tau)\left[\int_{t-\mu}^{t-d(t)}\dot{\boldsymbol{\zeta}}(s)^T S\dot{\boldsymbol{\zeta}}(s)\,ds + \int_{t-d(t)}^{t-\tau}\dot{\boldsymbol{\zeta}}(s)^T S\dot{\boldsymbol{\zeta}}(s)\,ds\right]\right.$$
$$\left. + (\nu-\mu)\int_{t-\nu}^{t-\mu}\dot{\boldsymbol{\zeta}}(s)^T T\dot{\boldsymbol{\zeta}}(s)\,ds\right\},$$

a convenient expression to be checked using Jensen's Inequality (Lemma II.0.3). The resulting $\dot{V}_4$ bound is convex with respect to $d(t)$. Indeed, this becomes clearer by defining

$$\mathbb{D}_1(t) := \frac{d(t)-\tau}{\mu-\tau}\in[0,1]\,,$$

and shows that a convex functional, with extrema at the edges of $\mathbb{D}_1(t)$ (0 and 1), checks $\dot{V}_4$, where

$$\dot{V}_4 \le \dot{\boldsymbol{\zeta}}^T\left[(\mu-\tau)^2\mathfrak{s} + (\nu-\mu)^2\mathfrak{t}\right]\dot{\boldsymbol{\zeta}} - \chi\left\{{\boldsymbol{\xi}_{11}}^T(\mathbb{D}_1\mathfrak{s}\mathbf{I})\,\boldsymbol{\xi}_{11} + {\boldsymbol{\xi}_{12}}^T(1-\mathbb{D}_1)\,\mathfrak{s}\mathbf{I}\boldsymbol{\xi}_{12}\right.$$
$$\left. + [\boldsymbol{\zeta}(t-\mu)-\boldsymbol{\zeta}(t-\nu)]^T\,\mathfrak{t}\mathbf{I}\,[\boldsymbol{\zeta}(t-\mu)-\boldsymbol{\zeta}(t-\nu)]\right\}. \tag{5.37}$$

with

$$\boldsymbol{\xi}_{11}(t) := \tfrac{\mu-\tau}{d(t)-\tau}\int_{t-d(t)}^{t-\tau}\dot{\boldsymbol{\zeta}}(s)\,ds,\quad \boldsymbol{\xi}_{12}(t) := \tfrac{\mu-\tau}{\mu-d(t)}\int_{t-\mu}^{t-d(t)}\dot{\boldsymbol{\zeta}}(s)\,ds.$$

$\dot{V}_3$ can also be upper bounded through Jensen's Inequality, by

$$\dot{V}_3 \le \tau^2\mathfrak{u}\dot{\boldsymbol{\zeta}}^T\dot{\boldsymbol{\zeta}} - \left[\int_{t-\tau}^{t}\dot{\boldsymbol{\zeta}}(s)\,ds\right]^T\mathfrak{u}\mathbf{I}\left[\int_{t-\tau}^{t}\dot{\boldsymbol{\zeta}}(s)\,ds\right]. \tag{5.38}$$

If closed-loop system (5.1)-(5.4) was linear, the differential equation that governs its state changes could be substituted for $\dot{\boldsymbol{\zeta}}$, and analysis could be carried on. This is not the case, however, because of nonlinearities introduced by rigid body kinematics. Since the goal is to obtain design conditions that can be written as LMIs, $\dot{\boldsymbol{\zeta}}$ must be dealt with. From (5.28) and triangle inequality,

$$\left\|\dot{\boldsymbol{\zeta}}\right\|^2 \le \frac{1}{4}\left\{\left\|[\boldsymbol{\zeta}]_\times(\kappa\boldsymbol{\zeta}(t-d(t))-\boldsymbol{r}_1)\right\|^2 + \eta^2\left\|\kappa\boldsymbol{\zeta}(t-d(t))-\boldsymbol{r}_1\right\|^2\right\}$$

$$\leq \frac{1}{4}\left\{\left[\|\boldsymbol{\zeta}\|^2+\eta^2\right]\|\kappa\boldsymbol{\zeta}(t-d(t))-\boldsymbol{r}_1\|^2\right\}$$
$$\leq \frac{1}{4}\|\kappa\boldsymbol{\zeta}(t-d(t))-\boldsymbol{r}_1\|^2, \tag{5.39}$$

since

$$\left\{[\boldsymbol{\zeta}]_\times(\kappa\boldsymbol{\zeta}(t-d(t))-\boldsymbol{r}_1)\right\}\cdot(\kappa\boldsymbol{\zeta}(t-d(t))-\boldsymbol{r}_1)=0,$$

and because $\boldsymbol{q}$ is unit-norm. Combining bounds (5.38), (5.37) and (5.39) yields

$$\dot{V}_3 \leq \frac{\tau^2\mathfrak{u}}{4}\left[\kappa\boldsymbol{\zeta}(t-d(t))-\boldsymbol{r}_1\right]^T\left[\kappa\boldsymbol{\zeta}(t-d(t))-\boldsymbol{r}_1\right]-\left[\int_{t-\tau}^{t}\dot{\boldsymbol{\zeta}}(s)\,ds\right]^T\mathfrak{u}\mathbf{I}\left[\int_{t-\tau}^{t}\dot{\boldsymbol{\zeta}}(s)\,ds\right],$$
$$\dot{V}_4 \leq \frac{(\mu-\tau)^2\mathfrak{s}+(\nu-\mu)^2\mathfrak{t}}{4}\left[\kappa^2\boldsymbol{\zeta}(t-d(t))^T\boldsymbol{\zeta}(t-d(t))-\kappa\boldsymbol{\zeta}(t-d(t))^T\boldsymbol{r}_1-\right.$$
$$\left.-\kappa\boldsymbol{r}_1^T\boldsymbol{\zeta}(t-d(t))+\boldsymbol{r}_1^T\boldsymbol{r}_1\right]-\left\{\boldsymbol{\xi}_{11}^T(\mathbb{D}_1\mathfrak{s}\mathbf{I})\boldsymbol{\xi}_{11}+\boldsymbol{\xi}_{12}^T(1-\mathbb{D}_1)\mathfrak{s}\mathbf{I}\boldsymbol{\xi}_{12}\right.$$
$$\left.+\left[\boldsymbol{\zeta}(t-\mu)-\boldsymbol{\zeta}(t-\nu)\right]^T\mathfrak{t}\mathbf{I}\left[\boldsymbol{\zeta}(t-\mu)-\boldsymbol{\zeta}(t-\nu)\right]\right\}. \tag{5.40}$$

Since $\dot{V}_4$ bound (5.40) is convex with respect to $d(t)$, it reaches peak value at $\mathbb{D}_1$ extrema, 0 and 1. This implies $\mathbb{D}_1$ and $1-\mathbb{D}_1$ are mutually exclusive, and either $\boldsymbol{\xi}_{11}$ or $\boldsymbol{\xi}_{12}$ vanishes from (5.40). Thus, summing up bounds (5.35), (5.36), (5.38) and (5.40) lead to LMI

$$\dot{V} \leq \tilde{\boldsymbol{\vartheta}}_{1l}^T\tilde{\Omega}\tilde{\boldsymbol{\vartheta}}_{1l},$$

with

$$\tilde{\boldsymbol{\vartheta}}_{1l}(t):=\left[\begin{array}{cccccccc}\boldsymbol{\zeta}(t)^T & \boldsymbol{\zeta}\left(t-\frac{\tau}{2}\right)^T & \boldsymbol{\zeta}(t-\tau)^T & \boldsymbol{\zeta}(t-\mu)^T & \boldsymbol{\zeta}(t-\nu)^T & \boldsymbol{\zeta}(t-d(t))^T & \boldsymbol{\xi}_{1l}(t)^T & \boldsymbol{r}_1(t)^T\end{array}\right], l\in\{1,2\},$$

and

$$\tilde{\Omega}=\bar{\Omega}+\Omega_{1|\overline{\mathbb{D}}_1},$$

with $\bar{\Omega}$ and $\Omega_{1|\overline{\mathbb{D}}_1}$ given by (5.32) and (5.33), respectively.

According to condition 1 from Definition 5.1.4, for the closed-loop system to achieve H_∞ performance, it must be asymptotically stable when $\boldsymbol{r}_1$ is absent. Denote $\tilde{\Omega}_{7\times7}$ the upper-left seven-by-seven diagonal block of $\tilde{\Omega}$, as in

$$\tilde{\Omega}=\begin{bmatrix}\tilde{\Omega}_{7\times7} & \tilde{\Omega}_{8\times1}\\ * & \Omega_{88}\end{bmatrix},$$

with

$$\tilde{\Omega}_{8\times1}:=\left[\begin{array}{ccccccc}\mathfrak{n}\mathbf{I} & \mathbf{0} & \mathbf{0} & \mathbf{0} & \mathbf{0} & \mathfrak{m}\mathbf{I} & \mathbf{0}\end{array}\right],$$
$$\Omega_{88}:=(\mathfrak{m}-\delta)\,\mathbf{I},$$

and define

$$\Omega:=\begin{bmatrix}\Omega_{7\times7} & \tilde{\Omega}_{8\times1}\\ * & \Omega_{88}\end{bmatrix},$$

where

$$\Omega_{7\times7}:=\tilde{\Omega}_{7\times7}-\text{diag}\left\{\alpha\mathbf{I},\mathbf{0}\right\}.$$

Assuming $\boldsymbol{r}_1$ to be zero, it follows that

$$\dot{V}\leq\boldsymbol{\vartheta}_{1l}^T\Omega_{7\times7}\boldsymbol{\vartheta}_{1l}$$

with

$$\boldsymbol{\vartheta}_{1l}{:=}\left[\boldsymbol{\zeta}\left(t\right)^T\ \boldsymbol{\zeta}\left(t-\tfrac{\tau}{2}\right)^T\ \boldsymbol{\zeta}\left(t-\tau\right)^T\ \boldsymbol{\zeta}\left(t-\mu\right)^T\ \boldsymbol{\zeta}\left(t-\nu\right)^T\ \boldsymbol{\zeta}\left(t-d\left(t\right)\right)^T\ \boldsymbol{\xi}_{1l}\left(t\right)^T\right],l{\in}\left\{1,2\right\}.$$

Consequently, if $\Omega_{7\times7}$ is negative definite, the closed-loop system is asymptotically stable. Note, however, that if $\tilde{\Omega}$ is negative definite, then so is $\Omega_{7\times7}$. This can be concluded using Schur-complement-based reasoning: from Lemma II.0.2 in Appendix II, if Ω is negative definite, then so is $\Omega_{7\times7}-\tilde{\Omega}_{8\times1}^T\Omega_{88}\tilde{\Omega}_{8\times1}$. Since Ω is negative definite, so must be right-lower diagonal block Ω_{88}, implying

$$\Omega_{7\times7}{\leq}\Omega_{7\times7}-\tilde{\Omega}_{8\times1}^T\Omega_{88}\Omega_{8\times1}.$$

Since

$$\Omega{=}\tilde{\Omega}-\text{diag}\left\{\alpha\mathbf{I},\mathbf{0}\right\}{\leq}\tilde{\Omega},$$

if $\tilde{\Omega}$ is negative definite, so is $\Omega_{7\times7}$.

Introducing more degrees of freedom in the form of free-weighting matrix $\mathscr{F}_1$, less conservative conditions can be obtained. This is possible via Finsler's Lemma, defining an orthogonal matrix $\mathscr{G}_1$. Thus, let $\mathscr{G}_1$ be defined as $\left[\overline{\mathscr{G}}_1\ \mathscr{G}_{1\overline{\mathbb{D}}_1}\ \mathbf{0}\right]$, $\overline{\mathscr{G}}_1$ as in (5.34) and

$$\hat{\mathscr{G}}_{1\mathbb{D}}{=}\begin{bmatrix}\overline{\mathbb{D}}_1\mathbf{I}\\\left(1-\overline{\mathbb{D}}_1\right)\mathbf{I}\end{bmatrix},$$

with $\overline{\mathbb{D}}_1$ in $\{0,1\}$. For $\overline{\mathbb{D}}_1$ equal to one, $d\left(t\right)$ equals μ, and it follows that

$$\begin{aligned}\lim_{d(t)\to\mu}\mathscr{G}_1\tilde{\boldsymbol{\vartheta}}_{1l}&{=}\lim_{d(t)\to\mu}\begin{bmatrix}-\boldsymbol{\zeta}\left(t-\tau\right)+\boldsymbol{\zeta}\left(t-d\left(t\right)\right)+\frac{\mu-\tau}{d(t)-\tau}\int_{t-d(t)}^{t-\tau}\dot{\boldsymbol{\zeta}}\left(s\right)ds\\\boldsymbol{\zeta}\left(t-\mu\right)-\boldsymbol{\zeta}\left(t-d\left(t\right)\right)-\mathbf{0}\dot{\boldsymbol{\zeta}}\left(t-d\left(t\right)\right)\end{bmatrix}\\&{=}\begin{bmatrix}-\boldsymbol{\zeta}\left(t-\tau\right)+\boldsymbol{\zeta}\left(t-\mu\right)+\left(\boldsymbol{\zeta}\left(t-\tau\right)-\boldsymbol{\zeta}\left(t-\mu\right)\right)\\\boldsymbol{\zeta}\left(t-\mu\right)-\boldsymbol{\zeta}\left(t-\mu\right)+\mathbf{0}\dot{\boldsymbol{\zeta}}\left(t-\mu\right)\end{bmatrix}\\&{=}\begin{bmatrix}\mathbf{0}\\\mathbf{0}\end{bmatrix}.\end{aligned}$$

Analogously, when $\overline{\mathbb{D}}_1$ equals zero, $\mathscr{G}_1\tilde{\boldsymbol{\vartheta}}_{1l}$ also equals zero, i.e., $\mathscr{G}_1$ and $\tilde{\boldsymbol{\vartheta}}_{1l}$ are orthogonal. Thus, from Finsler's Lemma (Lemma II.0.1), Ω is negative definite if, and only if,

$$\tilde{\Omega}{=}\Omega+\mathscr{F}_1\mathscr{G}_1+\mathscr{G}_1^T\mathscr{F}_1^T{<}0.$$

Since $\tilde{\boldsymbol{\vartheta}}_{1l}^T\tilde{\Omega}\tilde{\boldsymbol{\vartheta}}_{1l}$ remains convex with respect to $d\left(t\right)$, its extrema coincide with $\mathbb{D}_1$'s, i.e., $\tilde{\boldsymbol{\vartheta}}_{1l}^T\tilde{\Omega}\tilde{\boldsymbol{\vartheta}}_{1l}$ reaches its maximum when $\mathbb{D}_1$ equals one or zero. Thus, if $\tilde{\Omega}$ is negative definite, when $\mathbb{D}_1$ equals zero and one, then so is Ω, and $\dot{V}$ is negative definite. Therefore, the closed-loop system is stable considering the first delay scenario. Analogous analysis prove $\dot{V}$ is also definite negative for the second delay scenario $\mathbb{S}_2$. Therefore, if the hypotheses from Theorem 5.1.5 hold, $\dot{V}$ is negative definite, independent if d takes values in $\mathbb{S}_1$ or $\mathbb{S}_2$, and closed-loop system (5.28)-(5.4) is asymptotically stable when $\boldsymbol{r}_1$ is absent.

Nevertheless, the resulting expression is not in the form of an LMI. Indeed, because of the cross product between $\boldsymbol{\zeta}\left(t-d\left(t\right)\right)$ and $\boldsymbol{r}$, (5.39) carries terms both with κ and κ^2. In addition, the derivative of $\dot{V}_1$ introduces cross product term $\beta\kappa$, with β also a variable. Altogether, these issues would precede establishing conditions that could be cast as LMIs in order to design controllers.

Let κ be a positive real number. Then, congruence transformation Υ, given by diag $\{\mathbf{I}, \kappa\mathbf{I}_{3\times3}\}$, multiplying $\tilde{\Omega}$ as in $\Upsilon^T\tilde{\Omega}\Upsilon$ and additional variables

$$\mathfrak{n}{=}\beta\kappa,\ \mathfrak{m}{=}\kappa^2\frac{\left[(\mu-\tau)^2\mathfrak{s}+(\nu-\mu)^2\mathfrak{t}+\tau^2\mathfrak{u}\right]}{4}, \tag{5.41}$$

can remedy these issues. Since Υ has full rank (because κ is positive), the "sign" of $\tilde{\Omega}$ is not affected by Υ, i.e., $\tilde{\Omega}$ is negative definite if, and only if, $\Upsilon^T\tilde{\Omega}\Upsilon$ is negative definite. The reason for introducing variable β becomes apparent now, as it provides $\mathfrak{n}$ with an extra degree of freedom which lets κ loose and allows $\mathfrak{m}$ to set the gain κ, since $\mathfrak{u}, \mathfrak{s}$ and $\mathfrak{t}$ are also variables. Hence, from (5.41), gain κ is recovered through LMI variables as

$$\kappa{=}2\sqrt{\mathfrak{m}\left[(\mu-\tau)^2\mathfrak{s}+(\nu-\mu)^2\mathfrak{t}+\tau^2\mathfrak{u}\right]^{-1}}. \tag{5.42}$$

The effects of an exogenous perturbation on $\boldsymbol{\zeta}$ can be assessed by considering term $\gamma^2\boldsymbol{r}_1^T\boldsymbol{r}_1$, which is added to $\tilde{\boldsymbol{\vartheta}}_{1l}^T\tilde{\Omega}\tilde{\boldsymbol{\vartheta}}_{1l}$. Nevertheless, by doing that, γ^2 is also multiplied by κ^2 when congruence transformation Υ is done, once again resulting in nonlinear conditions. Nonetheless, introducing a new variable δ can circumvent this. Even though $\delta{=}\gamma^2\kappa^2$ might seem like an option, since the goal is to establish conditions that allow to cast the design of H_∞ controllers as an optimization problem where the perturbation attenuation bound γ is to be minimized, this choice of δ would imply minimizing the *product* $\gamma\kappa$, rather than γ. Hence, δ is defined as $-\gamma^{-2}\lambda^2$ instead. Variable λ is an extra degree of freedom transparent to the LMI which decouples the minimization of γ^2 from that of κ^2. Thus, LMIs (5.31) are obtained.

Now, that sufficient stability conditions are stated in form of LMIs, controller performance can be addressed. If (5.31) hold, then

$$\dot{V}+\boldsymbol{\zeta}^T\boldsymbol{\zeta}-\gamma^2\boldsymbol{r}_1^T\boldsymbol{r}_1{<}0. \tag{5.43}$$

Since V is positive definite and $\dot{V}$ is negative definite, integrating (5.43) and assuming zero initial condition yields

$$\int_0^{+\infty}\boldsymbol{\zeta}(s)^T\boldsymbol{\zeta}(s)\,ds{<}\gamma^2\int_0^{+\infty}\boldsymbol{r}_1(s)^T\boldsymbol{r}_1(s)\,ds,$$

that is

$$\|\boldsymbol{\zeta}\|_2^2{<}\gamma^2\|\boldsymbol{r}_1\|_2^2,$$

satisfying condition 2 of Definition 5.1.4. □

It is now possible to cast H_∞ controller design as a linear optimization problem with the conditions from Theorem 5.1.5 considered the constraints, as in

$$\min_{s.t.\ \overline{\Omega}+\Omega_l|_{\overline{\mathbb{D}}_l}+\mathscr{F}_l\mathscr{G}_l+\mathscr{G}_l^T\mathscr{F}_l^T<0\,(5.31)}\delta,$$

because the conditions are LMIs. Hence, using an appropriate optimization solver such as *SeDuMi* [51] or *SDPT3* [52], H_∞ performance controllers can be readily designed in an automated fashion.

5.1.3 Numerical Discussion

Theorem 5.1.5 provides LMI conditions that allow the design of H_∞ controllers, but can also be used as an instrument to assess the influence of different delay bounds τ and ν over the perturbation attenuation bound γ. The following experiments are conducted in MATLAB environment, simulations done in Simulink, and LMIs programmed using the YALMIP package [53]. SDPT3 solver [52] seems to have an edge over SeDuMi [51] at this particular optimization problem and, therefore, is adopted throughout this subsection.

The set of delay candidates is obtained by incrementing τ and ν in steps of 50 milliseconds, such that ν is greater than or equal to τ. This delay grid is then used to obtain the corresponding disturbance rejection norm bounds given by Theorem 5.1.5, yielding a three-dimensional surface, which provides a more qualitative way to understand the nature of the relationship between disturbance rejection and delays. Figure 5.1 exposes the detrimental effects of growing delay bounds τ and ν. As expected, the larger the delays, the worse the perturbation rejection. Nonetheless, Figure 5.1 surface also presents a surprisingly linear variation of γ with respect to both τ and ν. In particular, the specific ratio $\frac{\nu}{\tau}$ of 2.603 renders minimal disturbance rejection bounds according to Theorem 5.1.5. This "optimal ratio", however, is due to particular optimization conditions of Theorem 5.1.5 LMIs, and does not represent an actual physical phenomenon. Indeed, if the system is stable and rejects disturbances with H_∞ norm bound γ for a delay interval of $[\tau_1, \nu]$, then disturbance rejection should be at least γ for an interval $[\tau_2, \nu]$ if τ_2 is greater than or equal to τ_1, because this falls into a particular subcase of the previous scenario:$[\tau_2, \nu]$ belongs to $[\tau_1, \nu]$. In fact, when the interval length becomes smaller, the delay tends to constant value ν.

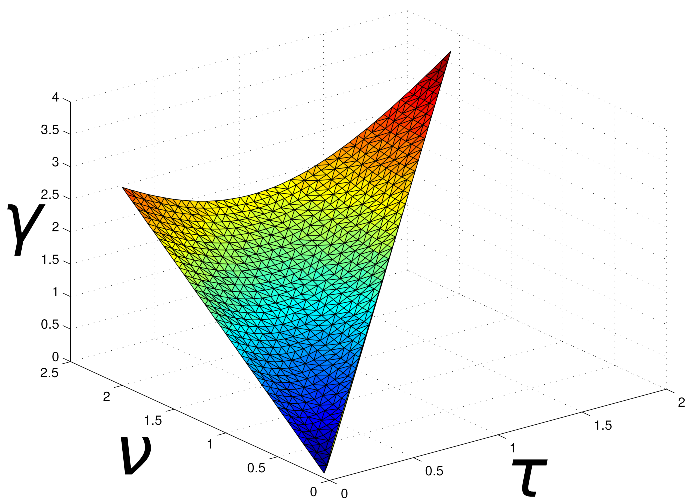

Figure 5.1: Perturbation attenuation upper bound γ for different delay bounds τ and ν.

Since numerical results suggest the conditions from Theorem 5.1.5 have mechanisms and characteristics that do not reflect real world's, the conservatism of the Theorem is gauged by comparing theoretical and experimental disturbance rejection performances. The procedure is to fix τ equal to zero, vary ν and obtain the corresponding theoretical disturbance rejection H_∞ norm bound, which can be compared with the actual disturbance rejection obtained experimentally using the controller designed through the same Theorem. For diversity's sake, two different disturbance profiles, that are shown in Table 5.1, are simulated. $\hat{\boldsymbol{r}}_1$ and $\tilde{\boldsymbol{r}}_1$ are multiplied by $\mathbf{1}_{3\times 1}$ vector and $\mathcal{N}\left(0, 0.005\right)$ denotes

Gaussian noise with zero average and variance of 0.005.

Table 5.1: Exogenous disturbance profiles $\hat{\boldsymbol{r}}_1$ and $\tilde{\boldsymbol{r}}_1$.

$t\,[s]$	$0 \leq t \leq 10$	$10 \leq t \leq 20$	$20 \leq t \leq 30$	$30 \leq t \leq 40$
$\hat{\boldsymbol{r}}_1\,(t)$	$0.1\cos(0.75\pi t)$	0.02	$0.05\sin(0.5\pi t)$	$\mathcal{N}(0, 0.005)$
$\tilde{\boldsymbol{r}}_1\,(t)$	$0.1\sin(2\pi t)$	0.1	$\mathcal{N}(0, 0.0035)$	$0.1\sin(\pi t) + \mathcal{N}\left(0, 3 * 10^{-6}\right)$

Figures from Table 5.2 quantify the trend previously noted: increasing ν deteriorates perturbation attenuation. The experimental disturbance attenuation γ_{exp}, which are numerically obtained by squaring $\|r_1\|$ and $\|\boldsymbol{\zeta}\|$ and taking the square root of MATLAB function *trapz*–that performs numerical integration of the data–, also validate bounds provided by Theorem 5.1.5, since experimental attenuation γ_{exp} is always smaller than theoretical one γ_{th}. Numerical evidence also disproves the linear relationship between disturbance attenuation and delay suggested by Figure 5.1's surface.

Table 5.2: Theoretical and simulated perturbation attenuation for different ν.

ν	0.001	0.011	0.087	0.43	0.92	3.73	6.19
γ_{th}	0.0015	0.0168	0.1326	0.6556	1.4026	5.6867	9.4372
γ_{exp}	0.0007	0.0073	0.0492	0.1932	0.2622	0.4921	0.6811

The second disturbance profile, denoted by $\tilde{\boldsymbol{r}}_1$ as in Table 5.1, is simulated changing the system's settings: controller κ is set equal to 25.1139 and time-delays uniformly distributed between 25 ms and 70 ms. Figure 5.2 shows the aftermath, depicting $\boldsymbol{\zeta}$ state norm and disturbance norm. In agreement with the theoretical H_∞ norm bound of 0.0840 provided by Theorem 5.1.5, numerical calculation using experimental data yield γ_{sim} smaller than γ_{exp}, and equal to 0.0376.

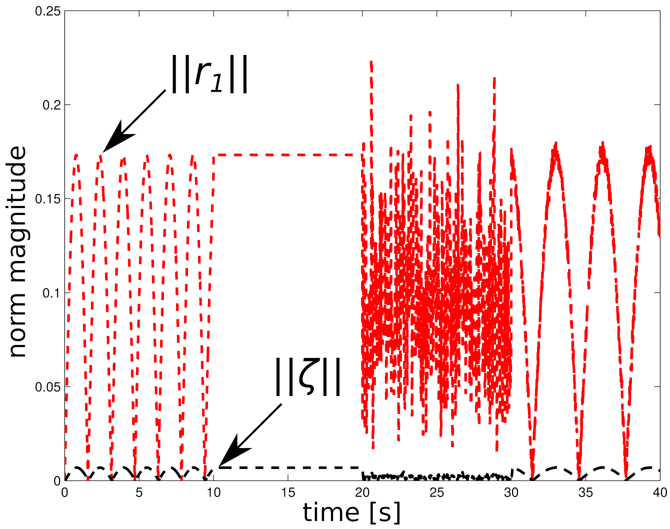

Figure 5.2: $\|\zeta\|$ superimposed on exogenous disturbance norm $\|\boldsymbol{r}_1\|$.

The conservative gap between experimental and theoretical results would have been made larger had the auxiliary variable δ not been introduced. Indeed, assuming previous delay interval of $[0.025, 0.07]$, Theorem 5.1.5 norm bound without δ is 4.257, opposed to 0.0608 when the variable is considered. This represents a roughly 70 times improvement. Analogous comparisons are shown in

Table 5.3, for different delay intervals, and reinforce the benefits of decoupling H_∞ norm bound and controller gain κ, as far as optimization is concerned.

Table 5.3: Disturbance rejection norm γ with and without δ.

Delay Interval [s]	$[0, 0.001]$	$[0, 1]$	$[50, 50.001]$	$[0, 150]$	$[1000, 1000.001]$
Theorem 5.1.5 with δ	0.0015	1.5246	96.9352	304.9171	$1.9387 * 10^3$
Theorem 5.1.5 without δ	0.1009	99.1489	$6.1975 * 10^3$	$2.1246 * 10^4$	$1.7459 * 10^5$

5.2 DYNAMIC ATTITUDE CONTROL

When rigid body dynamics cannot be assumed transparent for the purposes of control, it is necessary to take the relationship between angular momentum change and input torques into account. In this case, the control input is considered the net torque applied to the rigid body, and actual attitude is controlled indirectly via angular velocities through the angular momentum. The nonlinearities that arise, are quadratic-like, and make the so-called *dynamic attitude control* problem a challenging one.

5.2.1 Model-based Tracking with Delayed Attitude Measurements

Typical attitude control applications assign a rigid body desired trajectories to follow, instead of just stabilizing it at a certain orientation, and rigid body's dynamics may not be transparent for control purposes, i.e., it might only be possible to set angular velocity, which is governed by dynamics equation (3.22), through input torques. Considering these two realistic assumptions toughens attitude control, called the *dynamic tracking* problem. It is, however, possible to state dynamic tracking as an stabilization problem, if attitude and velocity errors are appropriately defined.

Consider a rigid body whose kinematics are contaminated with exogenous perturbations as in (5.28) and dynamics is given by (3.22), and let $\boldsymbol{q}_d$ and $\boldsymbol{\omega}_d$ represent the attitude and angular velocity states of a desired trajectory, relative to an inertial frame $\mathcal{I}$. The discrepancies between the desired and actual states can be captured by error states

$$\boldsymbol{q}_e = \boldsymbol{q}_d^{-1}\boldsymbol{q}, \tag{5.44}$$

$$\boldsymbol{\omega}_e = \boldsymbol{\omega} - \boldsymbol{\omega}_{\mathcal{B}}, \tag{5.45}$$

where

$$\boldsymbol{\omega}_{\mathcal{B}} = \mathcal{R}\left(\boldsymbol{q}\right)^T \boldsymbol{\omega}_d \tag{5.46}$$

is the desired angular velocity expressed in body frame $\mathcal{B}$ coordinates, and $\mathcal{R}\left(\boldsymbol{q}\right)$ can be obtained through Rodrigues' Formula (3.9). Equation (5.44) is convenient because the attitude error quaternion $\boldsymbol{q}_e$ is also unit-norm, since it is the product of two unit-norm quaternions, which form a group [44]. Thus, from (5.44) and (3.14), and assuming velocity inputs are affected by exogenous disturbance $\boldsymbol{r}_1$, it follows that attitude error kinematics evolves according to $\dot{\boldsymbol{q}}_e$, such that

$$\dot{\boldsymbol{q}}_e\left(t\right) = \begin{bmatrix} \dot{\eta}_e\left(t\right) \\ \dot{\boldsymbol{\zeta}}_e\left(t\right) \end{bmatrix} = \frac{1}{2}\begin{bmatrix} -\boldsymbol{\zeta}_e\left(t\right)^T \\ \eta_e\left(t\right)\mathbf{I} + \left[\boldsymbol{\zeta}_e\left(t\right)\right]_\times \end{bmatrix}\left[\boldsymbol{\omega}_e\left(t\right) + \boldsymbol{r}_1\left(t\right)\right]. \tag{5.47}$$

Analogously, from (5.45) and (3.22), angular velocity error dynamics is given by

$$J\dot{\boldsymbol{\omega}}_e = -\left[\boldsymbol{\omega}\right]_\times J\boldsymbol{\omega} + J\left(\left[\boldsymbol{\omega}_e\right]_\times \boldsymbol{\omega}_{\mathcal{B}} - \dot{\boldsymbol{\omega}}_{\mathcal{B}}\right) + u. \tag{5.48}$$

Thus, if attitude error system described by (5.47)-(5.48) is asymptotically stable, tracking errors converge to zero, which implies the original system (5.28)-(3.22) follows the desired trajectory. The states $\boldsymbol{\omega}_{\mathcal{B}}$ and $\dot{\boldsymbol{\omega}}_{\mathcal{B}}$ are assumed available, since the desired trajectory is known to the rigid body. The inertia matrix J is also considered known, and full state information is accessible, although attitude measurements $\boldsymbol{q}$ are deemed subjected to time-delays. Real-world applications back the last hypothesis, and prevent it from being considered artificial [15]. Indeed, attitude sensors are prone to considerably larger measurement delays than velocity sensors are. For example, star trackers may need up to ten seconds to produce attitude measurements [16].

Consider the feedforward-plus-proportional-derivative controller

$$u = \left[\boldsymbol{\omega}\right]_\times J\boldsymbol{\omega} - J\left(\left[\boldsymbol{\omega}_e\right]_\times \boldsymbol{\omega}_{\mathcal{B}} - \dot{\boldsymbol{\omega}}_{\mathcal{B}}\right) - \kappa_1\boldsymbol{\zeta}_e\left(t - d\left(t\right)\right) - \kappa_2\boldsymbol{\omega}_e, \tag{5.49}$$

with κ_1, κ_2 positive real numbers. Model knowledge enables the controller to compensate dynamic nonlinearities through the feedforward term $\left[\boldsymbol{\omega}\right]_\times J\boldsymbol{\omega} - J\left(\left[\boldsymbol{\omega}_e\right]_\times \boldsymbol{\omega}_{\mathcal{B}} - \dot{\boldsymbol{\omega}}_{\mathcal{B}}\right)$. On the other hand, kinematics' cannot be avoided. Fortunately, though, the source of kinematic nonlinearities, $\dot{\boldsymbol{\zeta}}_e$, is bounded by a linear term.

Proposition 5.2.1. *Let* $\boldsymbol{q}_e$ *be a unit quaternion satisfying* (5.47). *Then*

$$\left\|\dot{\boldsymbol{\zeta}}_e\left(t\right)\right\|^2 \leq \frac{1}{4}\left\|\boldsymbol{\omega}_e\left(t\right) + \boldsymbol{r}_1\left(t\right)\right\|^2, \forall t \geq 0.$$

Proof. From (5.47)

$$\left\|\dot{\boldsymbol{\zeta}}_e\right\|^2 = \dot{\boldsymbol{\zeta}}_e^T\dot{\boldsymbol{\zeta}}_e = \frac{1}{4}\left\{\left(\eta_e\mathbf{I} + \left[\boldsymbol{\zeta}_e\right]_\times\right)\left(\boldsymbol{\omega}_{\boldsymbol{e}} + \boldsymbol{r}_1\right)\right\}^T\left\{\left(\eta_e\mathbf{I} + \left[\boldsymbol{\zeta}_e\right]_\times\right)\left(\boldsymbol{\omega}_{\boldsymbol{e}} + \boldsymbol{r}_1\right)\right\}.$$

Noting that

$$\eta_e\left(\left[\boldsymbol{\zeta}_e\right]_\times\left(\boldsymbol{\omega}_e + \boldsymbol{r}_1\right)\right)^T\left(\boldsymbol{\omega}_{\boldsymbol{e}} + \boldsymbol{r}_1\right) = 0,$$

from $\left[\cdot\right]_\times$ property $\left\|\left[\boldsymbol{\zeta}_e\right]_\times\right\| \leq \left\|\boldsymbol{\zeta}_e\right\|$ (I.6), and unit-norm quaternion constraint (5.3), it follows that

$$\begin{aligned}
\left\|\dot{\boldsymbol{\zeta}}_e\right\|^2 &= \frac{1}{4}\left\{\eta_e^2\left(\boldsymbol{\omega}_e + \boldsymbol{r}_1\right)^T\left(\boldsymbol{\omega}_e + \boldsymbol{r}_1\right) + \left(\left[\boldsymbol{\zeta}_e\right]_\times\left(\boldsymbol{\omega}_e + \boldsymbol{r}_1\right)\right)^T\left(\left[\boldsymbol{\zeta}_e\right]_\times\left(\boldsymbol{\omega}_e + \boldsymbol{r}_1\right)\right)\right\} \\
&= \frac{1}{4}\left\{\eta_e^2\left\|\boldsymbol{\omega}_e + \boldsymbol{r}_1\right\|^2 + \left\|\left[\boldsymbol{\zeta}_e\right]_\times\left(\boldsymbol{\omega}_e + \boldsymbol{r}_1\right)\right\|^2\right\} \\
&\leq \frac{1}{4}\left(\eta_e^2 + \left\|\left[\boldsymbol{\zeta}_e\right]_\times\right\|^2\right)\left\|\boldsymbol{\omega}_e + \boldsymbol{r}_1\right\|^2 \\
&\leq \frac{1}{4}\left(\eta_e^2 + \left\|\boldsymbol{\zeta}_e\right\|^2\right)\left\|\boldsymbol{\omega}_e + \boldsymbol{r}_1\right\|^2 \\
&\leq \frac{1}{4}\left\|\boldsymbol{\omega}_e + \boldsymbol{r}_1\right\|^2.
\end{aligned}$$

□

Proposition 5.2.2. *Let* $P \in \mathbb{S}^n$ *be a positive definite matrix and let* ρ *be a positive real number. Then, for* $\boldsymbol{x}, \boldsymbol{y}$ *vectors in* $\mathbb{R}^n$

$$\pm 2\boldsymbol{x}^T P\boldsymbol{y} \leq \rho\boldsymbol{x}^T P\boldsymbol{x} + \frac{1}{\rho}\boldsymbol{y}^T P\boldsymbol{y}.$$

Proof. Let $\tilde{\rho}$ be a nonzero real number. Since P is positive definite,

$$0 \leq \left(\tilde{\rho}\boldsymbol{x} \pm \frac{1}{\tilde{\rho}}\boldsymbol{y}\right)^T P \left(\tilde{\rho}\boldsymbol{x} \pm \frac{1}{\tilde{\rho}}\boldsymbol{y}\right) = \tilde{\rho}^2\boldsymbol{x}^T P\boldsymbol{x} \pm 2\boldsymbol{x}^T P\boldsymbol{y} + \frac{1}{\tilde{\rho}^2}\boldsymbol{y}^T P\boldsymbol{y},$$

and the result follows by considering ρ equal to $\tilde{\rho}^2$. □

Since only attitude measurements are subjected to time-delays, LKF candidate used to obtain controller design conditions in Subsection 5.1.2 suffices to handle kinematics. But because dynamics is also considered, extra terms are required to ensure the stability of velocity error state $\boldsymbol{\omega}_e$. Thus, consider LKF given by

$$V = \sum_{i=1}^{4} V_i\left(t\right), \tag{5.50}$$

with

$$V_1 = 2\mathfrak{a}\left[\boldsymbol{\zeta}_e^T\boldsymbol{\zeta}_e + \left(1-\eta_e\right)^2\right] + \mathfrak{b}\boldsymbol{\omega}_e^T J\boldsymbol{\omega}_e + 2\mathfrak{c}\boldsymbol{\zeta}_e^T J\boldsymbol{\omega}_e, \tag{5.51}$$

$$\begin{aligned} V_2 = &\int_{t-\frac{\tau}{2}}^{t} \begin{bmatrix} \boldsymbol{\zeta}_e\left(s\right) \\ \boldsymbol{\zeta}_e\left(s-\frac{\tau}{2}\right) \end{bmatrix}^T M \begin{bmatrix} \boldsymbol{\zeta}_e\left(s\right) \\ \boldsymbol{\zeta}_e\left(s-\frac{\tau}{2}\right) \end{bmatrix} ds \\ &+ \int_{t-\mu}^{t-\tau} \begin{bmatrix} \boldsymbol{\zeta}_e\left(s\right) \\ \boldsymbol{\zeta}_e\left(s-\mu+\tau\right) \end{bmatrix}^T N \begin{bmatrix} \boldsymbol{\zeta}_e\left(s\right) \\ \boldsymbol{\zeta}_e\left(s-\mu+\tau\right) \end{bmatrix} ds, \end{aligned} \tag{5.52}$$

$$V_3 = \tau\int_{-\tau}^{0}\int_{t+\beta}^{t} \dot{\boldsymbol{\zeta}}_e\left(s\right)^T \mathfrak{r}\dot{\boldsymbol{\zeta}}_e\left(s\right) ds d\beta, \tag{5.53}$$

$$V_4 = \left(\mu-\tau\right)\int_{-\mu}^{-\tau}\int_{t+\beta}^{t} \dot{\boldsymbol{\zeta}}_e\left(s\right)^T \mathfrak{s}\dot{\boldsymbol{\zeta}}_e\left(s\right) ds d\beta + \left(\nu-\mu\right)\int_{-\nu}^{-\mu}\int_{t+\beta}^{t} \dot{\boldsymbol{\zeta}}_e\left(s\right)^T \mathfrak{t}\dot{\boldsymbol{\zeta}}_e\left(s\right) ds\beta, \tag{5.54}$$

where $\mathfrak{a}, \mathfrak{b}, \mathfrak{c}, \mathfrak{r}, \mathfrak{s}$ and $\mathfrak{t}$ are real numbers and M, N symmetric matrices. LKF terms V_1, V_2 and V_3 all facilitate the use of TDS analysis techniques discussed in Subsection 4.4. Namely, V_1 enables FA (4.4.2) and PAM (4.4.1), while V_3 and V_4 allow using PAM (4.4.1) and PAM plus CA (4.4.3), respectively.

Because terms (5.52)-(5.54) consist of quadratic forms, positiveness of the corresponding scalar and matrix variables suffices to guarantee positiveness of the V_2, V_3 and V_4. Nevertheless, because of cross term $2\mathfrak{c}\boldsymbol{\zeta}_e^T\boldsymbol{\omega}_e$ in (5.51), $\mathfrak{a}$ and $\mathfrak{b}$ being positive does not suffice to ensure V_1 is positive definite (even if $\mathfrak{c}$ is positive). Indeed, suppose $\mathfrak{a}$ and $\mathfrak{b}$ are positive. From Proposition 5.2.2,

$$\begin{aligned} V_1 &= 2\mathfrak{a}\left[\boldsymbol{\zeta}_e^T\boldsymbol{\zeta}_e + \left(1-\eta_e\right)^2\right] + \mathfrak{b}\boldsymbol{\omega}_e^T J\boldsymbol{\omega}_e + 2\mathfrak{c}\boldsymbol{\zeta}_e^T J\boldsymbol{\omega}_e \\ &\geq 2\mathfrak{a}\boldsymbol{\zeta}_e^T\boldsymbol{\zeta}_e + \mathfrak{b}\boldsymbol{\omega}_e^T J\boldsymbol{\omega}_e + 2\mathfrak{c}\boldsymbol{\zeta}_e^T J\boldsymbol{\omega}_e \\ &\geq \frac{2\mathfrak{a}}{\lambda_{\max}\left(J\right)}\boldsymbol{\zeta}_e^T J\boldsymbol{\zeta}_e + \mathfrak{b}\boldsymbol{\omega}_e^T J\boldsymbol{\omega}_e - \left|\mathfrak{c}\right|\boldsymbol{\zeta}_e^T J\boldsymbol{\zeta}_e - \left|\mathfrak{c}\right|\boldsymbol{\omega}_e^T J\boldsymbol{\omega}_e \\ &= \left(\frac{2\mathfrak{a}}{\lambda_{\max}\left(J\right)} - \left|\mathfrak{c}\right|\right)\boldsymbol{\zeta}_e^T J\boldsymbol{\zeta}_e + \left(\mathfrak{b}-\left|\mathfrak{c}\right|\right)\boldsymbol{\omega}_e^T J\boldsymbol{\omega}_e, \end{aligned}$$

which reveals that the coefficients $\frac{2\mathfrak{a}}{\lambda_{\max}(J)} - \left|\mathfrak{c}\right|$ and $\mathfrak{b}-\left|\mathfrak{c}\right|$ must also be positive. Therefore, (5.50) is positive definite if

$$\begin{gathered} \mathfrak{a} > 0, \quad \mathfrak{b} > 0, \quad \mathfrak{b} > \left|\mathfrak{c}\right|, \quad 2\mathfrak{a} > \lambda_{\max}\left(J\right)\left|\mathfrak{c}\right|, \quad \mathfrak{r} > 0, \quad \mathfrak{s} > 0, \quad \mathfrak{t} > 0, \\ M = \begin{bmatrix} M_{11} & M_{12} \\ * & M_{22} \end{bmatrix} > 0, N = \begin{bmatrix} N_{11} & N_{12} \\ * & N_{22} \end{bmatrix} > 0. \end{gathered} \tag{5.55}$$

Theorem 5.2.3. *Given nonnegative real numbers τ and ν, and positive controller gains κ_1 and κ_2, the closed-loop system* (5.47)-(5.49) *is stable with positive disturbance rejection upper bound γ if there exist positive real numbers $\mathfrak{a}, \mathfrak{b}, \mathfrak{c}, \mathfrak{r}, \mathfrak{s}, \mathfrak{t}$, and matrices M, N, satisfying* (5.55)*, as well as free-weighting matrices $\mathscr{F}_l$ such that*

$$\bar{\Omega} + \Omega_l|_{\overline{\mathbb{D}}_l} + \mathscr{F}_l\mathscr{G}_l + \mathscr{G}_l^T\mathscr{F}_l^T < 0, \tag{5.56}$$

hold for all $\overline{\mathbb{D}}_l \in \{0,1\}$ and $l \in \{1,2\}$, where

$$\bar{\Omega} = \begin{bmatrix} \Omega_{11} & \Omega_{12} & \Omega_{13} & \mathbf{0} & \mathbf{0} & \Omega_{16} & \Omega_{17} & \mathbf{0} & \Omega_{19} \\ * & \Omega_{22} & \Omega_{23} & \mathbf{0} & \mathbf{0} & \mathbf{0} & \mathbf{0} & \mathbf{0} & \mathbf{0} \\ * & * & \Omega_{33} & \Omega_{34} & \mathbf{0} & \mathbf{0} & \mathbf{0} & \mathbf{0} & \mathbf{0} \\ * & * & * & \Omega_{44} & \Omega_{45} & \mathbf{0} & \mathbf{0} & \mathbf{0} & \mathbf{0} \\ * & * & * & * & \Omega_{55} & \mathbf{0} & \mathbf{0} & \mathbf{0} & \mathbf{0} \\ * & * & * & * & * & \mathbf{0} & \Omega_{67} & \mathbf{0} & \mathbf{0} \\ * & * & * & * & * & * & \Omega_{77} & \mathbf{0} & \Omega_{79} \\ * & * & * & * & * & * & * & \mathbf{0} & \mathbf{0} \\ * & * & * & * & * & * & * & * & \Omega_{99} \end{bmatrix} \tag{5.57}$$

with

$$\begin{aligned}
\Omega_{11} &= M_{11} - \mathfrak{r}\mathbf{I} + \mathbf{I}, & \Omega_{34} &= N_{12}, \\
\Omega_{12} &= M_{12}, & \Omega_{44} &= N_{22} - N_{11}, \\
\Omega_{13} &= \mathfrak{r}\mathbf{I}, & \Omega_{45} &= -N_{12}, \\
\Omega_{16} &= -\kappa_1\mathfrak{c}\mathbf{I}, & \Omega_{55} &= -N_{22}, \\
\Omega_{17} &= (\mathfrak{a} - \kappa_2\mathfrak{c})\,\mathbf{I}, & \Omega_{67} &= -\kappa_1\mathfrak{b}\mathbf{I}, \\
\Omega_{19} &= \mathfrak{a}\mathbf{I}, & \Omega_{77} &= \mathfrak{c}J + [M_J\mathfrak{c} + \mathfrak{m} - 2\kappa_2\mathfrak{b}]\,\mathbf{I}, \\
\Omega_{22} &= M_{22} - M_{11}, & \Omega_{79} &= (\mathfrak{m} + M_J\mathfrak{c})\,\mathbf{I}, \\
\Omega_{23} &= -M_{12}, & \Omega_{99} &= (\mathfrak{m} + M_J\mathfrak{c})\,\mathbf{I} - \gamma\mathbf{I}, \\
\Omega_{33} &= N_{11} - M_{22} - \mathfrak{r}\mathbf{I}, & \mathfrak{m} &= \frac{1}{4}\left[\tau^2\mathfrak{r} + (\mu-\tau)^2\,\mathfrak{s} + (\nu-\mu)^2\,\mathfrak{t}\right],
\end{aligned}$$

$$\Omega_1|_{\overline{\mathbb{D}}_1} = -\mathfrak{t}\,(\mathbb{J}_4 - \mathbb{J}_5)^T\,(\mathbb{J}_4 - \mathbb{J}_5) - \mathfrak{s}\mathbb{J}_8^T\mathbb{J}_8, \quad \Omega_2|_{\overline{\mathbb{D}}_2} = -\mathfrak{s}\,(\mathbb{J}_3 - \mathbb{J}_4)^T\,(\mathbb{J}_3 - \mathbb{J}_4) - \mathfrak{t}\mathbb{J}_8^T\mathbb{J}_8, \tag{5.58}$$

$$\mathscr{G}_1 = \begin{bmatrix} \bar{\mathscr{G}_1} & \bar{\mathscr{G}}_{1\overline{\mathbb{D}}_1} & \mathbf{0} \end{bmatrix}, \qquad \mathscr{G}_2 = \begin{bmatrix} \bar{\mathscr{G}_2} & \bar{\mathscr{G}}_{2\overline{\mathbb{D}}_2} & \mathbf{0} \end{bmatrix}, \tag{5.59}$$

$$\bar{\mathscr{G}_1} = \begin{bmatrix} \mathbf{0} & \mathbf{0} & -\mathbf{I} & \mathbf{0} & \mathbf{0} & \mathbf{I} & \mathbf{0} \\ \mathbf{0} & \mathbf{0} & \mathbf{0} & \mathbf{I} & \mathbf{0} & -\mathbf{I} & \mathbf{0} \end{bmatrix}, \qquad \bar{\mathscr{G}_2} = \begin{bmatrix} \mathbf{0} & -\mathbf{I} & \mathbf{0} & \mathbf{0} & \mathbf{0} & \mathbf{I} & \mathbf{0} \\ \mathbf{0} & \mathbf{0} & \mathbf{I} & \mathbf{0} & \mathbf{0} & -\mathbf{I} & \mathbf{0} \end{bmatrix},$$

$$\mathscr{G}_{1\overline{\mathbb{D}}_1} = \begin{bmatrix} \overline{\mathbb{D}}_1\mathbf{I} \\ \left(1 - \overline{\mathbb{D}}_1\right)\mathbf{I} \end{bmatrix}, \qquad \mathscr{G}_{2\overline{\mathbb{D}}_2} = \begin{bmatrix} \overline{\mathbb{D}}_2\mathbf{I} \\ \left(1 - \overline{\mathbb{D}}_2\right)\mathbf{I} \end{bmatrix},$$

and $\mathbb{J}_k \in \mathbb{R}^{3\times 27}, k \in \{1, \ldots, 9\}$, are block entry matrices with nine elements whose k-th element is the identity and all the others are null, e.g., $\mathbb{J}_9 = \begin{bmatrix} \mathbf{0} & \mathbf{0} & \mathbf{0} & \mathbf{0} & \mathbf{0} & \mathbf{0} & \mathbf{0} & \mathbf{0} & \mathbf{I} \end{bmatrix}$.

Proof. Once more, the goal is to establish sufficient conditions that satisfy Lyapunov-Krasovskii theorem. In this sense, assume $\mathfrak{a}, \mathfrak{b}, \mathfrak{c}, \mathfrak{r}, \mathfrak{s}, \mathfrak{t}$, and M, N, satisfy (5.55). Then, LKF candidate (5.50) is positive definite. It remains to show its derivative along trajectories of $\boldsymbol{q}_e$ is definite negative.

Let V_{1a}, V_{1b} be such that

$$V_1 = V_{1a} + V_{1b},$$

with

$$\begin{aligned} V_{1a} &= 2\mathfrak{a}\left[\boldsymbol{\zeta}_e^T\boldsymbol{\zeta}_e + (1-\eta_e)^2\right], \\ V_{1b} &= \mathfrak{b}\boldsymbol{\omega}_e^T J\boldsymbol{\omega}_e + 2\mathfrak{c}\boldsymbol{\zeta}_e^T J\boldsymbol{\omega}_e. \end{aligned}$$

From the error kinematics (5.47), and since $\boldsymbol{q}_e$ is also unit norm,

$$\dot{V}_{1a} = 2\frac{d}{dt}\mathfrak{a}\left[\boldsymbol{\zeta}_e^T\boldsymbol{\zeta}_e + (1-\eta_e)^2\right] = 2\mathfrak{a}\frac{d}{dt}(2-2\eta_e) = -4\mathfrak{a}\dot{\eta}_e = 2\mathfrak{a}\boldsymbol{\zeta}_e^T(\boldsymbol{\omega}_e + \boldsymbol{r}_1). \tag{5.60}$$

Taking into account closed-loop error system (5.47)-(5.48)-(5.49), $\left\|\dot{\boldsymbol{\zeta}}_e\right\|^2$ bound given by Proposition 5.2.1, and assuming $\mathfrak{c}$ to be positive gives

$$\frac{d}{dt}\left(\mathfrak{b}\boldsymbol{\omega}_e^T J\boldsymbol{\omega}_e\right) = -2\mathfrak{b}\kappa_1\boldsymbol{\zeta}_e(t-d(t))^T\boldsymbol{\omega}_e - 2\mathfrak{b}\kappa_2\boldsymbol{\omega}_e^T\boldsymbol{\omega}_e, \tag{5.61}$$

$$\begin{aligned} \frac{d}{dt}\left(2\mathfrak{c}\boldsymbol{\zeta}_e^T J\boldsymbol{\omega}_e\right) &= 2\mathfrak{c}\boldsymbol{\omega}_e^T J\dot{\boldsymbol{\zeta}}_e + 2\mathfrak{c}\boldsymbol{\zeta}_e^T\left[-\kappa_1\boldsymbol{\zeta}_e(t-d(t)) - \kappa_2\boldsymbol{\omega}_e\right] \\ &\leq \mathfrak{c}\left[\boldsymbol{\omega}_e^T J\boldsymbol{\omega}_e + \dot{\boldsymbol{\zeta}}_e^T J\dot{\boldsymbol{\zeta}}_e\right] - 2\mathfrak{c}\kappa_1\boldsymbol{\zeta}_e^T\boldsymbol{\zeta}_e(t-d(t)) - 2\mathfrak{c}\kappa_2\boldsymbol{\zeta}_e^T\boldsymbol{\omega}_e \qquad (5.62) \\ &= \mathfrak{c}\boldsymbol{\omega}_e^T J\boldsymbol{\omega}_e + \frac{1}{4}(\boldsymbol{\omega}_e + \boldsymbol{r}_1)^T\left(\eta_e\mathbf{I} + [\boldsymbol{\zeta}_e]_\times\right)^T J\left(\eta_e\mathbf{I} + [\boldsymbol{\zeta}_e]_\times\right)(\boldsymbol{\omega}_e + \boldsymbol{r}_1) \\ &- 2\mathfrak{c}\kappa_1\boldsymbol{\zeta}_e^T\boldsymbol{\zeta}_e(t-d(t)) - 2\mathfrak{c}\kappa_2\boldsymbol{\zeta}_e^T\boldsymbol{\omega}_e \\ &\leq \mathfrak{c}\boldsymbol{\omega}_e^T J\boldsymbol{\omega}_e + \frac{1}{4}\mathfrak{c}\left(\|\eta_e\| + \|\boldsymbol{\zeta}_e\|\right)^2 M_J(\boldsymbol{\omega}_e + \boldsymbol{r}_1)^T(\boldsymbol{\omega}_e + \boldsymbol{r}_1) \\ &- 2\mathfrak{c}\kappa_1\boldsymbol{\zeta}_e^T\boldsymbol{\zeta}_e(t-d(t)) - 2\mathfrak{c}\kappa_2\boldsymbol{\zeta}_e^T\boldsymbol{\omega}_e \\ &\leq -2\mathfrak{c}\kappa_1\boldsymbol{\zeta}_e^T\boldsymbol{\zeta}_e(t-d(t)) - 2\mathfrak{c}\kappa_2\boldsymbol{\zeta}_e^T\boldsymbol{\omega}_e + \mathfrak{c}\boldsymbol{\omega}_e^T(J + M_J\mathbf{I})\boldsymbol{\omega}_e \\ &+ 2\mathfrak{c}\boldsymbol{\omega}_e^T M_J\mathbf{I}\boldsymbol{r}_1 + \mathfrak{c}\boldsymbol{r}_1^T M_J\mathbf{I}\boldsymbol{r}_1. \qquad (5.63) \end{aligned}$$

Note that $\boldsymbol{\omega}_e^T JJ^T\boldsymbol{\omega}_e + \dot{\boldsymbol{\zeta}}_e^T\dot{\boldsymbol{\zeta}}_e$, rather than $\boldsymbol{\omega}_e^T J\boldsymbol{\omega}_e + \dot{\boldsymbol{\zeta}}_e^T J\dot{\boldsymbol{\zeta}}_e$, could have been used to bound $2\boldsymbol{\omega}_e^T J\dot{\boldsymbol{\zeta}}_e$ in inequality (5.62). The resulting expression, in this case, would be $\mathfrak{c}\boldsymbol{\omega}_e^T\left(JJ^T + \mathbf{I}\right)\boldsymbol{\omega}_e + 2\mathfrak{c}\boldsymbol{\omega}_e^T\boldsymbol{r}_1 + \mathfrak{c}\boldsymbol{r}_1^T\boldsymbol{r}_1$. The latter can be more advantageous in case of large J, since the diagonal element Ω_{99} needs to compensate large M_J, forcing γ to be grow, which means a more conservative disturbance rejection bound. On the other hand, JJ^T too large can compromise feasibility of the LMI because of its presence in diagonal submatrix Ω_{77}. Thus, the choice for $\boldsymbol{\omega}_e^T J\boldsymbol{\omega}_e + \dot{\boldsymbol{\zeta}}_e^T J\dot{\boldsymbol{\zeta}}_e$ is because J is considered small in examples.

Combining (5.61), and (5.63) with (5.60) gives

$$\begin{aligned} \dot{V}_1 \leq& -2\mathfrak{c}\kappa_1\boldsymbol{\zeta}_e^T\boldsymbol{\zeta}_e(t-d(t)) + 2\boldsymbol{\zeta}_e^T(\mathfrak{a} - \mathfrak{c}\kappa_2)\mathbf{I}\boldsymbol{\omega}_e + 2\mathfrak{a}\boldsymbol{\zeta}_e^T\boldsymbol{r}_1 - 2\mathfrak{b}\kappa_1\boldsymbol{\zeta}_e(t-d(t))^T\boldsymbol{\omega}_e \\ &+ \boldsymbol{\omega}_e^T\left[\mathfrak{c}(J + M_J\mathbf{I}) - 2\mathfrak{b}\kappa_2\mathbf{I}\right]\boldsymbol{\omega}_e + 2\mathfrak{c}\boldsymbol{\omega}_e^T M_J\mathbf{I}\boldsymbol{r}_1 + \mathfrak{c}\boldsymbol{r}_1^T M_J\mathbf{I}\boldsymbol{r}_1. \end{aligned} \tag{5.64}$$

The remaining three terms of $\dot{V}$ are given by

$$\dot{V}_2(t) = \begin{bmatrix} \boldsymbol{\zeta}_e(t) \\ \boldsymbol{\zeta}_e\left(t-\frac{\tau}{2}\right) \end{bmatrix}^T M \begin{bmatrix} \boldsymbol{\zeta}_e \\ \boldsymbol{\zeta}_e\left(t-\frac{\tau}{2}\right) \end{bmatrix} - \begin{bmatrix} \boldsymbol{\zeta}_e\left(t-\frac{\tau}{2}\right) \\ \boldsymbol{\zeta}_e(t-\tau) \end{bmatrix}^T M \begin{bmatrix} \boldsymbol{\zeta}_e\left(t-\frac{\tau}{2}\right) \\ \boldsymbol{\zeta}_e(t-\tau) \end{bmatrix}$$

$$+\begin{bmatrix}\boldsymbol{\zeta}_e(t-\tau)\\ \boldsymbol{\zeta}_e(t-\mu)\end{bmatrix}^T N\begin{bmatrix}\boldsymbol{\zeta}_e(t-\tau)\\ \boldsymbol{\zeta}_e(t-\mu)\end{bmatrix}-\begin{bmatrix}\boldsymbol{\zeta}_e(t-\mu)\\ \boldsymbol{\zeta}_e(t-\nu)\end{bmatrix}^T N\begin{bmatrix}\boldsymbol{\zeta}_e(t-\mu)\\ \boldsymbol{\zeta}_e(t-\nu)\end{bmatrix}, \tag{5.65}$$

$$\dot{V}_3(t)=\tau^2\dot{\boldsymbol{\zeta}}_e(t)^T\mathfrak{r}\dot{\boldsymbol{\zeta}}_e(t)-\tau\int_{t-\tau}^{t}\dot{\boldsymbol{\zeta}}_e(s)^T\mathfrak{r}\mathbf{I}\dot{\boldsymbol{\zeta}}_e(s)\,ds, \tag{5.66}$$

$$\dot{V}_4(t)=\dot{V}_{4(0)}(t)+\dot{V}_{4(I)}(t),$$

$$\dot{V}_{4(0)}(t)=(\mu-\tau)^2\dot{\boldsymbol{\zeta}}_e(t)^T\mathfrak{s}\dot{\boldsymbol{\zeta}}_e(t)+(\nu-\mu)^2\dot{\boldsymbol{\zeta}}_e(t)^T\mathfrak{t}\dot{\boldsymbol{\zeta}}_e(t), \tag{5.67}$$

$$\dot{V}_{4(I)}(t)=-(\mu-\tau)\int_{t-\mu}^{t-\tau}\dot{\boldsymbol{\zeta}}_e(s)^T\mathfrak{s}\mathbf{I}\dot{\boldsymbol{\zeta}}_e(s)\,ds-(\nu-\mu)\int_{t-\eta}^{t-\mu}\dot{\boldsymbol{\zeta}}_e(s)^T\mathfrak{t}\mathbf{I}\dot{\boldsymbol{\zeta}}_e(s)\,ds. \tag{5.68}$$

Jensen's Inequality (Lemma II.0.3) and Proposition 5.2.1 allow to conclude that

$$\begin{aligned}\dot{V}_3&\le\tau^2\dot{\boldsymbol{\zeta}}_e(t)^T\mathfrak{r}\dot{\boldsymbol{\zeta}}_e(t)-\left[\int_{t-\tau}^{t}\dot{\boldsymbol{\zeta}}_e(s)\,ds\right]^T\mathfrak{r}\mathbf{I}\left[\int_{t-\tau}^{t}\dot{\boldsymbol{\zeta}}_e(s)\,ds\right]\\&\le\frac{\tau^2\mathfrak{r}}{4}\left(\boldsymbol{\omega}_e^T\boldsymbol{\omega}_e+2\boldsymbol{\omega}_e^T\boldsymbol{r}_1+\boldsymbol{r}_1^T\boldsymbol{r}_1\right)+\begin{bmatrix}\boldsymbol{\zeta}_e(t)\\ \boldsymbol{\zeta}_e(t-\tau)\end{bmatrix}^T\begin{bmatrix}-\mathfrak{r}\mathbf{I}&\mathfrak{r}\mathbf{I}\\ \mathfrak{r}\mathbf{I}&-\mathfrak{r}\mathbf{I}\end{bmatrix}\begin{bmatrix}\boldsymbol{\zeta}_e(t)\\ \boldsymbol{\zeta}_e(t-\tau)\end{bmatrix}\end{aligned} \tag{5.69}$$

$$\dot{V}_{4(0)}\le\left[\frac{(\mu-\tau)^2\mathfrak{s}+(\nu-\mu)^2\mathfrak{t}}{4}\right]\left(\boldsymbol{\omega}_e^T\boldsymbol{\omega}_e+2\boldsymbol{\omega}_e^T\boldsymbol{r}_1+\boldsymbol{r}_1^T\boldsymbol{r}_1\right). \tag{5.70}$$

Instead of rushing to bound (5.68) using Jensen's Inequality, which would hinder convex techniques (Section 4.4.3) from being used, the analysis is broken in two by taking into account two distinct delay scenarios $\mathbb{S}_1$ and $\mathbb{S}_2$, corresponding to subintervals $[\tau,\mu]$ and $(\mu,\nu]$, respectively, similarly to (5.17). Based on $\mathbb{S}_1$ and $\mathbb{S}_2$, indicator function χ (4.10) allows $\dot{V}_{4(I)}$ to be rewritten as the sum of two mutually exclusive terms $\dot{V}_{4(\mathbb{S}_1)}$ and $\dot{V}_{4(\mathbb{S}_2)}$, and the integral term in (5.68) can be divided to explore convexity. Namely, for the first scenario,

$$\begin{aligned}\dot{V}_{4(\mathbb{S}_1)}(t)=-\chi(d(t))\Bigg[&(\mu-\tau)\int_{t-\mu}^{t-d(t)}\dot{\boldsymbol{\zeta}}_e(s)^T\mathfrak{s}\mathbf{I}\dot{\boldsymbol{\zeta}}_e(s)\,ds+(\mu-\tau)\int_{t-d(t)}^{t-\tau}\dot{\boldsymbol{\zeta}}_e(s)^T\mathfrak{s}\dot{\boldsymbol{\zeta}}_e(s)\,ds\\&+(\nu-\mu)\int_{t-\nu}^{t-\mu}\dot{\boldsymbol{\zeta}}_e(s)^T\mathfrak{t}\mathbf{I}\dot{\boldsymbol{\zeta}}_e(s)\,ds\Bigg].\end{aligned} \tag{5.71}$$

The convexity of $\dot{V}_4$'s bound becomes clearer when auxiliary states $\boldsymbol{\xi}_{11}$ and $\boldsymbol{\xi}_{12}$ are defined, as in (5.20). Therefore, taking $\dot{V}_{4(0)}$ bound (5.70) into account and applying Jensen's Inequality (Lemma II.0.3) to bound (5.71), gives

$$\begin{aligned}\dot{V}_4\le&\left[\frac{(\mu-\tau)^2\mathfrak{s}+(\nu-\mu)^2\mathfrak{t}}{4}\right]\left(\boldsymbol{\omega}_e^T\boldsymbol{\omega}_e+2\boldsymbol{\omega}_e^T\boldsymbol{r}_1+\boldsymbol{r}_1^T\boldsymbol{r}_1\right)-\chi\left\{\boldsymbol{\xi}_{11}^T(\mathbb{D}_1\mathfrak{s}\mathbf{I})\boldsymbol{\xi}_{11}\right.\\&\left.+\boldsymbol{\xi}_{12}^T(1-\mathbb{D}_1)\mathfrak{s}\mathbf{I}\boldsymbol{\xi}_{12}+[\boldsymbol{\zeta}_e(t-\mu)-\boldsymbol{\zeta}_e(t-\nu)]^T\mathfrak{t}\mathbf{I}[\boldsymbol{\zeta}_e(t-\mu)-\boldsymbol{\zeta}_e(t-\nu)]\right\},\end{aligned} \tag{5.72}$$

which is convex with respect to $d(t)$ because

$$\mathbb{D}_1(d(t)):=\frac{d(t)-\tau}{\mu-\tau}\in[0,1],$$

is convex with respect to $d(t)$. Thus, $\dot{V}_4$'s bound (5.72) reaches its maximum at the edges of $\mathbb{D}_1$, 0 or 1. Since at each extremum of $\mathbb{D}_1$, either $\boldsymbol{\xi}_{11}$ or $\boldsymbol{\xi}_{12}$ will be weighted by a zero matrix, define

$$\tilde{\boldsymbol{\vartheta}}_{1l}{:=}\begin{bmatrix} \boldsymbol{\zeta}_e^T & \boldsymbol{\zeta}_e\left(t-\frac{\tau}{2}\right)^T & \boldsymbol{\zeta}_e\left(t-\tau\right)^T & \boldsymbol{\zeta}_e\left(t-\mu\right)^T & \boldsymbol{\zeta}_e\left(t-\nu\right)^T & \boldsymbol{\zeta}_e\left(t-d\left(t\right)\right)^T & \boldsymbol{\omega}_e^T & \boldsymbol{\xi}_{1l}^T & \boldsymbol{r}_1^T \end{bmatrix}^T, l{\in}\{1,2\},$$

and let $\tilde{\Omega}$ be such that

$$\tilde{\Omega}{=}\bar{\Omega}+\Omega_1|_{\mathbb{D}_1},$$

with $\bar{\Omega}$ and $\Omega_1|_{\overline{\mathbb{D}}_1}$ given by (5.57) and (5.58), respectively. Combining bounds (5.64), (5.65), (5.69) and (5.72), it follows that for both extrema

$$\dot{V}{\leq}\tilde{\boldsymbol{\vartheta}}_{1l}^T\tilde{\Omega}\tilde{\boldsymbol{\vartheta}}_{1l}, l{\in}\{1,2\}.$$

According to condition 1 from definition 5.1.4, for the closed-loop to achieve H_∞ performance, it must be asymptotically stable when $\boldsymbol{r}_1$ is zero. Denote $\tilde{\Omega}_{8\times8}$ the upper-left eight-by-eight block of $\tilde{\Omega}$ such that

$$\tilde{\Omega}{=}\begin{bmatrix} \tilde{\Omega}_{8\times8} & \tilde{\Omega}_{9\times1} \\ * & \Omega_{99} \end{bmatrix},$$

with

$$\tilde{\Omega}_{9\times1}{=}\begin{bmatrix} \Omega_{19}^T & \mathbf{0} & \mathbf{0} & \mathbf{0} & \mathbf{0} & \mathbf{0} & \Omega_{79}^T & \mathbf{0} \end{bmatrix}^T,$$

and define

$$\Omega{=}\begin{bmatrix} \Omega_{8\times8} & \tilde{\Omega}_{9\times1} \\ * & \Omega_{99} \end{bmatrix}$$

with

$$\Omega_{8\times8}{=}\tilde{\Omega}_{8\times8}-\text{diag}\{\mathbf{I},\mathbf{0}\}.$$

Assuming $\boldsymbol{r}_1$ is zero, it follows that

$$\dot{V}{\leq}\boldsymbol{\vartheta}_{1l}^T\Omega_{8\times8}\boldsymbol{\vartheta}_{1l},$$

where

$$\boldsymbol{\vartheta}_{1l}{=}\begin{bmatrix} \boldsymbol{\zeta}_e^T & \boldsymbol{\zeta}_e\left(t-\frac{\tau}{2}\right)^T & \boldsymbol{\zeta}_e\left(t-\tau\right)^T & \boldsymbol{\zeta}_e\left(t-\mu\right)^T & \boldsymbol{\zeta}_e\left(t-\nu\right)^T & \boldsymbol{\zeta}_e\left(t-d\left(t\right)\right)^T & \boldsymbol{\omega}_e^T & \boldsymbol{\xi}_{1l}^T \end{bmatrix}^T, l{\in}\{1,2\}.$$

Consequently, if $\Omega_{8\times8}$ is negative definite, the closed-loop system is asymptotically stable. Note, however, that if $\tilde{\Omega}$ is negative definite, then so is $\Omega_{8\times8}$. This can be seen using a Schur-complement-type argument: from Lemma II.0.2, if Ω is negative definite, then so is $\Omega_{8\times8}-\tilde{\Omega}_{9\times1}^T\Omega_{99}\tilde{\Omega}_{9\times1}$. Nonetheless, since Ω is negative definite, so must be Ω_{99}, which implies that

$$\Omega_{8\times8}{\leq}\Omega_{8\times8}-\tilde{\Omega}_{9\times1}^T\Omega_{99}\tilde{\Omega}_{9\times1}{<}0.$$

Since

$$\Omega{=}\tilde{\Omega}-\text{diag}\left\{\mathbf{I},\mathbf{0}\right\}{\leq}\tilde{\Omega},$$

if $\tilde{\Omega}$ is negative definite, then so is $\Omega_{8\times8}$.

From Finsler's Lemma (Lemma II.0.1), $\tilde{\Omega}$ is negative definite if, and only if, $\tilde{\Omega}+\mathscr{F}_1\mathscr{G}_1+\mathscr{G}_1^T\mathscr{F}_1^T$ is negative definite, where $\mathscr{F}_1$ is a free-weighting matrix and $\mathscr{G}_1$ is given by (5.59). Since,

$\tilde{\boldsymbol{\vartheta}}\left(\tilde{\Omega}+\mathscr{F}_1\mathscr{G}_1+\mathscr{G}_1^T\mathscr{F}_1^T\right)\tilde{\boldsymbol{\vartheta}}$ remains convex with respect to $d(t)$, $\tilde{\Omega}+\mathscr{F}_1\mathscr{G}_1+\mathscr{G}_1^T\mathscr{F}_1^T$ need be negative definite only at the extrema of $\mathbb{D}_1$. Therefore, if (5.56) holds, the error closed-loop system is asymptotically stable. The second scenario $\mathbb{S}_2$ is amenable to similar arguments. Thus, closed-loop system (5.47)-(5.49) is asymptotically stable when $\boldsymbol{r}_1$ is zero, and condition 1 from Definition 5.1.4 is satisfied.

Therefore, it remains to prove the second condition from Definition 5.1.4 is also valid. Assuming $\boldsymbol{r}_1$ is nonzero, and using (5.56), gives

$$\dot{V}+\boldsymbol{\zeta}_e^T\boldsymbol{\zeta}_e+\boldsymbol{r}_1^T\boldsymbol{r}_1<0. \tag{5.73}$$

Since V is positive definite and $\dot{V}$ is negative definite, assuming null initial conditions, integrating (5.73) gives

$$\int_0^{+\infty}\boldsymbol{\zeta}_e^T\boldsymbol{\zeta}_e<\gamma^2\int_0^{+\infty}\boldsymbol{r}_1^T\boldsymbol{r}_1,$$

that is,

$$\|\boldsymbol{\zeta}_e\|_2^2\leq\|\boldsymbol{r}_1\|_2^2\,,\forall t\geq 0.$$

□

5.2.1.1 Experimental Analysis

Since Theorem 5.2.3 ensures the same disturbance attenuation bounds regardless of the trajectory to be followed, it is reasonable to question whether this also holds in practice. Considering disturbance behavior $\boldsymbol{r}_1$ in Table 5.4, the stabilization disturbance rejection performance is compared with actual tracking's. The desired trajectory evolves according to $\dot{\boldsymbol{\omega}}_{\mathcal{B}}$, also in Table 5.4, and initial conditions of the desired trajectory expressed in body frame $\mathcal{B}$ are assumed

$$\boldsymbol{q}_d(0)=\begin{bmatrix}0.298 & -0.536 & 0.318 & 0.723\end{bmatrix},\quad \boldsymbol{\omega}_{\mathcal{B}}=\begin{bmatrix}0 & 0.1 & 0.05\end{bmatrix}.$$

Note that the rigid body's initial conditions must match the desired trajectory's since Theorem 5.2.3 assumes zero initial conditions, i.e., $\boldsymbol{q}_e$ and $\boldsymbol{\omega}_e$ must equal $\mathbf{1}$ and $\mathbf{0}$, respectively. Attitude feedback time-delays are considered uniformly distributed between 0 and 100 milliseconds, and the rigid body's inertia is deemed [22]

$$J=10^{-2}*\begin{bmatrix}4.65 & -0.07 & 0.04\\ -0.07 & 4.86 & -0.21\\ 0.04 & -0.21 & 4.82\end{bmatrix}.$$

In addition, assume control gains κ_1 equal to 5 and κ_2 equal to 1.

Table 5.4: Exogenous disturbance $\boldsymbol{r}_1(t)$ and desired trajectory's acceleration $\dot{\boldsymbol{\omega}}_{\mathcal{B}}$.

$t\,[s]$	$0\leq t\leq 10$	$10\leq t\leq 20$	$20\leq t\leq 30$	$30\leq t\leq 60$
$\boldsymbol{r}_1(t)$	$0.07\sin(1.25\pi t)$	$0.1+\mathcal{N}\left(0,3*10^{-4}\right)$	$0.1\sin(0.75\pi t)+\mathcal{N}\left(0,5*10^{-5}\right)$	$\mathcal{N}(0,0.035)$
$\dot{\boldsymbol{\omega}}_{\mathcal{B}}(t)$	$0.3\sin(1.25t)$	0.01	$0.07\sin(0.75t)$	$0.05\sin(t)$

Experimental disturbance rejection, calculated using numerical integration through MATLAB function *trapz*, is 0.1275, which is less than theoretical H_∞ norm bound of 1.0063. The experimental figure confirms the visual intuition from Figure 5.3a that, even in the stabilizing case, taken rigid body's dynamics into account impairs the controller's ability to reject disturbances compared with the kinematic controller. Performance deteriorates further with actual tracking, as it can be seen in Figure 5.3b, with γ_{exp} of 0.1862.

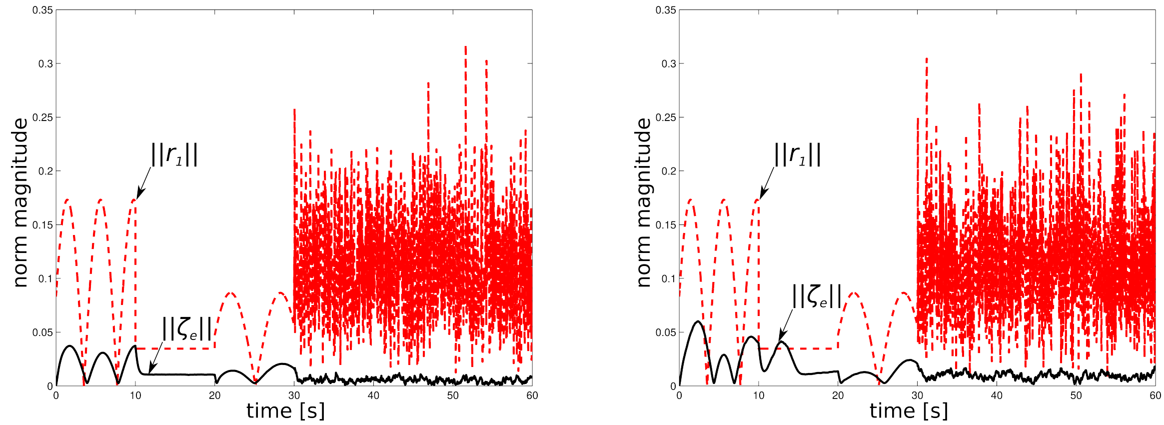

(a) Stabilization. (b) Tracking.

Figure 5.3: $\|\zeta_e\|$ and $\|\boldsymbol{r}_1\|$ norms.

Since the desired trajectory is not continuous and simulation duration is not long, part of the error norm could be attributed to asymptotic stability. Thus, removing disturbances indicates the contribution of actual tracking error to poor disturbance rejection and, consequently, show how well can the rigid body follow the desired trajectory. Numerical integration provides $\|\zeta_e\|$ equal to 0.0982, which, as depicted in Figure 5.4a, confirms that part of the deterioration in disturbance rejection performance is because of tracking errors.

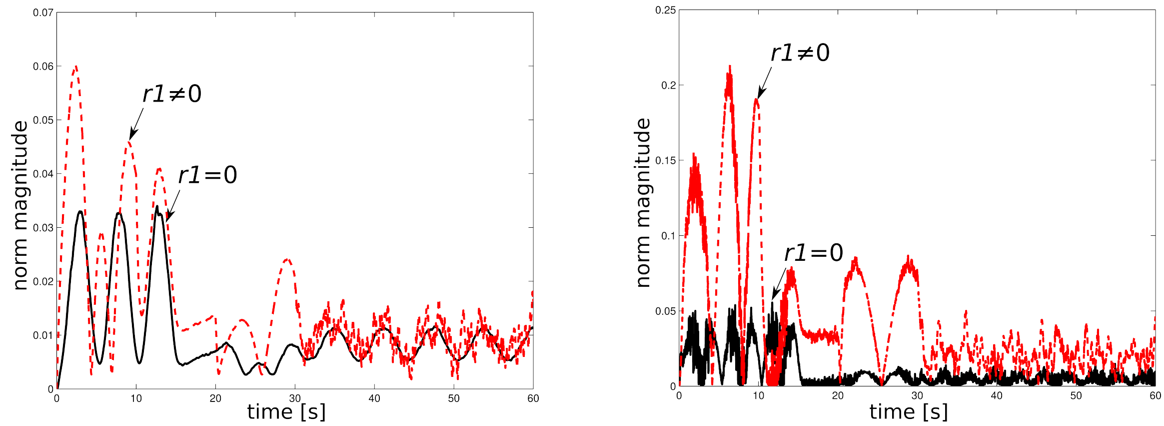

(a) Tracking $\|\zeta_e\|$. (b) Tracking $\|\boldsymbol{\omega}_e\|$.

Figure 5.4: Tracking errors with and without disturbances.

Note, however, norm magnitude spikes occur because $\dot{\boldsymbol{\omega}}_{\mathcal{B}}$ is discontinuous and contribute to error norm as well, as shown in Figure 5.5a. Indeed, as the trajectories move away from discontinuities, the bounces tend to decrease, which is evidenced by Figure 5.5b, and the rigid body successfully follows the desired trajectories.

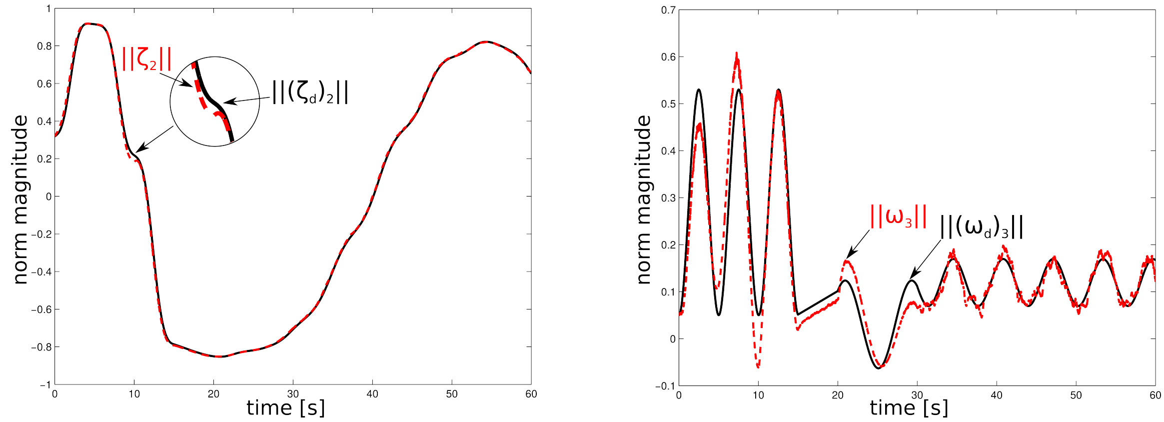

(a) $\boldsymbol{\zeta}_2$ and $(\boldsymbol{\zeta}_d)_2$.

(b) $\boldsymbol{\omega}_d$ and $\boldsymbol{\omega}$ under disturbance.

Figure 5.5: Desired and actual trajectories.

5.2.2 Robust Dynamic Stabilization

This subsection addresses model-independent dynamic stability subjected to heterogeneous measurement delays. By heterogeneous delays, it is meant that d_1 and d_2, the attitude and angular velocity measurement delays, are independent delays and may have different bounds, such that

$$\begin{aligned} 0 \leq \tau_1 \leq d_1(t) \leq \nu_1, t \geq 0, \\ 0 \leq \tau_2 \leq d_2(t) \leq \nu_2, t \geq 0. \end{aligned} \tag{5.74}$$

As it will be seen, asymptotic stability can be achieved without information of matrix inertia J. The only assumption is the existence of known norm bounds M_J and m_J to J, i.e.,

$$m_J \leq \lambda_{\min}(J) \leq \|J\| = \lambda_{\max}(J) \leq M_J. \tag{5.75}$$

Let κ_1, κ_2 be positive real numbers, and consider PD control law

$$\boldsymbol{u}(t) = -\kappa_1 \boldsymbol{\zeta}_{d_1} - \kappa_2 \boldsymbol{\omega}_{d_2}, \tag{5.76}$$

where $\boldsymbol{\zeta}_{d_1}$ denotes $\boldsymbol{\zeta}(t - d_1(t))$ and $\boldsymbol{\omega}_{d_2}$ denotes $\boldsymbol{\omega}(t - d_2(t))$. Assuming controller (5.76) is used, the closed-loop rigid body's dynamics equation can be rewritten as

$$J\dot{\boldsymbol{\omega}} = -[\boldsymbol{\omega}]_\times J\boldsymbol{\omega} - \kappa_1 \boldsymbol{\zeta}_{d_1} - \kappa_2 \boldsymbol{\omega}_{d_2}. \tag{5.77}$$

The following results will support the arguments used to prove stability in this subsection.

Proposition 5.2.4. *Given positive definite matrix P in $\mathbb{S}^n$, $\boldsymbol{x}$ and $\boldsymbol{y}$ in $\mathbb{R}^n$, then*

$$2\boldsymbol{x}^T\boldsymbol{y} \leq \boldsymbol{x}^T P \boldsymbol{x} + \boldsymbol{y}^T P^{-1} \boldsymbol{y}$$

holds.

Proof. Since P is positive definite, there exists[1] an invertible $P^{\frac{1}{2}}$ such that P equals $\left(P^{\frac{1}{2}}\right)^2$, and it follows that

$$0 \leq \left(P^{\frac{1}{2}}\boldsymbol{x} - P^{-\frac{1}{2}}\boldsymbol{y}\right)^T \left(P^{\frac{1}{2}}\boldsymbol{x} - P^{-\frac{1}{2}}\boldsymbol{y}\right) = \boldsymbol{x}^T P\boldsymbol{x} - 2\boldsymbol{x}^T\boldsymbol{y} + \boldsymbol{y}^T P^{-1}\boldsymbol{y}.$$

□

Lemma 5.2.5. *[22]Consider dynamics*

$$J\dot{\boldsymbol{\omega}} = -\left[\boldsymbol{\omega}\right]_\times J\boldsymbol{\omega} + \boldsymbol{u},$$

with positive definite J in $\mathbb{S}^n$, $\boldsymbol{\omega}$ in $\mathbb{R}^3$ and $\boldsymbol{u}(t)$ a continuous map from $\mathbb{R}_{\geq 0}$ into $\mathbb{R}^3$, bounded by positive constant M_u for t greater than or equal to t_0. Then, for t_0 greater than zero, and t greater than t_0,

$$\boldsymbol{\omega}(t)^T J\boldsymbol{\omega}(t) \leq \left(\boldsymbol{\omega}(0)^T J\boldsymbol{\omega}(0)\right) e^{t-t_0} + M_u^2 m_J^{-1}\left(e^{t-t_0} - 1\right) \tag{5.78}$$

holds.

Proof. Taking the derivative of $\boldsymbol{\omega}(t)^T J\boldsymbol{\omega}(t)$ yields

$$2\boldsymbol{\omega}(t)^T J\dot{\boldsymbol{\omega}}(t) = 2\boldsymbol{\omega}(t)^T\left(-\left[\boldsymbol{\omega}(t)\right]_\times J\boldsymbol{\omega}(t) + \boldsymbol{u}(t)\right) = 2\boldsymbol{\omega}(t)^T\boldsymbol{u}(t).$$

Then, Proposition 5.2.4 gives

$$2\boldsymbol{\omega}(t)^T\boldsymbol{u}(t) \leq \boldsymbol{\omega}(t)^T J\boldsymbol{\omega}(t) + \boldsymbol{u}(t)^T J^{-1}\boldsymbol{u}(t) \leq \boldsymbol{\omega}(t)^T J\boldsymbol{\omega}(t) + m_J^{-1}M_u^2.$$

Substituing $2\boldsymbol{\omega}(t)^T\boldsymbol{u}(t)$ for $2\boldsymbol{\omega}(t)^T J\dot{\boldsymbol{\omega}}(t)$, and integrating the previous inequality, one recovers (5.78). □

Up to this point, results have been proved using Lyapunov-Krasovskii arguments, where an LKF is built, and its derivative is shown to be upper bounded by some negative definite matrix, which allows Lyapunov-Krasovskii Theorem to be used. When angular velocity delays are considered, however, some technical issues arise. So far, the device used to introduce terms $-\boldsymbol{\zeta}^T\boldsymbol{\zeta}$ and $-\boldsymbol{\zeta}_{d_1}^T\boldsymbol{\zeta}_{d_1}$, has been the integral $\int_{-\nu}^{0}\int_{t+l}^{t}\dot{\boldsymbol{\zeta}}^T\dot{\boldsymbol{\zeta}}$. The term $\dot{\boldsymbol{\zeta}}^T\dot{\boldsymbol{\zeta}}$ also arises, which can be handled because nonlinear kinematics is linearly bounded. For the dynamic case, a similar procedure would introduce $\dot{\boldsymbol{\omega}}^T\dot{\boldsymbol{\omega}}$. This quadratic form, however, can only be bounded by something proportional to $\|\boldsymbol{\omega}\|^4$, because of gyroscopic term $\left[\boldsymbol{\omega}\right]_\times J\boldsymbol{\omega}$. Thus, a different approach is needed. The next lemma provides another path to determine stability.

Lemma 5.2.6. *Barbalat's Lemma [29]*

Let $f : \mathbb{R} \to \mathbb{R}$ be a uniformly continuous map on $[0, +\infty)$, and suppose $\lim_{t\to+\infty}\int_0^t f(s)\,ds$ exists and is finite. Then,

$$\lim_{t\to+\infty} f(t) = 0.$$

[1]Consider the diagonal decomposition $Q^T DQ$ of P and take $P^{\frac{1}{2}}$ as $Q^T D^{\frac{1}{2}}Q$, where $D^{\frac{1}{2}}$ corresponds to the diagonal matrix composed of the square roots of P eigenvalues. Since P is positive definite, all eigenvalues are positive and $P^{\frac{1}{2}}$ is invertible.

Although the proof of stability will rely on Barbalat's lemma instead of Lyapunov-Krasovskii theorem, a positive definite functional of states $\boldsymbol{x}_t$ is also necessary. Thus, consider energy-like function

$$V = \sum_{i=1}^{3} V_i, \tag{5.79}$$

with

$$V_1 = 2\mathfrak{a}\left[\boldsymbol{\zeta}^T\boldsymbol{\zeta} + (1-\eta)^2\right] + \mathfrak{b}\boldsymbol{\omega}^T J\boldsymbol{\omega} + 2\mathfrak{c}\boldsymbol{\zeta}^T J\boldsymbol{\omega}, \tag{5.80}$$

$$V_2 = \nu_1\mathfrak{p}_1\int_{-\nu_1}^{0}\int_{t+l}^{t}\dot{\boldsymbol{\zeta}}(s)^T\dot{\boldsymbol{\zeta}}(s)\,ds dl + \nu_2\mathfrak{p}_2\int_{-\nu_2}^{0}\int_{t+l}^{t}\dot{\boldsymbol{\omega}}(s)^T\dot{\boldsymbol{\omega}}(s)\,ds dl, \tag{5.81}$$

real number $\mathfrak{c}$ and positive real numbers $\mathfrak{a}, \mathfrak{b}, \mathfrak{p}_1, \mathfrak{p}_2$ and $\mathfrak{r}$.

Because of cross term $\mathfrak{c}\boldsymbol{\zeta}^T J\boldsymbol{\omega}$, the positivity of term V_1 (5.80) is not ensured if real numbers $\mathfrak{a}$ and $\mathfrak{b}$ are greater than zero (even if $\mathfrak{c}$ is positive). Indeed, using quadratic inequality from Proposition 5.1.1, cross-term bound from Proposition 5.2.2 and $\lambda_{\max}(J)$ bound M_J (5.75), gives

$$\begin{aligned}
V_1 &= 2\mathfrak{a}\left[\boldsymbol{\zeta}^T\boldsymbol{\zeta} + (1-\eta)^2\right] + \mathfrak{b}\boldsymbol{\omega}^T J\boldsymbol{\omega} + 2\mathfrak{c}\boldsymbol{\zeta}^T J\boldsymbol{\omega} \\
&\geq 2\mathfrak{a}\boldsymbol{\zeta}^T\boldsymbol{\zeta} + \mathfrak{b}\boldsymbol{\omega}^T J\boldsymbol{\omega} + 2\mathfrak{c}\boldsymbol{\zeta}^T J\boldsymbol{\omega} \\
&\geq \frac{2}{\lambda_{\max}(J)}\mathfrak{a}\boldsymbol{\zeta}^T J\boldsymbol{\zeta} + \mathfrak{b}\boldsymbol{\omega}^T J\boldsymbol{\omega} - |\mathfrak{c}|\,\boldsymbol{\zeta}^T J\boldsymbol{\zeta} - |\mathfrak{c}|\,\boldsymbol{\omega}^T J\boldsymbol{\omega} \\
&\geq \frac{2}{M_J}\mathfrak{a}\boldsymbol{\zeta}^T J\boldsymbol{\zeta} + \mathfrak{b}\boldsymbol{\omega}^T J\boldsymbol{\omega} - |\mathfrak{c}|\,\boldsymbol{\zeta}^T J\boldsymbol{\zeta} - |\mathfrak{c}|\,\boldsymbol{\omega}^T J\boldsymbol{\omega} \\
&= \left(\frac{2}{M_J}\mathfrak{a} - |\mathfrak{c}|\right)\boldsymbol{\zeta}^T J\boldsymbol{\zeta} + (\mathfrak{b} - |\mathfrak{c}|)\,\boldsymbol{\omega}^T J\boldsymbol{\omega}.
\end{aligned}$$

Note that $\mathfrak{c}$ need not be positive, but $|\mathfrak{c}|$must be taken to lower bound cross-term $2\mathfrak{c}\boldsymbol{\zeta}^T J\boldsymbol{\omega}$. Thus, for V to be positive, the constraints

$$\mathfrak{a} > 0, \quad 2\mathfrak{a} > M_J\,|\mathfrak{c}|, \quad \mathfrak{b} > 0, \quad \mathfrak{b} > |\mathfrak{c}|, \quad \mathfrak{p}_1 > 0, \quad \mathfrak{p}_2 > 0, \tag{5.82}$$

must hold.

Theorem 5.2.7. *Let τ_1, τ_2, ν_1 and ν_2 be nonnegative real numbers satisfying delay bounds* (5.74)*, let M_ω be a positive real number such that $\|\boldsymbol{\omega}(t)\|$ is less than or equal to M_ω for all t in $[-\nu, 0]$, where ν is given by* $\max\{\nu_1, \nu_2\}$*, and consider parameter $M_{\mathfrak{p}_2}$ a positive real number. Then, if there exist real numbers $\mathfrak{a}, \mathfrak{b}, \mathfrak{c}, \mathfrak{p}_1$, and $\mathfrak{p}_2$ such that* (5.82)*,*

$$\Omega = \begin{bmatrix} \Omega_{11} & \Omega_{12} & \Omega_{13} & \Omega_{14} \\ * & \Omega_{22} & \Omega_{23} & \Omega_{24} \\ * & * & \Omega_{33} & \Omega_{34} \\ * & * & * & \Omega_{44} \end{bmatrix} < 0, \tag{5.83}$$

and

$$m_J^{-1} < \mathfrak{b}, \quad \mathfrak{p}_2 < M_{\mathfrak{p}_2}, \quad M_V < \mathfrak{m}, \tag{5.84}$$

hold, where

$$\Omega_{11} = -\mathfrak{p}_1\mathbf{I}, \qquad \Omega_{22} = \left(m_J^{-2}(1+\kappa_1)\kappa_1\nu_2^2\mathfrak{p}_2 - \mathfrak{p}_1\right)\mathbf{I},$$

$$\begin{aligned}
&\Omega_{12}{=}(\mathfrak{p}_1-\kappa_1\mathfrak{c})\,\mathbf{I}, && \Omega_{24}{=}m_J^{-2}\nu_2^2\kappa_1\kappa_2\mathfrak{p}_2\mathbf{I},\\
&\Omega_{13}{=}\mathfrak{a}\mathbf{I}, && \Omega_{33}{=}\left(\frac{\nu_1^2}{4}\mathfrak{p}_1+4M_J\left|\mathfrak{c}\right|+\frac{\nu_2^2}{m_J^2}\left(M_J^2-m_J^2\right)\left(1+\kappa_1+\kappa_2\right)M_{\mathfrak{p}_2}\mathfrak{m}-\mathfrak{p}_2\right)\mathbf{I},\\
&\Omega_{14}{=}-\kappa_2\mathfrak{c}\mathbf{I}, && \Omega_{34}{=}(\mathfrak{p}_2-\kappa_2\mathfrak{b})\,\mathbf{I},\\
&\Omega_{23}{=}-\kappa_1\mathfrak{b}\mathbf{I}, && \Omega_{44}{=}\left(m_J^{-2}\left(1+\kappa_2\right)\kappa_2\nu_2^2-1\right)\mathfrak{p}_2\mathbf{I},
\end{aligned}$$

$$M_u{=}(\kappa_1+\kappa_2M_\omega)^2\,,\;\; M_{\|\omega\|}{=}\left[e^\tau m_J^{-1}M_JM_\omega^2+(e^\tau-1)\,m_J^{-2}M_u^2\right]^{\frac{1}{2}}\,,\;\; M_1{=}\max\left\{M_{\|\omega\|},M_\omega\right\},$$

$$\begin{aligned}
M_V{=}&8\mathfrak{a}+\left[e^\tau M_JM_\omega^2+(e^\tau-1)\,m_J^{-1}\left(\kappa_1+\kappa_2M_\omega\right)^2\right]\mathfrak{b}+2M_JM_{\|\omega\|}\mathfrak{c}\\
&+\frac{\nu_1^3}{8}M_1^2\mathfrak{p}_1+\frac{\nu_2^3}{2}m_J^{-2}\left(M_J^2M_1^4+2M_JM_1^2M_u+M_u^2\right)\mathfrak{p}_2,
\end{aligned}$$

then closed-loop system (3.14)-(5.77) *is asymptotically stable.*

Proof. The path to prove the theorem is based on a two-step argument. First, using Barbalat's Lemma, a conditional proof of asymptotic stability is given depending on an upper bound of V, which is then obtained in the final part of the argument. The aggregate requirements form the conditions stated by the theorem.

Take V_{1a} and V_{1b}, such that

$$\begin{aligned}
V_{1a}&=2\mathfrak{a}\left[\boldsymbol{\zeta}^T\boldsymbol{\zeta}+(1-\eta)^2\right]+\mathfrak{b}\boldsymbol{\omega}^TJ\boldsymbol{\omega},\\
V_{1b}&=2\mathfrak{c}\boldsymbol{\zeta}^TJ\boldsymbol{\omega}.
\end{aligned}$$

Then, using cross-term bound from Proposition 5.2.2 and quadratic upper bound from Proposition 5.1.1, and substituting (5.1) for $\dot{\boldsymbol{\zeta}}$ and (5.77) for $\dot{\boldsymbol{\omega}}$, results in

$$\begin{aligned}
\dot{V}_{1a}&=\frac{d}{dt}\left\{2\mathfrak{a}\left[\boldsymbol{\zeta}^T\boldsymbol{\zeta}+(1-\eta)^2\right]+\mathfrak{b}\boldsymbol{\omega}^TJ\boldsymbol{\omega}\right\}\\
&=\frac{d}{dt}\left\{2\mathfrak{a}\left[\boldsymbol{\zeta}^T\boldsymbol{\zeta}+1-2\eta+\eta^2\right]\right\}+2\mathfrak{b}\boldsymbol{\omega}^TJ\dot{\boldsymbol{\omega}}\\
&=\frac{d}{dt}\left\{4\mathfrak{a}\left(1-\eta\right)\right\}+2\mathfrak{b}\boldsymbol{\omega}^T\left(-\left[\boldsymbol{\omega}\right]_\times J\boldsymbol{\omega}-\kappa_1\boldsymbol{\zeta}_{d_1}-\kappa_2\boldsymbol{\omega}_{d_2}\right)\\
&=-4\mathfrak{a}\dot{\eta}-2\kappa_1\mathfrak{b}\boldsymbol{\omega}^T\boldsymbol{\zeta}_{d_1}-2\kappa_2\mathfrak{b}\boldsymbol{\omega}^T\boldsymbol{\omega}_{d_2}\\
&=2\mathfrak{a}\boldsymbol{\zeta}^T\boldsymbol{\omega}-2\kappa_1\mathfrak{b}\boldsymbol{\omega}^T\boldsymbol{\zeta}_{d_1}-2\kappa_2\mathfrak{b}\boldsymbol{\omega}^T\boldsymbol{\omega}_{d_2}\\
&=\begin{bmatrix}\boldsymbol{\zeta}\\ \boldsymbol{\zeta}_{d_1}\\ \boldsymbol{\omega}\\ \boldsymbol{\omega}_{d_2}\end{bmatrix}^T\begin{bmatrix}\mathbf{0}&\mathbf{0}&\mathfrak{a}\mathbf{I}&\mathbf{0}\\ *&\mathbf{0}&-\kappa_1\mathfrak{b}\mathbf{I}&\mathbf{0}\\ *&*&\mathbf{0}&-\kappa_2\mathfrak{b}\mathbf{I}\\ *&*&*&\mathbf{0}\end{bmatrix}\begin{bmatrix}\boldsymbol{\zeta}\\ \boldsymbol{\zeta}_{d_1}\\ \boldsymbol{\omega}\\ \boldsymbol{\omega}_{d_2}\end{bmatrix}. \qquad (5.85)\\
\dot{V}_{1b}&=2\mathfrak{c}\dot{\boldsymbol{\zeta}}^TJ\boldsymbol{\omega}+2\mathfrak{c}\boldsymbol{\zeta}^TJ\dot{\boldsymbol{\omega}}\\
&=\mathfrak{c}\boldsymbol{\omega}^T\left(\eta\mathbf{I}+\left[\boldsymbol{\zeta}\right]_\times\right)^TJ\boldsymbol{\omega}+2\mathfrak{c}\boldsymbol{\zeta}^T\left(-\left[\boldsymbol{\omega}\right]_\times J\boldsymbol{\omega}-\kappa_1\boldsymbol{\zeta}_{d_1}-\kappa_2\boldsymbol{\omega}_{d_2}\right)\\
&\leq 2M_J\left|\mathfrak{c}\right|\boldsymbol{\omega}^T\boldsymbol{\omega}-2\mathfrak{c}\boldsymbol{\zeta}^T\left(\left[\boldsymbol{\omega}\right]_\times J\boldsymbol{\omega}\right)-2\kappa_1\mathfrak{c}\boldsymbol{\zeta}^T\boldsymbol{\zeta}_{d_1}-2\kappa_2\mathfrak{c}\boldsymbol{\zeta}^T\boldsymbol{\omega}_{d_2}\\
&\leq 4M_J\left|\mathfrak{c}\right|\boldsymbol{\omega}^T\boldsymbol{\omega}-2\kappa_1\mathfrak{c}\boldsymbol{\zeta}^T\boldsymbol{\zeta}_{d_1}-2\kappa_2\mathfrak{c}\boldsymbol{\zeta}^T\boldsymbol{\omega}_{d_2}
\end{aligned}$$

$$
= \begin{bmatrix} \boldsymbol{\zeta} \\ \boldsymbol{\zeta}_{d_1} \\ \boldsymbol{\omega} \\ \boldsymbol{\omega}_{d_2} \end{bmatrix}^T \begin{bmatrix} \mathbf{0} & -\kappa_1 \mathfrak{c}\mathbf{I} & \mathbf{0} & -\kappa_2 \mathfrak{c}\mathbf{I} \\ * & \mathbf{0} & \mathbf{0} & \mathbf{0} \\ * & * & 4M_J \left|\mathfrak{c}\right| \mathbf{I} & \mathbf{0} \\ * & * & * & \mathbf{0} \end{bmatrix} \begin{bmatrix} \boldsymbol{\zeta} \\ \boldsymbol{\zeta}_{d_1} \\ \boldsymbol{\omega} \\ \boldsymbol{\omega}_{d_2} \end{bmatrix}. \tag{5.86}
$$

Note that, in order to bound the terms $\mathfrak{c}\boldsymbol{\omega}^T \left(\eta\mathbf{I} + [\boldsymbol{\zeta}]_\times\right) J\boldsymbol{\omega}$ and $2\mathfrak{c}\boldsymbol{\zeta}^T \left([\boldsymbol{\omega}]_\times J\boldsymbol{\omega}\right)$,$|\mathfrak{c}|$ must be used, since $\mathfrak{c}$ is not necessarily positive. Indeed, from the unit quaternion norm constraint (5.3) and property $\left\|[\boldsymbol{\zeta}]_\times\right\| \leq \|\boldsymbol{\zeta}\|$ (I.6), it follows that

$$
\begin{aligned}
\mathfrak{c}\boldsymbol{\omega}^T \left(\eta\mathbf{I} + [\boldsymbol{\zeta}]_\times\right)^T J\boldsymbol{\omega} \leq |\mathfrak{c}| \left\|\boldsymbol{\omega}^T \left(\eta\mathbf{I} + [\boldsymbol{\zeta}]_\times\right)^T J\boldsymbol{\omega}\right\| &\leq |\mathfrak{c}| \left\|\eta\mathbf{I} + [\boldsymbol{\zeta}]_\times\right\| \|J\| \|\boldsymbol{\omega}\|^2 \\
&\leq 2\left|\mathfrak{c}\right| M_J \boldsymbol{\omega}^T\boldsymbol{\omega}, \\
-2\mathfrak{c}\boldsymbol{\zeta}^T \left([\boldsymbol{\omega}]_\times J\boldsymbol{\omega}\right) \leq 2\left|\mathfrak{c}\right| \left\|\boldsymbol{\zeta}^T \left([\boldsymbol{\omega}]_\times J\boldsymbol{\omega}\right)\right\| &\leq 2\left|\mathfrak{c}\right| \|\boldsymbol{\zeta}\| \|J\| \|\boldsymbol{\omega}\|^2 \\
&\leq 2\left|\mathfrak{c}\right| M_J \boldsymbol{\omega}^T\boldsymbol{\omega}.
\end{aligned}
$$

The combination of derivative terms $\dot{V}_{1a}$ (5.85) and $\dot{V}_{1b}$ (5.86) results in

$$
\begin{aligned}
\dot{V}_1 &= \dot{V}_{1a} + \dot{V}_{1b} \\
&\leq \begin{bmatrix} \boldsymbol{\zeta} \\ \boldsymbol{\zeta}_{d_1} \\ \boldsymbol{\omega} \\ \boldsymbol{\omega}_{d_2} \end{bmatrix}^T \begin{bmatrix} \mathbf{0} & \mathbf{0} & \mathfrak{a}\mathbf{I} & \mathbf{0} \\ * & \mathbf{0} & -\kappa_1 \mathfrak{b}\mathbf{I} & \mathbf{0} \\ * & * & \mathbf{0} & -\kappa_2 \mathfrak{b}\mathbf{I} \\ * & * & * & \mathbf{0} \end{bmatrix} \begin{bmatrix} \boldsymbol{\zeta} \\ \boldsymbol{\zeta}_{d_1} \\ \boldsymbol{\omega} \\ \boldsymbol{\omega}_{d_2} \end{bmatrix} \\
&+ \begin{bmatrix} \boldsymbol{\zeta} \\ \boldsymbol{\zeta}_{d_1} \\ \boldsymbol{\omega} \\ \boldsymbol{\omega}_{d_2} \end{bmatrix}^T \begin{bmatrix} \mathbf{0} & -\kappa_1 \mathfrak{c}\mathbf{I} & \mathbf{0} & -\kappa_2 \mathfrak{c}\mathbf{I} \\ * & \mathbf{0} & \mathbf{0} & \mathbf{0} \\ * & * & 4M_J \left|\mathfrak{c}\right| \mathbf{I} & \mathbf{0} \\ * & * & * & \mathbf{0} \end{bmatrix} \begin{bmatrix} \boldsymbol{\zeta} \\ \boldsymbol{\zeta}_{d_1} \\ \boldsymbol{\omega} \\ \boldsymbol{\omega}_{d_2} \end{bmatrix} \\
&= \begin{bmatrix} \boldsymbol{\zeta} \\ \boldsymbol{\zeta}_{d_1} \\ \boldsymbol{\omega} \\ \boldsymbol{\omega}_{d_2} \end{bmatrix}^T \begin{bmatrix} \mathbf{0} & -\kappa_1 \mathfrak{c}\mathbf{I} & \mathfrak{a}\mathbf{I} & -\kappa_2 \mathfrak{c}\mathbf{I} \\ * & \mathbf{0} & -\kappa_1 \mathfrak{b}\mathbf{I} & \mathbf{0} \\ * & * & 4M_J \left|\mathfrak{c}\right| \mathbf{I} & -\kappa_2 \mathfrak{b}\mathbf{I} \\ * & * & * & \mathbf{0} \end{bmatrix} \begin{bmatrix} \boldsymbol{\zeta} \\ \boldsymbol{\zeta}_{d_1} \\ \boldsymbol{\omega} \\ \boldsymbol{\omega}_{d_2} \end{bmatrix}.
\end{aligned} \tag{5.87}
$$

From delay bounds (5.74), and invoking Jensen's Inequality, it follows $\dot{V}_2$ is also bounded, such that

$$
\begin{aligned}
\dot{V}_2 &= \nu_1\mathfrak{p}_1 \int_{-\nu_1}^{0} \left[\dot{\boldsymbol{\zeta}}(t)^T \dot{\boldsymbol{\zeta}}(t) - \dot{\boldsymbol{\zeta}}(t+l)^T \dot{\boldsymbol{\zeta}}(t+l)\right] dl \\
&+ \nu_2\mathfrak{p}_2 \int_{-\nu_2}^{0} \left[\dot{\boldsymbol{\omega}}(t)^T \dot{\boldsymbol{\omega}}(t) - \dot{\boldsymbol{\omega}}(t+l)^T \dot{\boldsymbol{\omega}}(t+l)\right] dl \\
&= \nu_1^2\mathfrak{p}_1\dot{\boldsymbol{\zeta}}^T\dot{\boldsymbol{\zeta}} - \nu_1\mathfrak{p}_1 \int_{t-\nu_1}^{t} \dot{\boldsymbol{\zeta}}(s)^T \dot{\boldsymbol{\zeta}}(s)\, ds + \nu_2^2\mathfrak{p}_2\dot{\boldsymbol{\omega}}^T\dot{\boldsymbol{\omega}} - \nu_2\mathfrak{p}_2 \int_{t-\nu_2}^{t} \dot{\boldsymbol{\omega}}(s)^T \dot{\boldsymbol{\omega}}(s)\, ds \\
&= \nu_1^2\mathfrak{p}_1\dot{\boldsymbol{\zeta}}^T\dot{\boldsymbol{\zeta}} + \nu_2^2\mathfrak{p}_2\dot{\boldsymbol{\omega}}^T\dot{\boldsymbol{\omega}} - \nu_1\mathfrak{p}_1 \int_{t-d_1(t)}^{t} \dot{\boldsymbol{\zeta}}(s)^T \dot{\boldsymbol{\zeta}}(s)\, ds - \nu_1\mathfrak{p}_1 \int_{t-\nu_1}^{t-d_1(t)} \dot{\boldsymbol{\zeta}}(s)^T \dot{\boldsymbol{\zeta}}(s)\, ds \\
&- \nu_2\mathfrak{p}_2 \int_{t-d_2(t)}^{t} \dot{\boldsymbol{\omega}}(s)^T \dot{\boldsymbol{\omega}}(s)\, ds - \nu_2\mathfrak{p}_2 \int_{t-\nu_2}^{t-d_2(t)} \dot{\boldsymbol{\omega}}(s)^T \dot{\boldsymbol{\omega}}(s)\, ds
\end{aligned}
$$

$$
\begin{aligned}
&\leq \nu_1^2 \mathfrak{p}_1 \dot{\boldsymbol{\zeta}}^T \dot{\boldsymbol{\zeta}} + \nu_2^2 \mathfrak{p}_2 \dot{\boldsymbol{\omega}}^T \dot{\boldsymbol{\omega}} - \nu_1 \mathfrak{p}_1 \int_{t-d_1(t)}^{t} \dot{\boldsymbol{\zeta}}(s)^T \dot{\boldsymbol{\zeta}}(s)\, ds - \nu_2 \mathfrak{p}_2 \int_{t-d_2(t)}^{t} \dot{\boldsymbol{\omega}}(s)^T \dot{\boldsymbol{\omega}}(s)\, ds \\
&\leq \nu_1^2 \mathfrak{p}_1 \dot{\boldsymbol{\zeta}}^T \dot{\boldsymbol{\zeta}} - \nu_1 \frac{\mathfrak{p}_1}{d_1(t)} \left[\int_{t-d_1(t)}^{t} \dot{\boldsymbol{\zeta}}(s)\, ds\right]^T \left[\int_{t-d_1(t)}^{t} \dot{\boldsymbol{\zeta}}(s)\, ds\right] \\
&+ \nu_2^2 \mathfrak{p}_2 \dot{\boldsymbol{\omega}}^T \dot{\boldsymbol{\omega}} - \nu_2 \frac{\mathfrak{p}_2}{d_2(t)} \left[\int_{t-d_2(t)}^{t} \dot{\boldsymbol{\omega}}(s)\, ds\right]^T \left[\int_{t-d_2(t)}^{t} \dot{\boldsymbol{\omega}}(s)\, ds\right] \\
&\leq \nu_1^2 \mathfrak{p}_1 \dot{\boldsymbol{\zeta}}^T \dot{\boldsymbol{\zeta}} - \mathfrak{p}_1 \left[\boldsymbol{\zeta} - \boldsymbol{\zeta}_{d_1}\right]^T \left[\boldsymbol{\zeta} - \boldsymbol{\zeta}_{d_1}\right] + \nu_2^2 \mathfrak{p}_2 \dot{\boldsymbol{\omega}}^T \dot{\boldsymbol{\omega}} - \mathfrak{p}_2 \left[\boldsymbol{\omega} - \boldsymbol{\omega}_{d_2}\right]^T \left[\boldsymbol{\omega} - \boldsymbol{\omega}_{d_2}\right] \\
&\leq \nu_1^2 \mathfrak{p}_1 \dot{\boldsymbol{\zeta}}^T \dot{\boldsymbol{\zeta}} + \nu_2^2 \mathfrak{p}_2 \dot{\boldsymbol{\omega}}^T \dot{\boldsymbol{\omega}} + \begin{bmatrix} \boldsymbol{\zeta} \\ \boldsymbol{\zeta}_{d_1} \\ \boldsymbol{\omega} \\ \boldsymbol{\omega}_{d_2} \end{bmatrix}^T \begin{bmatrix} -\mathfrak{p}_1 \mathbf{I} & \mathfrak{p}_1 \mathbf{I} & 0 & 0 \\ * & -\mathfrak{p}_1 \mathbf{I} & 0 & 0 \\ * & * & -\mathfrak{p}_2 \mathbf{I} & \mathfrak{p}_2 \mathbf{I} \\ * & * & * & -\mathfrak{p}_2 \mathbf{I} \end{bmatrix} \begin{bmatrix} \boldsymbol{\zeta} \\ \boldsymbol{\zeta}_{d_1} \\ \boldsymbol{\omega} \\ \boldsymbol{\omega}_{d_2} \end{bmatrix}
\end{aligned}
$$

Now, let V_{2a}, V_{2b} be such that

$$
\begin{aligned}
\dot{V}_2 &= \dot{V}_{2a} + \dot{V}_{2b}, \\
\dot{V}_{2a} &= \nu_1^2 \mathfrak{p}_1 \dot{\boldsymbol{\zeta}}(t)^T \dot{\boldsymbol{\zeta}}(t) + \nu_2^2 \mathfrak{p}_2 \dot{\boldsymbol{\omega}}(t)^T \dot{\boldsymbol{\omega}}(t), \\
\dot{V}_{2b} &\leq \begin{bmatrix} \boldsymbol{\zeta} \\ \boldsymbol{\zeta}_{d_1} \\ \boldsymbol{\omega} \\ \boldsymbol{\omega}_{d_2} \end{bmatrix}^T \begin{bmatrix} -\mathfrak{p}_1 \mathbf{I} & \mathfrak{p}_1 \mathbf{I} & 0 & 0 \\ * & -\mathfrak{p}_1 \mathbf{I} & 0 & 0 \\ * & * & -\mathfrak{p}_2 \mathbf{I} & \mathfrak{p}_2 \mathbf{I} \\ * & * & * & -\mathfrak{p}_2 \mathbf{I} \end{bmatrix} \begin{bmatrix} \boldsymbol{\zeta} \\ \boldsymbol{\zeta}_{d_1} \\ \boldsymbol{\omega} \\ \boldsymbol{\omega}_{d_2} \end{bmatrix}.
\end{aligned} \tag{5.88}
$$

From inequality $\left\|[\boldsymbol{\zeta}]_\times\right\| \leq \|\boldsymbol{\zeta}\|$ (I.6), $\left\|\dot{\boldsymbol{\zeta}}\right\|^2$ can be linearly bounded because

$$
\begin{aligned}
\dot{\boldsymbol{\zeta}}^T \dot{\boldsymbol{\zeta}} = \frac{1}{4} \boldsymbol{\omega}^T \left(\eta \mathbf{I} - [\boldsymbol{\zeta}]_\times\right) \left(\eta \mathbf{I} + [\boldsymbol{\zeta}]_\times\right) \boldsymbol{\omega} = \frac{1}{4} \boldsymbol{\omega}^T \left(\eta^2 \mathbf{I} - [\boldsymbol{\zeta}]_\times^2\right) \boldsymbol{\omega} &\leq \frac{\eta^2 + \|\boldsymbol{\zeta}\|^2}{4} \boldsymbol{\omega}^T \boldsymbol{\omega} \\
&= \frac{1}{4} \boldsymbol{\omega}^T \boldsymbol{\omega}.
\end{aligned}
$$

On the other hand, using cross-term bounds[2], and $\|J\|$ norm bounds (5.75)[3]

$$
\begin{aligned}
m_J^2 \dot{\boldsymbol{\omega}}^T \dot{\boldsymbol{\omega}} &\overset{(i)}{\leq} \dot{\boldsymbol{\omega}}^T J J \dot{\boldsymbol{\omega}} \\
&= \left(-[\boldsymbol{\omega}]_\times J \boldsymbol{\omega} - \kappa_1 \boldsymbol{\zeta}_{d_1} - \kappa_2 \boldsymbol{\omega}_{d_2}\right)^T \left(-[\boldsymbol{\omega}]_\times J \boldsymbol{\omega} - \kappa_1 \boldsymbol{\zeta}_{d_1} - \kappa_2 \boldsymbol{\omega}_{d_2}\right) \\
&= \left([\boldsymbol{\omega}]_\times J \boldsymbol{\omega}\right)^T \left([\boldsymbol{\omega}]_\times J \boldsymbol{\omega}\right) + 2\kappa_1 \left([\boldsymbol{\omega}]_\times J \boldsymbol{\omega}\right)^T \boldsymbol{\zeta}_{d_1} + 2\kappa_2 \left([\boldsymbol{\omega}]_\times J \boldsymbol{\omega}\right)^T \boldsymbol{\omega}_{d_2} \\
&+ \kappa_1^2 \boldsymbol{\zeta}_{d_1}^T \boldsymbol{\zeta}_{d_1} + 2\kappa_1 \kappa_2 \boldsymbol{\zeta}_{d_1}^T \boldsymbol{\omega}_{d_2} + \kappa_2^2 \boldsymbol{\omega}_{d_2}^T \boldsymbol{\omega}_{d_2} \\
&\leq (1 + \kappa_1 + \kappa_2) \underbrace{\left([\boldsymbol{\omega}]_\times J \boldsymbol{\omega}\right)^T \left([\boldsymbol{\omega}]_\times J \boldsymbol{\omega}\right)}_{= \|\boldsymbol{\omega}\|^2 \|J \boldsymbol{\omega}\|^2 - (\boldsymbol{\omega}^T J \boldsymbol{\omega})^2} + \kappa_1 \boldsymbol{\zeta}_{d_1}^T \boldsymbol{\zeta}_{d_1} + \kappa_2 \boldsymbol{\omega}_{d_2}^T \boldsymbol{\omega}_{d_2} \\
&+ \kappa_1^2 \boldsymbol{\zeta}_{d_1}^T \boldsymbol{\zeta}_{d_1} + 2\kappa_1 \kappa_2 \boldsymbol{\zeta}_{d_1}^T \boldsymbol{\omega}_{d_2} + \kappa_2^2 \boldsymbol{\omega}_{d_2}^T \boldsymbol{\omega}_{d_2} \\
&\leq \left(M_J^2 - m_J^2\right) (1 + \kappa_1 + \kappa_2) \|\boldsymbol{\omega}\|^4 + \kappa_1 \boldsymbol{\zeta}_{d_1}^T \boldsymbol{\zeta}_{d_1} + \kappa_2 \boldsymbol{\omega}_{d_2}^T \boldsymbol{\omega}_{d_2}
\end{aligned}
$$

[2] The term $2\kappa_1 \nu_2 \mathfrak{p}_2 \left([\boldsymbol{\omega}]_\times J \boldsymbol{\omega}\right)^T \boldsymbol{\zeta}$ can also be checked using cross-term bound from Proposition 5.2.2.

[3] Since J is positive definite, it admits diagonal decomposition $Q^T D Q$, with Q orthonormal and D diagonal. Thus

$$
J^2 = \left(Q^T D Q\right) \left(Q^T D Q\right) = Q^T D^2 Q,
$$

which means $\lambda\left(J^2\right)$ and $\lambda\left(J\right)^2$ define the same set. This proves inequality (i).

$$+\kappa_1^2\boldsymbol{\zeta}_{d_1}^T\boldsymbol{\zeta}_{d_1}+2\kappa_1\kappa_2\boldsymbol{\zeta}_{d_1}^T\boldsymbol{\omega}_{d_2}+\kappa_2^2\boldsymbol{\omega}_{d_2}^T\boldsymbol{\omega}_{d_2}.$$

From the definition of V, and imposing $m_J^{-1}\leq\mathfrak{b}$, inequalities

$$\boldsymbol{\omega}^T\boldsymbol{\omega}\leq\frac{m_J^{-1}}{\mathfrak{b}}\mathfrak{b}\boldsymbol{\omega}^TJ\boldsymbol{\omega}\leq\mathfrak{b}\boldsymbol{\omega}^TJ\boldsymbol{\omega}\leq V$$

hold, which means that

$$\dot{V}_{2a}\leq\boldsymbol{\vartheta}^T\Omega_{2a}\boldsymbol{\vartheta},\ \ \Omega_{2a}=\begin{bmatrix}\mathbf{0}&\mathbf{0}&\mathbf{0}&\mathbf{0}\\ *&(\Omega_{2a})_{22}&\mathbf{0}&(\Omega_{2a})_{24}\\ *&*&(\Omega_{2a})_{33}&\mathbf{0}\\ *&*&*&(\Omega_{2a})_{44}\end{bmatrix},\ \ \boldsymbol{\vartheta}=\begin{bmatrix}\boldsymbol{\zeta}\\ \boldsymbol{\zeta}_{d_1}\\ \boldsymbol{\omega}\\ \boldsymbol{\omega}_{d_2}\end{bmatrix}, \tag{5.89}$$

with

$$(\Omega_{2a})_{22}=\frac{\nu_2^2}{m_J^2}\left(1+\kappa_1\right)\kappa_1\mathfrak{p}_2\mathbf{I},\qquad(\Omega_{2a})_{33}=\frac{\nu_1^2}{4}\mathfrak{p}_1\mathbf{I}+V\frac{\nu_2^2}{m_J^2}\left(M_J^2-m_J^2\right)\left(1+\kappa_1+\kappa_2\right)\mathfrak{p}_2\mathbf{I},$$
$$(\Omega_{2a})_{24}=\frac{\nu_2^2}{m_J^2}\kappa_1\kappa_2\mathfrak{p}_2\mathbf{I},\qquad(\Omega_{2a})_{44}=\frac{\nu_2^2}{m_J^2}\left(1+\kappa_2\right)\kappa_2\mathfrak{p}_2\mathbf{I}.$$

Combining inequalities (5.87) and (5.89) with identity (5.88) results in

$$\begin{aligned}\dot{V}&\leq\dot{V}_1+\dot{V}_2\\ &\leq\begin{bmatrix}\boldsymbol{\zeta}\\ \boldsymbol{\zeta}_{d_1}\\ \boldsymbol{\omega}\\ \boldsymbol{\omega}_{d_2}\end{bmatrix}^T\begin{bmatrix}\mathbf{0}&-\kappa_1\mathfrak{c}\mathbf{I}&\mathfrak{a}\mathbf{I}&-\kappa_2\mathfrak{c}\mathbf{I}\\ *&\mathbf{0}&-\kappa_1\mathfrak{b}\mathbf{I}&\mathbf{0}\\ *&*&4M_J\left|\mathfrak{c}\right|\mathbf{I}&-\kappa_2\mathfrak{b}\mathbf{I}\\ *&*&*&\mathbf{0}\end{bmatrix}\begin{bmatrix}\boldsymbol{\zeta}\\ \boldsymbol{\zeta}_{d_1}\\ \boldsymbol{\omega}\\ \boldsymbol{\omega}_{d_2}\end{bmatrix}\\ &\quad+\begin{bmatrix}\boldsymbol{\zeta}\\ \boldsymbol{\zeta}_{d_1}\\ \boldsymbol{\omega}\\ \boldsymbol{\omega}_{d_2}\end{bmatrix}^T\begin{bmatrix}-\mathfrak{p}_1\mathbf{I}&\mathfrak{p}_1\mathbf{I}&\mathbf{0}&\mathbf{0}\\ *&-\mathfrak{p}_1\mathbf{I}&\mathbf{0}&\mathbf{0}\\ *&*&-\mathfrak{p}_2\mathbf{I}&\mathfrak{p}_2\mathbf{I}\\ *&*&*&-\mathfrak{p}_2\mathbf{I}\end{bmatrix}\begin{bmatrix}\boldsymbol{\zeta}\\ \boldsymbol{\zeta}_{d_1}\\ \boldsymbol{\omega}\\ \boldsymbol{\omega}_{d_2}\end{bmatrix}+\boldsymbol{\vartheta}^T\Omega_{2a}\boldsymbol{\vartheta}\\ &=\boldsymbol{\vartheta}^T\Omega\boldsymbol{\vartheta},\end{aligned} \tag{5.90}$$

where

$$\Omega=\begin{bmatrix}\Omega_{11}&\Omega_{12}&\Omega_{13}&\Omega_{14}\\ *&\Omega_{22}&\Omega_{23}&\Omega_{24}\\ *&*&\Omega_{33}&\Omega_{34}\\ *&*&*&\Omega_{44}\end{bmatrix},$$

$$\begin{aligned}&\Omega_{11}=-\mathfrak{p}_1\mathbf{I} &&\Omega_{22}=\left(m_J^{-2}\left(1+\kappa_1\right)\kappa_1\nu_2^2\mathfrak{p}_2-\mathfrak{p}_1\right)\mathbf{I}\\ &\Omega_{12}=\left(\mathfrak{p}_1-\kappa_1\mathfrak{c}\right)\mathbf{I} &&\Omega_{24}=m_J^{-2}\nu_2^2\kappa_1\kappa_2\mathfrak{p}_2\mathbf{I}\\ &\Omega_{13}=\mathfrak{a}\mathbf{I} &&\Omega_{33}=\left(\frac{\nu_1^2}{4}\mathfrak{p}_1+4M_J\left|\mathfrak{c}\right|+V\nu_2^2\frac{\left(M_J^2-m_J^2\right)}{m_J^2}\left(1+\kappa_1+\kappa_2\right)\mathfrak{p}_2-\mathfrak{p}_2\right)\mathbf{I}\\ &\Omega_{14}=-\kappa_2\mathfrak{c}\mathbf{I} &&\Omega_{34}=\left(\mathfrak{p}_2-\kappa_2\mathfrak{b}\right)\mathbf{I}\\ &\Omega_{23}=-\kappa_1\mathfrak{b}\mathbf{I} &&\Omega_{44}=\left(m_J^{-2}\left(1+\kappa_2\right)\kappa_2\nu_2^2-1\right)\mathfrak{p}_2\mathbf{I}\end{aligned}$$

Now, let τ be defined by $\min\{\tau_1, \tau_2\}$, and suppose $V(\tau)$ is less than $\mathfrak{m}$, with $\mathfrak{m}$ such that it makes Ω negative definite if V is replaced by $\mathfrak{m}$ in Ω_{33}. Then, $V(t)$ is less than $\mathfrak{m}$ for all t greater than or equal to τ. Indeed, by contradiction, assume that there is t_c greather than τ, such that $V(t_c){=}\mathfrak{m}$. This implies that there exists some t_p in $[\tau, t_c]$ such that $\dot{V}(t_p)$ is positive. For t in $[\tau, t_p)$, $\dot{V}(t)$ is nonpositive, which means that $V(t)$ is less than $\mathfrak{m}$. Then, because V is continuous, $V(t_p)$ must be less than or equal to $\mathfrak{m}$. Thus, inequality (5.90) implies

$$\dot{V}(t_p){\leq}\boldsymbol{\vartheta}(t_p)^T\Omega|_{V(t_p)}\boldsymbol{\vartheta}(t_p){\leq}\boldsymbol{\vartheta}(t_p)^T\Omega|_{\mathfrak{m}}\boldsymbol{\vartheta}(t_p){<}0.$$

Contradicting the hypothesis that $\dot{V}(t_p)$ is positive. Therefore, $\dot{V}(\boldsymbol{x}_t)$ is negative for t greater than or equal to τ. This implies that $\boldsymbol{\omega}(t)$ is bounded, and as a consequence, from (5.1)-(5.77), it follows that $\dot{\boldsymbol{q}}(t)$ and $\dot{\boldsymbol{\omega}}(t)$ are both bounded. Thus, it can be concluded via the Mean-value Theorem that $\boldsymbol{q}(t)$ and $\boldsymbol{\omega}(t)$ are uniformly continuous [58].

Because Ω is negative definite for t greater than or equal to τ, then

$$\dot{V}(\boldsymbol{x}_t){\leq}\boldsymbol{\vartheta}(t)^T\,\Omega\boldsymbol{\vartheta}(t){<}0,$$

holds for all t greater than or equal to τ. Integrating previous inequality from τ to t yields

$$V(\boldsymbol{x}_t) - V(\boldsymbol{x}_\tau){\leq}\int_\tau^t \boldsymbol{\vartheta}(s)^T\,\Omega\boldsymbol{\vartheta}(s)\,ds{<}0. \tag{5.91}$$

Let $\lambda_{\max}(\Omega)$ be the largest eigenvalue of Ω, which is negative because Ω is negative definite. For $V(\boldsymbol{x}_t)$ is nonnegative, it can be concluded via (5.91) that

$$-\lambda_{\max}(\Omega)\int_\tau^t \boldsymbol{\vartheta}(s)^T\,\boldsymbol{\vartheta}(s)\,ds{\leq}\int_\tau^t \boldsymbol{\vartheta}(s)^T\,(-\Omega)\,\boldsymbol{\vartheta}(s)\,ds{\leq}V(\boldsymbol{x}_\tau)\,.$$

This implies that $\int_\tau^t \boldsymbol{\vartheta}(s)^T\,\boldsymbol{\vartheta}(s)\,ds$ is finite. Since $\boldsymbol{\vartheta}$ is uniformly continuous, from Barbalat's Lemma 5.2.6, it follows that $\boldsymbol{\vartheta}(t)$ converges to zero, that is, $\boldsymbol{q}(t)$ and $\boldsymbol{\omega}(t)$ both converge to zero. Therefore, the system is asymptotically stable.

Now, it remains to obtain the conditions that $\mathfrak{m}$ must satisfy in order to bound $V(\tau)$. Note that, since $\mathfrak{m}$ is considered a variable, and $\mathfrak{p}_2$ multiplies $\mathfrak{m}$, term Ω_{33} makes the inequality nonlinear. In this sense, imposing an extra constraint

$$\mathfrak{p}_2{<}M_{\mathfrak{p}_2},$$

with $M_{\mathfrak{p}_2}$ a given positive real number parameter, makes Ω linear with respect to the decision variables. An additional variable accounting for the product $\mathfrak{p}_2\mathfrak{m}$ could have been defined instead. Nevertheless, the constraint to ensure $\mathfrak{m}$ is, in fact, greater than $V(\tau)$, would again make the constraints nonlinear[4]. Thus, Ω_{33} is considered

$$\Omega_{33}{=}\left(4M_J\,|\mathfrak{c}| + \nu_2^2 m_J^{-2}\left(M_J^2 - m_J^2\right)(1 + \kappa_1 + \kappa_2)\,M_{\mathfrak{p}_2}\mathfrak{m} - \mathfrak{p}_2\right)\mathbf{I}.$$

[4]Indeed, this would imply inequality

$$M_V\mathfrak{p}_2{<}\mathfrak{p}_{\mathfrak{m}}{=}\mathfrak{p}_2\mathfrak{m},$$

which is not linear because M_V carries decision variables.

Now, the exact expression that bounds $V(\tau)$ must be obtained, so that $\mathfrak{m}$ can be greater than it, satisfying the assumption required to prove the theorem. Suppose $\|\boldsymbol{\omega}(t)\|$ is less than M_ω for all t in $[-\nu, 0]$, with ν given by $\max\{\nu_1, \nu_2\}$. This implies

$$\begin{aligned}
\boldsymbol{u}(t)^T \boldsymbol{u}(t) =& \|-\kappa_1 \boldsymbol{\zeta}(t - d_1(t)) - \kappa_2 \boldsymbol{\omega}(t - d_2(t))\|^2 \\
=& \kappa_1^2 \boldsymbol{\zeta}(t - d_1(t))^T \boldsymbol{\zeta}(t - d_1(t)) + 2\kappa_1\kappa_2 \boldsymbol{\zeta}(t - d_1(t))^T \boldsymbol{\omega}(t - d_2(t)) \\
&+ \kappa_2^2 \boldsymbol{\omega}(t - d_2(t))^T \boldsymbol{\omega}(t - d_2(t)) \\
\leq& \kappa_1^2 + 2\kappa_1\kappa_2 \|\boldsymbol{\zeta}(t - d_1(t))\| \|\boldsymbol{\omega}(t - d_2(t))\| + \kappa_2^2 M_\omega^2 \\
\leq& \kappa_1^2 + 2\kappa_1\kappa_2 M_\omega + \kappa_2^2 M_\omega^2 \\
\leq& (\kappa_1 + \kappa_2 M_\omega)^2 \\
=& M_u^2,
\end{aligned} \tag{5.92}$$

for all t in $[0, \tau]$ (note that $t - d_2(t)$ belongs to $[-\nu, 0]$). Substituting (5.92) for M_u in the inequality from Lemma 5.78 shows that

$$\boldsymbol{\omega}(t)^T J \boldsymbol{\omega}(t) \leq e^\tau \left(\boldsymbol{\omega}(0)^T J \boldsymbol{\omega}(0)\right) + (e^\tau - 1)(\kappa_1 + \kappa_2 M_\omega)^2 m_J^{-1}$$

holds for all t in $[0, \tau]$. By hypothesis, $\|\boldsymbol{\omega}(t)\|$ is less than M_ω for all t in $[-\nu, 0]$. This implies that

$$\begin{aligned}
\boldsymbol{\omega}(t)^T \boldsymbol{\omega}(t) \leq& m_J^{-1} \boldsymbol{\omega}(t)^T J \boldsymbol{\omega}(t) \\
\leq& m_J^{-1} \left[e^\tau \left(\boldsymbol{\omega}(0)^T J \boldsymbol{\omega}(0)\right) + (e^\tau - 1) m_J^{-1} (\kappa_1 + \kappa_2 M_\omega)^2\right] \\
\leq& \left[e^\tau m_J^{-1} M_J M_\omega^2 + (e^\tau - 1) m_J^{-2} (\kappa_1 + \kappa_2 M_\omega)^2\right] \\
=& M_{\|\omega\|}^2
\end{aligned}$$

that is,

$$\|\boldsymbol{\omega}(t)\| \leq \left[e^\tau m_J^{-1} M_J M_\omega^2 + (e^\tau - 1) m_J^{-2} (\kappa_1 + \kappa_2 M_\omega)^2\right]^{\frac{1}{2}} = M_{\|\omega\|} \tag{5.93}$$

for all t in $[0, \tau]$. On the other hand, substituting (3.14) for $\dot{\boldsymbol{\zeta}}$, and (5.77) for $\dot{\boldsymbol{\omega}}$, and using initial conditions upper bound M_ω, it can be concluded that, for all t in $[0, \tau]$, inequalities

$$\begin{aligned}
\int_{-\nu_1}^{0} \int_{t+l}^{t} \dot{\boldsymbol{\zeta}}(s)^T \dot{\boldsymbol{\zeta}}(s)\, ds dl =& \int_{-\nu_1}^{0} \int_{t+l}^{t} \left\| \frac{1}{2} \left(\eta(s) \mathbf{I} + [\boldsymbol{\zeta}(s)]_\times\right)^T \boldsymbol{\omega}(s) \right\|^2 ds dl \\
\leq& \frac{1}{4} \int_{-\nu_1}^{0} \int_{t+l}^{t} \|\boldsymbol{\omega}(s)\|^2 ds dl \\
\leq& \frac{1}{4} \int_{-\nu_1}^{0} \int_{t+l}^{t} M_1^2 ds dl \\
=& \frac{1}{4} M_1^2 \int_{-\nu_1}^{0} l dl \\
=& \frac{\nu_1^2}{8} M_1^2,
\end{aligned} \tag{5.94}$$

with M_1 given by $\max\left\{M_{\|\omega\|}, M_\omega\right\}$, and

$$\int_{-\nu_2}^{0} \int_{t+l}^{t} \dot{\boldsymbol{\omega}}(s)^T \dot{\boldsymbol{\omega}}(s)\, ds dl \leq \int_{-\nu_2}^{0} \int_{t+l}^{t} m_J^{-2} \dot{\boldsymbol{\omega}}(s)^T J J \dot{\boldsymbol{\omega}}(s)\, ds dl$$

$$
\begin{aligned}
&= m_J^{-2} \int_{-\nu_2}^{0} \int_{t+l}^{t} \left\| - \left[\boldsymbol{\omega}(s)\right]_\times J\boldsymbol{\omega}(s) + \boldsymbol{u}(s) \right\|^2 dsdl \\
&\leq m_J^{-2} \int_{-\nu_2}^{0} \int_{t+l}^{t} \left(M_J^2 M_1^4 + 2M_J M_1^2 M_u + M_u^2\right) dsdl \\
&= m_J^{-2} \left(M_J^2 M_1^4 + 2M_J M_1^2 M_u + M_u^2\right) \int_{-\nu_2}^{0} ldl \\
&= \frac{\nu_2^2}{2} m_J^{-2} \left(M_J^2 M_1^4 + 2M_J M_1^2 M_u + M_u^2\right),
\end{aligned} \tag{5.95}
$$

must hold. Note that, because t is in $[0, \tau]$ and l is in $[-\nu_1, 0]$, the limits of the first inner integral $\int_{t+l}^{t} \|\boldsymbol{\omega}(s)\|^2 ds$ are between $[-\nu, \tau]$. Thus, $\|\boldsymbol{\omega}(s)\|$ is limited by M_1 in the integral since $\|\boldsymbol{\omega}(s)\|$ is less than or equal to M_ω for s in $[-\nu, 0]$ and less than or equal to $M_{\|\omega\|}$ for s in $[0, \tau]$. The integrand of the second inner integral is bounded using an analogous argument.

Combining inequalities (5.93), (5.94), and (5.95), yields

$$
\begin{aligned}
V_1(t) &= 2\mathfrak{a}\left[\boldsymbol{\zeta}^T\boldsymbol{\zeta} + (1-\eta)^2\right] + \mathfrak{b}\boldsymbol{\omega}^T J\boldsymbol{\omega} + 2\mathfrak{c}\boldsymbol{\zeta}^T J\boldsymbol{\omega} \\
&\leq 4\mathfrak{a}\left[1-\eta\right] + \mathfrak{b}\left[e^\tau M_J M_\omega^2 + \left(e^\tau - 1\right) m_J^{-1} \left(\kappa_1 + \kappa_2 M_\omega\right)^2\right] + 2\mathfrak{c}\left\|\boldsymbol{\zeta}\right\| \left\|J\boldsymbol{\omega}\right\| \\
&\leq 8\mathfrak{a} + \left[e^\tau M_J M_\omega^2 + \left(e^\tau - 1\right) m_J^{-1} \left(\kappa_1 + \kappa_2 M_\omega\right)^2\right] \mathfrak{b} + 2M_J M_{\|\omega\|}\mathfrak{c},
\end{aligned} \tag{5.96}
$$

$$
\begin{aligned}
V_2(t) &= \nu_1\mathfrak{p}_1 \int_{-\nu_1}^{0} \int_{t+l}^{t} \dot{\boldsymbol{\zeta}}(s)^T \dot{\boldsymbol{\zeta}}(s)\, dsdl + \nu_2\mathfrak{p}_2 \int_{-\nu_2}^{0} \int_{t+l}^{t} \dot{\boldsymbol{\omega}}(s)^T \dot{\boldsymbol{\omega}}(s)\, dsdl \\
&\leq \nu_1\mathfrak{p}_1 \frac{\nu_1^2}{8} M_1^2 + \nu_2\mathfrak{p}_2 \frac{\nu_2^2}{2} m_J^{-2} \left(M_J^2 M_1^4 + 2M_J M_1^2 M_u + M_u^2\right) \\
&= \frac{\nu_1^3}{8} M_1^2 \mathfrak{p}_1 + \frac{\nu_2^3}{2} m_J^{-2} \left(M_J^2 M_1^4 + 2M_J M_1^2 M_u + M_u^2\right) \mathfrak{p}_2,
\end{aligned} \tag{5.97}
$$

and

$$
\begin{aligned}
V(t) \leq\, & 8\mathfrak{a} + \left[e^\tau M_J M_\omega^2 + \left(e^\tau - 1\right) m_J^{-1} \left(\kappa_1 + \kappa_2 M_\omega\right)^2\right] \mathfrak{b} + 2M_J M_{\|\omega\|}\mathfrak{c} \\
& + \frac{\nu_1^3}{8} M_1^2 \mathfrak{p}_1 + \frac{\nu_2^3}{2} m_J^{-2} \left(M_J^2 M_1^4 + 2M_J M_1^2 M_u + M_u^2\right) \mathfrak{p}_2 \\
=\, & M_V.
\end{aligned}
$$

for all t in $[0, \tau]$. Therefore, if $\mathfrak{m}$ is greater than M_V, it follows that

$$
V(t) < \mathfrak{m}
$$

holds for all t in $[0, \tau]$. In particular, $V(\tau)$ is less than $\mathfrak{m}$. □

The idea of using initial conditions to overcome the fourth power of $\|\boldsymbol{\omega}\|$ is not new [21, 22]. Nevertheless, in previous approaches, the delay was considered constant, known and d_1 equal to d_2. In addition, more conservative techniques were used to establish inequalities based on the sum of negative quadratic forms of $\boldsymbol{q}$ and $\boldsymbol{\omega}$ only, instead of LMI conditions that embrace the delayed states. The outcome is simpler and less conservative conditions. Another positive aspect of this approach is that by imposing some relaxations, controller design can be envisioned, which to best of the author knowledge, has not been accomplished so far. Moreover, even though TDS techniques were spared for the sake of simplicity in the proof, it is expected that including these strategies will lead to even less conservative results.

Although some terms of LMI set (5.83)-(5.84) seem algebraically complicated, especially Ω_{33} and M_V, they carry a considerable amount of information that can provide intuition on how the system behaves. As expected, the presence of squares ν_1^2 and ν_2^2 in the diagonal terms Ω_{22}, Ω_{33} and Ω_{44} shows that delay increase can rapidly degrade stability. In fact, stability deteriorates at an even higher rate, because of cubes ν_1^3 and ν_2^3 in M_V, which must be smaller than $\mathfrak{m}$. Thus, $\mathfrak{m}$ must grow, making Ω_{33} less negative, and as a diagonal term, this makes it harder for Ω to be negative definite. The diagonal sub matrices also carry terms proportional to squared gains κ_1^2 and κ_2^2, showing that large gains ultimately reduce stability margin. This also explains why larger inertia J, which translates into larger M_J, tends to deteriorate stability. Indeed, if J grows, larger gains are required to steer the rigid body, decreasing stability margin. Initial conditions also negatively affect stability, since the farthest the rigid body initially is from equilibrium, the higher control signals must be, implying higher controller gains and, therefore, decreased stability margin. Numerically, this phenomenon manifests through M_V because of terms proportional to M_ω and M_ω^2, that force $\mathfrak{m}$ to grow.

Some patterns, on the other hand, are less obvious. Dynamic nonlinearities, unequivocally the greatest challenge in controlling rigid body orientation, arise because of gyroscopic term $[\boldsymbol{\omega}]_\times J\boldsymbol{\omega}$. The term is also quadratic-like in nature, so it carries most of the system's energy that must be contained in order to steer the rigid body. If, however, J is proportional to identity matrix, then the term cancels out and nonlinearities disappear. When J approaches the identity, its eigenvalues also converge, that is, m_J and M_J converge to the same value. Then, the term $M_J^2 - m_J^2$, which multiplies $\mathfrak{m}$, tends to zero. Numerically, this means $\mathfrak{m}$ can grow without affecting diagonal Ω_{33} so much, and also provides some more room for larger delays, gains and initial conditions, because M_V does not strain $\mathfrak{m}$ anymore. This also explains why larger m_J are numerically beneficial to the LMI by means of terms m_J^{-2}. Indeed, since m_J is less than or equal to M_j, instead of larger J, they suggest rigid bodies whose inertia is closer to identity (m_J is closer to M_J) are more stable.

5.2.2.1 Numerical experiments

Assuming identical delay upper bounds equal to 100 milliseconds, and lower delays bounds equal to zero, the region of feasible $\{\kappa_1, \kappa_2\}$ pairs is numerically assessed. For this, κ_2 is incremented from 0 to 0.18 in one millisecond steps. Then, given κ_2, the maximum and minimum feasible κ_1 are found using a binary-search-based algorithm. The process starts by determining a search interval $[\kappa_{\min}, \kappa_{\max}]$ and testing the feasibility of its midpoint κ. If LMI conditions of Theorem 5.2.7 are feasible, the search continues in interval $[\kappa, \kappa_{\max}]$. If not, interval $[\kappa_{\min}, \kappa]$ is considered. The process goes on until two consecutive feasible gains κ are less than a parameter $precision$ apart, or the search interval itself is already smaller than $precision$ parameter (i.e., no feasible κ_1 for that κ_2). Algorithm 5.1 illustrates the procedure considering 0.001 $precision$, and initial κ guess of 0.125. The search for a minimum κ_1 is analogous, except that the lower half of $[\kappa_{\min}, \kappa_{\max}]$ is taken in case κ is feasible, and *vice versa*. After the increments are exhausted, each κ_2 has been assigned a feasible interval $[\kappa_{1\,\min}, \kappa_{1\,\max}]_{\kappa_2}$. Computing the convex hull of these slices through MATLAB function *bwconvhull*, a feasible region is obtained.

Algorithm 5.1 Maximum stable κ_2 according to Theorem 5.2.7 using binary search.

```
precision ← 10^{-3}
κ_low, κ_feas1, κ_feas2 ← 0
κ_upp ← 0.25
κ ← (κ_low + κ_upp)/2
while abs(κ_feas1 − κ_feas2) > precision ∨ κ_feas2 == 0 ∧ κ > precision do
    if Theorem 5.2.7 feasible then
        κ_feas2 = κ_feas1, κ_feas1 = κ
        κ_low = κ, κ = (κ_low + κ_upp)/2
    else
        κ_upp = κ, κ = (κ_low + κ_upp)/2
    end if
end while
```

The feasible gain regions shown in Figure 5.6 confirm the shrink rate of feasible gain area is highly nonlinear, becoming faster as initial conditions get more aggressive. Indeed, a nearly 300 time increase in M_ω from 0.03 rad/s to 9 rad/s represented a reduction in feasible gain area of approximately two thirds, depicted from the wavy grey to the dark grey shapes in Figure 5.6, while only 22 percent faster initial velocities caused a plunge of 73 percent in feasible gain area, displayed as the light grey shape. Also, the figure suggests the existence of an "optimal" $\{\kappa_1, \kappa_2\}$ pair, when it comes to robustness to initial conditions. This pair is given by what seems to be the regions are converging to as M_ω grows. Figure 5.6 also supports that in general, higher κ_1 gains are tolerable, compared to κ_2. A comparison with previous results from [22] corroborates that, though the relationship between feasible κ_1 and κ_2 is not exactly the same. Nevertheless, the strategy adopted in Theorem 5.2.7 produced a considerably larger area of feasible gains, which mean faster convergence.

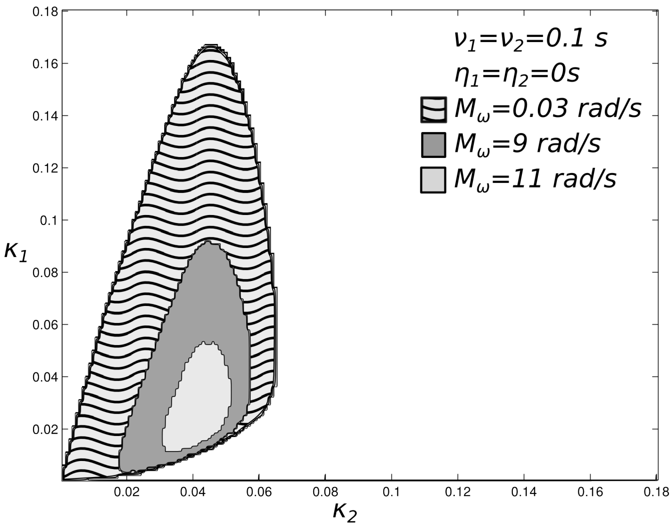

Figure 5.6: Feasible κ_1, κ_2 for ν_1 and ν_2 equal to 0.1 s, and M_ω equal to 0.03 rad/s.

In order to determine if these observations are merely artificial numerical factoids, consequences of LMIs from Theorem 5.2.7, or if they actually hold in reality, a series of simulations are performed. First, for the same delay settings described in Figure 5.6, a few runs are made with alternating values

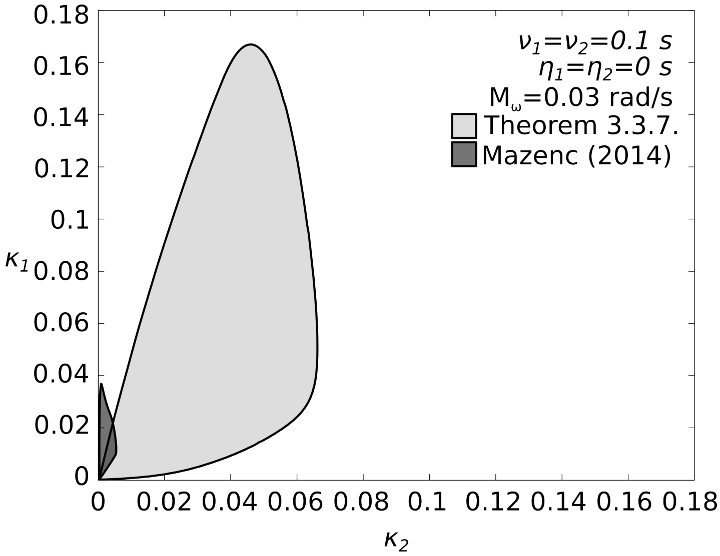

Figure 5.7: Feasible κ_1, κ_2 for ν_1 and ν_2 equal to 0.1 s, and M_ω equal to 0.03 rad/s.

of $\{\kappa_1, \kappa_2\}$, that is, controller gains are simulated, and then swapped and simulated again. Controller pairs $\{0.16, 0.04\}$ and $\{0.04, 0.16\}$ are chosen. The former is at the edge of the wavy region, whereas the latter is not feasible according to theorem for M_ω greater than or equal to 0.03 rad/s . As a means to gauge the conservatism of Theorem 5.2.7, initial conditions are set to $3*\mathbf{1}$, where $\mathbf{1} = \begin{bmatrix} 1 & 1 & 1 \end{bmatrix}^T$, roughly 173 times larger than the what the wavy region in Figure 5.6 represents. Initial attitude is considered $\begin{bmatrix} \frac{-1}{\sqrt{2}} & -\sqrt{\frac{3}{16}} & \sqrt{\frac{4}{16}} & -\sqrt{\frac{1}{16}} \end{bmatrix}^T$. As it can be seen in Figure 5.8, both controllers stabilize the system, although it takes a lot longer in the second case because of smaller attitude feedback gain.

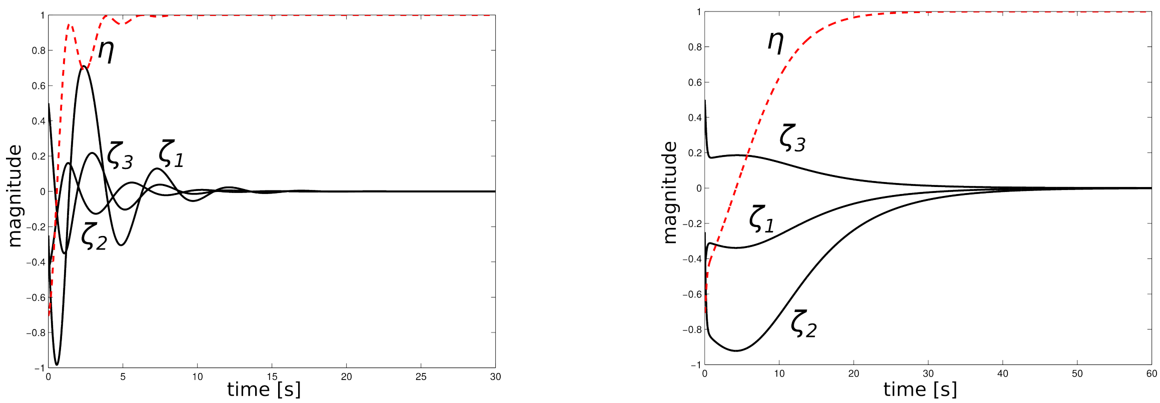

(a) $\{\kappa_1, \kappa_2\}$ set to $\{0.16, 0.04\}$.

(b) $\{\kappa_1, \kappa_2\}$ set to $\{0.04, 0.16\}$.

Figure 5.8: Dynamic attitude stabilization with different gains and M_ω equal to $3 * \mathbf{1}$.

Motivated by this apparent insensitivity to initial conditions, M_ω is systematically increased, with $\{\kappa_1, \kappa_2\}$ considered $\{0.7, 0.7\}$. As Figure 5.9a illustrates, when M_ω equals $3*\mathbf{1}$, oscillatory behavior is already observed. Surprisingly, however, even for initial conditions set to $3 * 10^2 * \mathbf{1}$, the controller is still capable of stabilizing the closed-loop system, despite the long convergence period observed in Figure 5.9b. Nevertheless, when M_ω is increased tenfold and reaches $3 * 10^3 * \mathbf{1}$, the system finally becomes unstable, as it can be seen in Figure 5.9c. This experimentally shows that closed-loop stability does depend on initial conditions, in sharp contrast with the kinematic case, where stability is achieved despite initial conditions. In addition, this also differs from the delay-free dynamic case, which can be stabilized by PD controllers [19]. The relationship between stability and initial velocity conditions is perhaps explained by the quadratic-like gyroscopic term $[\boldsymbol{\omega}]_\times J\boldsymbol{\omega}$, since feedback is only proportional to angular velocity. Thus, given κ_2, the controller ultimately becomes unable to contain the nonlinear term when initial angular velocities are too high. These remarks suggest that other controller structures should be studied, including quadratic compensation, for example.

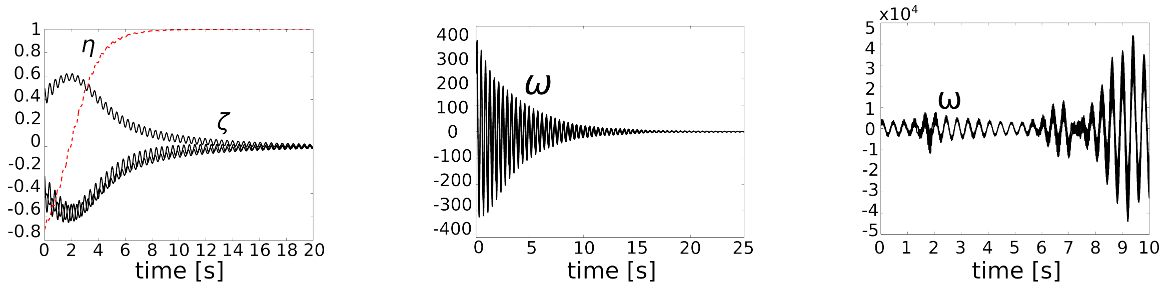

(a) $\boldsymbol{\omega}(0)$ set to $3 * \mathbf{1}$. (b) $\boldsymbol{\omega}(0)$ set to $3 * 10^2 * \mathbf{1}$. (c) $\boldsymbol{\omega}(0)$ set to $3 * 10^3 * \mathbf{1}$.

Figure 5.9: Closed-loop behavior for different initial conditions.

6 CONCLUSION

The general problem of rigid body attitude control subjected to closed-loop time-delays has been addressed. The approach was based on the quaternion representation, which is the minimum singularity-free global attitude parametrization and is also advantageous from the computational standpoint.

The main contribution was to provide stability and controller design LMI conditions by developing novel techniques to circumvent the challenges imposed by quaternion and dynamics nonlinearities. These conditions can be readily verified using efficient computational algorithms and at same time provide insight into the role of each of the system's components in terms of stability.

Important generalizations of the problem were solved, such as heterogeneous measurement delays, model-independent and H_∞ performance controllers. At the best of the authors knowledge, this was the first time the problem was solved using LMI techniques, especially under such general hypothesis.

The next step is to use the approach to develop multi-agent attitude synchronization and encompass translation control. Indeed, although there exist results concerning the former, at the best of the authors knowledge, none of them considered self-delays, i.e., time-delays afflicting local attitude control in addition to inter-agent communication delays. The latter should also be an interesting development, since results already involve quaternions and the transition to the dual quaternion setting should be smoother. Moreover, the last result concerning attitude dynamics showed that PD controllers are incapable of guaranteeing stability regardless of initial conditions. In this sense, other controller structures should be investigated in order to address the very core of the issue.

APPENDICES

I. AUXILIARY ATTITUDE RESULTS

This appendix presents some important properties of the $[\cdot]_\times$ operator that are instrumental to the proofs in this dissertation, and derives the quaternion equivalent of arbitrary rotations.

I.1 PROPERTIES OF THE $[\cdot]_\times$ OPERATOR

The skew-operator $[\cdot]_\times$ describes the nonlinearities in rigid body kinematics and dynamics, and for this reason is ubiquitous in this dissertation. Thus, exploring a few of its properties will come in handy. $[\cdot]_\times$ is defined as

$$\begin{aligned}[\cdot]_\times : \mathbb{R}^3 &\to \mathfrak{o}(3)\\ \boldsymbol{x} &\mapsto [\boldsymbol{x}]_\times\end{aligned}$$

where $\mathfrak{o}(3)$ denotes the set of three-by-three skew-symmetric matrices (i.e., $[\boldsymbol{x}]_\times^T = -[\boldsymbol{x}]_\times$), and

$$[\boldsymbol{x}]_\times := \begin{bmatrix} 0 & -x_3 & x_2 \\ x_3 & 0 & -x_1 \\ -x_2 & x_1 & 0 \end{bmatrix}. \tag{I.1}$$

From (I.1), it follows that $[\cdot]_\times$ is bijective. Indeed, if $[\boldsymbol{x}]_\times$ equals $[\boldsymbol{y}]_\times$, then x_i equals y_i for every i in $\{1,2,3\}$. Thus, $\boldsymbol{x}$ equals $\boldsymbol{y}$ and $[\cdot]_\times$ is injective. Now, let S be a skew-symmetric matrix. From the definition of a skew-symmetric matrix, it can be concluded that

$$S = -S^T \Rightarrow S_{11} = S_{22} = S_{33} = 0, S_{12} = -S_{21}, S_{13} = -S_{31}, S_{23} = -S_{32},$$

that is,

$$S = \begin{bmatrix} 0 & -S_{21} & S_{13} \\ S_{21} & 0 & -S_{32} \\ -S_{13} & S_{32} & 0 \end{bmatrix} = [\boldsymbol{s}]_\times,$$

where $\boldsymbol{s}$ is given by $\begin{bmatrix} S_{32} & S_{13} & S_{21} \end{bmatrix}$. Therefore, $[\cdot]_\times$ is bijective.

Consider scalars α, β, vectors $\boldsymbol{x}, \boldsymbol{y}$ in $\mathbb{R}^3$ and a rotation R in $SO(3)$. $[\cdot]_\times$ satisfies the following properties

$$[\alpha\boldsymbol{x} + \beta\boldsymbol{y}]_\times = \alpha[\boldsymbol{x}]_\times + \beta[\boldsymbol{y}]_\times, \tag{I.2}$$

$$[\boldsymbol{x}]_\times \boldsymbol{y} = \boldsymbol{x} \times \boldsymbol{y}, \tag{I.3}$$

$$R\left([\boldsymbol{x}]_\times \boldsymbol{y}\right) = [R\boldsymbol{x}]_\times R\boldsymbol{y}, \tag{I.4}$$

$$R[\boldsymbol{x}]_\times R^T = [R\boldsymbol{x}]_\times. \tag{I.5}$$

Indeed, properties (I.2)-(I.4) follow from direct calculation, and prove (I.5), since

$$\begin{aligned} R\left([\boldsymbol{x}]_\times R^T\boldsymbol{y}\right) &\overset{\text{(I.4)}}{=} [R\boldsymbol{x}]_\times \left(RR^T\boldsymbol{y}\right) \\ &= [R\boldsymbol{x}]_\times \boldsymbol{y}. \end{aligned}$$

Note that if R is not orthogonal, (I.4) is not valid, in general.

Let $\boldsymbol{v}$ be a vector in $\mathbb{R}^3$. Often, it is important to compare the norms of $\boldsymbol{v}$ and $[\boldsymbol{v}]_\times$. In this sense, regarding the $[\cdot]_\times$'s linear operator facet, i.e.,

$$\begin{aligned} [\boldsymbol{v}]_\times : \mathbb{R}^3 &\to \mathbb{R}^3 \\ \boldsymbol{x} &\mapsto \boldsymbol{v} \times \boldsymbol{x} \end{aligned}$$

and taking its induced norm, gives

$$\left\| [\boldsymbol{v}]_\times \right\| = \sup_{\|\boldsymbol{x}\|=1} \frac{\left\| [\boldsymbol{v}]_\times \boldsymbol{x} \right\|}{\|\boldsymbol{x}\|} = \sup_{\|\boldsymbol{x}\|=1} \frac{\|\boldsymbol{v}\| \, \|\boldsymbol{x}\| \sin\theta}{\|\boldsymbol{x}\|} \leq \sup_{\|\boldsymbol{x}\|=1} \|\boldsymbol{v}\| = \|\boldsymbol{v}\| \,, \tag{I.6}$$

where θ is the angle between $\boldsymbol{v}$ and $\boldsymbol{x}$.

I.2 ROTATIONS

Consider a three-dimensional vector $\boldsymbol{x}$, which is rotated by an angle θ about axis $\boldsymbol{n}$ according to the right-hand rule, as illustrated in Figure I.1. Since $\mathbb{R}^3$ is a Hilbert space, $\boldsymbol{x}$ can be decomposed as

$$\boldsymbol{x} = \boldsymbol{x}_{\|} + \boldsymbol{x}_{\perp}, \tag{I.7}$$

where $\boldsymbol{x}_{\|}$ and $\boldsymbol{x}_{\perp}$ are vectors parallel and orthogonal to $\boldsymbol{n}$, such that

$$\boldsymbol{x}_{\|} = (\boldsymbol{x} \cdot \boldsymbol{n})\, \boldsymbol{n} = (\|\boldsymbol{x}\| \cos\theta)\, \boldsymbol{n}, \tag{I.8}$$

$$\boldsymbol{x}_{\perp} = \boldsymbol{x} - \boldsymbol{x}_{\|} = \boldsymbol{x} - (\boldsymbol{x} \cdot \boldsymbol{n})\, \boldsymbol{n}. \tag{I.9}$$

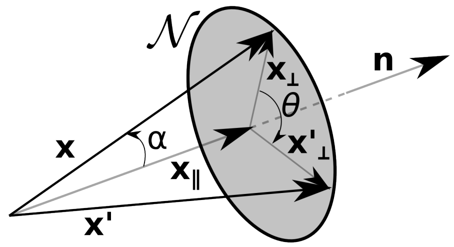

Figure I.1: Three-dimensional vector $\boldsymbol{x}$ rotated by θ about $\boldsymbol{n}$.

Since $\boldsymbol{x}_{\|}$ is the projection of $\boldsymbol{x}$ onto $\boldsymbol{n}$, it does not undergo any rotation, whereas $\boldsymbol{x}_{\perp}$ experiences the full θ rotation about $\boldsymbol{n}$. Now, consider the normal plane $\mathcal{N}$ defined by $\boldsymbol{n}$, represented by the gray ellipsis in Figure I.1. Then,

$$\begin{aligned} \boldsymbol{e}_1 &= \boldsymbol{x}_{\perp}, \\ \boldsymbol{e}_2 &= \boldsymbol{n} \times \boldsymbol{x}_{\perp} = \boldsymbol{n} \times \boldsymbol{x}_{\perp} + \boldsymbol{n} \times \boldsymbol{x}_{\|} = \boldsymbol{n} \times \boldsymbol{x}, \end{aligned}$$

form a basis $\{\boldsymbol{e}_1, \boldsymbol{e}_2\}$ of $\mathcal{N}$. It follows that

$$\boldsymbol{x}'_{\perp} = \boldsymbol{e}_1 \cos\theta + \boldsymbol{e}_2 \sin\theta = \boldsymbol{x}_{\perp} \cos\theta + (\boldsymbol{n} \times \boldsymbol{x}) \sin\theta,$$

and

$$\boldsymbol{x}' = \boldsymbol{x}_{\|} + \boldsymbol{x}'_{\perp}$$

$$= \boldsymbol{x}_{\|} + \boldsymbol{x}_{\perp} \cos\theta + (\boldsymbol{n} \times \boldsymbol{x}) \sin\theta, \tag{I.10}$$

known as the *vector rotation formula*. In fact, (I.10) can be used to verify that the quaternion equivalent of $(\boldsymbol{n}, \theta)$ is $\boldsymbol{q} = \begin{bmatrix} \cos\left(\frac{\theta}{2}\right) & \sin\left(\frac{\theta}{2}\right) \boldsymbol{n}^T \end{bmatrix}^T$. Indeed, considering the vector rotation form and quaternion multiplication

$$\boldsymbol{x}' = \boldsymbol{q} \otimes \boldsymbol{x} \otimes \overline{\boldsymbol{q}},$$

with

$$\begin{bmatrix} 0 \\ \boldsymbol{x}' \end{bmatrix} = \begin{bmatrix} \cos\left(\frac{\theta}{2}\right) \\ \sin\left(\frac{\theta}{2}\right) \boldsymbol{n} \end{bmatrix} \otimes \begin{bmatrix} 0 \\ \boldsymbol{x} \end{bmatrix} \otimes \begin{bmatrix} \cos\left(\frac{\theta}{2}\right) \\ -\sin\left(\frac{\theta}{2}\right) \boldsymbol{n} \end{bmatrix},$$

then

$$\begin{aligned} \boldsymbol{x}' &= \boldsymbol{x} \cos^2 \frac{\theta}{2} + 2 (\boldsymbol{n} \times \boldsymbol{x}) \sin \frac{\theta}{2} \cos \frac{\theta}{2} - \left[\boldsymbol{x} \left(\boldsymbol{n}^T \boldsymbol{n} \right) - 2 \boldsymbol{n} \left(\boldsymbol{n}^T \boldsymbol{x} \right) \right] \sin^2 \frac{\theta}{2} \\ &= \boldsymbol{x} \left(\cos^2 \frac{\theta}{2} - \sin^2 \frac{\theta}{2} \right) + (\boldsymbol{n} \times \boldsymbol{x}) \left(2 \sin \frac{\theta}{2} \cos \frac{\theta}{2} \right) + \boldsymbol{n} \left(\boldsymbol{n}^T \boldsymbol{x} \right) \left(2 \sin^2 \frac{\theta}{2} \right) \\ &= \boldsymbol{x} \cos\theta + (\boldsymbol{n} \times \boldsymbol{x}) \sin\theta + \boldsymbol{n} \left(\boldsymbol{n}^T \boldsymbol{x} \right) (1 - \cos\theta) \\ &= \left(\boldsymbol{x} - \boldsymbol{n}\boldsymbol{n}^T \boldsymbol{x} \right) \cos\theta + \boldsymbol{n}\boldsymbol{n}^T \boldsymbol{x} + (\boldsymbol{n} \times \boldsymbol{x}) \sin\theta \\ &= \boldsymbol{x}_{\perp} \cos\theta + \boldsymbol{x}_{\|} + (\boldsymbol{n} \times \boldsymbol{x}) \sin\theta, \end{aligned}$$

retrieving (I.10).

II. TDS TOOLS

In this section, a few results which are commonly used in analysis techniques for Time-delay Systems (TDS) are introduced.

Lemma II.0.1. *Finsler's Lemma [10]*

Let $\boldsymbol{x} \in \mathbb{R}^n, \Omega \in \mathbb{S}^n$ and $\mathscr{G} \in \mathbb{R}^{m\times n}$ such that $\operatorname{rank}(\mathscr{G}) < n$. The following statements are equivalent:

1. $\boldsymbol{x}^T\Omega\boldsymbol{x} < 0$, *for all* $\mathscr{G}\boldsymbol{x} = 0, \boldsymbol{x} \neq 0$.
2. $\left(\mathscr{G}^{\perp}\right)^T \Omega\mathscr{G}^{\perp} < 0$.
3. $\exists\mu \in \mathbb{R} : \Omega - \mu\mathscr{G}^T\mathscr{G} < 0$.
4. $\exists\mathscr{F} \in \mathbb{R}^{n\times m} : \Omega + \mathscr{F}\mathscr{G} + \mathscr{G}^T\mathscr{F}^T < 0$.

Remark. $\mathscr{G}^{\perp}$ represents a *basis* for null space of $\mathscr{G} \in \mathbb{R}^{m\times n}$. That is, for all $\boldsymbol{x}$ in $\mathbb{R}^n$ such that $\mathscr{G}\boldsymbol{x} = 0$, there exists $\boldsymbol{z}$ in $\mathbb{R}^n$ such that $\boldsymbol{x} = \mathscr{G}^{\perp}\boldsymbol{z}$.

SCHUR COMPLEMENTS

Lyapunov analysis always comes down to obtaining and verifying inequalities, and often enough, these are equivalent to matrix positiveness/negativeness. Nevertheless, dimensionality issues make assessing these inequalities both computationally and analytically difficult. In this sense, the so-called Schur Complement comes in handy since the "sign" of matrices can be stated in terms of its Schur Complement, which has lower dimensions and can also be an important trick to dodge products of variables and obtaining linear conditions (LMIs).

Let Ω be a real matrix in $\mathbb{R}^{n\times n}$ which can be written as a two-by-two block matrix

$$P = \begin{bmatrix} A & B \\ C & D \end{bmatrix},$$

with A in $\mathbb{R}^{p\times p}$, D in $\mathbb{R}^{q\times q}$, and B, C^T in $\mathbb{R}^{p\times q}$[1]. Consider $\boldsymbol{x}, \boldsymbol{y}, \boldsymbol{z}$ and $\boldsymbol{w}$ vectors in $\mathbb{R}^3$, and the linear system

$$\begin{bmatrix} A & B \\ C & D \end{bmatrix} \begin{bmatrix} \boldsymbol{x} \\ \boldsymbol{y} \end{bmatrix} = \begin{bmatrix} \boldsymbol{z} \\ \boldsymbol{w} \end{bmatrix}.$$

Assuming D invertible and solving for $\boldsymbol{y}$ results in

$$\boldsymbol{y} = D^{-1}\left(\boldsymbol{w} - C\boldsymbol{x}\right).$$

Substituting this expression for $\boldsymbol{y}$ yields

$$\left(A - BD^{-1}C\right)\boldsymbol{x} = \boldsymbol{z} - BD^{-1}\boldsymbol{w}.$$

[1]From the definition of Ω, p and q must be such that $n = p + q$.

Then, if $\left(A - BD^{-1}C\right)$ is also invertible, the system can be solved as

$$\boldsymbol{x} = \left(A - BD^{-1}C\right)^{-1}\left(\boldsymbol{z} - BD^{-1}\boldsymbol{w}\right), \tag{II.1}$$

$$\boldsymbol{y} = D^{-1}\left(\boldsymbol{z} - C\left(A - BD^{-1}C\right)^{-1}\left(\boldsymbol{z} - BD^{-1}\boldsymbol{w}\right)\right). \tag{II.2}$$

If D is invertible, the matrix $A - BD^{-1}C$ is called the *Schur Complement* of D in P. Analogously, if A is invertible, the Schur complement of A in P is given by $D - CA^{-1}B$.

Expanding (II.1)-(II.2) and stacking vectors, one obtains

$$\begin{bmatrix} \boldsymbol{x} \\ \boldsymbol{y} \end{bmatrix} = \begin{bmatrix} \left(A - BD^{-1}C\right)^{-1} & -\left(A - BD^{-1}C\right)^{-1}BD^{-1} \\ -D^{-1}C\left(A - BD^{-1}C\right)^{-1} & D^{-1} + D^{-1}C\left(A - BD^{-1}C\right)^{-1}BD^{-1} \end{bmatrix} \begin{bmatrix} \boldsymbol{z} \\ \boldsymbol{w} \end{bmatrix},$$

which means the inverse of P can actually be written in terms of its Schur complement as

$$\begin{aligned} \begin{bmatrix} A & B \\ C & D \end{bmatrix}^{-1} &= \begin{bmatrix} \left(A - BD^{-1}C\right)^{-1} & -\left(A - BD^{-1}C\right)^{-1}BD^{-1} \\ -D^{-1}C\left(A - BD^{-1}C\right)^{-1} & D^{-1} + D^{-1}C\left(A - BD^{-1}C\right)^{-1}BD^{-1} \end{bmatrix} \\ &= \begin{bmatrix} \left(A - BD^{-1}C\right)^{-1} & \mathbf{0} \\ -D^{-1}C\left(A - BD^{-1}C\right)^{-1} & D^{-1} \end{bmatrix} \begin{bmatrix} I & -BD^{-1} \\ \mathbf{0} & I \end{bmatrix} \\ &= \begin{bmatrix} I & \mathbf{0} \\ -D^{-1}C & I \end{bmatrix} \begin{bmatrix} \left(A - BD^{-1}C\right)^{-1} & \mathbf{0} \\ \mathbf{0} & D^{-1} \end{bmatrix} \begin{bmatrix} I & -BD^{-1} \\ \mathbf{0} & I \end{bmatrix}. \end{aligned}$$

Consequently, P can also be decomposed in terms of its Schur complement

$$\begin{bmatrix} A & B \\ C & D \end{bmatrix} = \begin{bmatrix} I & BD^{-1} \\ \mathbf{0} & I \end{bmatrix} \begin{bmatrix} A - BD^{-1}C & \mathbf{0} \\ \mathbf{0} & D \end{bmatrix} \begin{bmatrix} I & \mathbf{0} \\ D^{-1}C & I \end{bmatrix}.$$

In particular, if P is symmetric, i.e., $C = B^T$, then

$$\begin{bmatrix} A & B \\ C & D \end{bmatrix} = \begin{bmatrix} I & BD^{-1} \\ \mathbf{0} & I \end{bmatrix} \begin{bmatrix} A - BD^{-1}B^T & \mathbf{0} \\ \mathbf{0} & D \end{bmatrix} \begin{bmatrix} I & \mathbf{0} \\ D^{-1}B^T & I \end{bmatrix},$$

which shows the Schur complement (along with one of the diagonal matrices) is actually what determines if a matrix is positive or negative definite. This fact is formalized in the following Lemma.

Lemma II.0.2. *Let P be a symmetric matrix of the form[10, 3]*

$$P = \begin{bmatrix} A & B \\ B^T & C \end{bmatrix}.$$

If C is invertible, then

1. *$P > 0$ if, and only if, $C > 0$ and $A - BC^{-1}B^T > 0$.*

2. *If $C > 0$, then $P \geq 0$ if, and only if, $A - BC^{-1}B^T \geq 0$.*

Lemma II.0.2 can be used to prove the following form of Jensen's Inequality, which is one of the most important tools throughout the technical proofs in this dissertation.

Lemma II.0.3. *Jensen's Inequality[70]*

Given scalars r_1, r_2 such that r_2 is greater than or equal to r_1, and positive definite matrix P in $\mathbb{S}^m$, then for any $\boldsymbol{x} : [r_1, r_2] \to \mathbb{R}^m$,

$$\int_{r_1}^{r_2} \boldsymbol{x}(s)^T P \boldsymbol{x}(s)\, ds \geq \frac{1}{r_2 - r_1} \left(\int_{r_1}^{r_2} \boldsymbol{x}(s)^T\, ds \right)^T P \left(\int_{r_1}^{r_2} \boldsymbol{x}(s)\, ds \right).$$

All the technical proofs in this dissertation use Jensen's Inequality in either the "greater than or equal to direction" as stated in Lemma II.0.3 or with the inverted inequality, when the terms are negative.

Bibliography

[1] J. Hale and S. Verduyn, *Introduction to Functional Differential Equations*. Springer-Verlag, 1993.

[2] V. Kharitonov, *Time-Delay Systems*, 2013, vol. 1.

[3] E. Fridman, *Introduction to Time-Delay Systems*, 2014, vol. 1.

[4] K. Ogata, *Discrete-Time Control Systems, 2nd Edition*. Pearson, 1995.

[5] N. Nise, *Control Systems Engineering*. John Wiley & Sons, 2010.

[6] M. Sidi, *Spacecraft Dynamics and Control*. New York: Press Syndicate of the University of Cambridge, 1997.

[7] J. Vilela, L. Figueredo, J. Ishihara, and G. Borges, "Quaternion-based Hinf kinematic attitude control subjected to input time-varying delays," *Conference on Decision and Control (CDC)*, no. Cdc, pp. 7066–7071, 2015.

[8] A. Ailon, R. Segev, and S. Arogeti, "A simple velocity-free controller for attitude regulation of a spacecraft with delayed feedback," *IEEE Transactions on Automatic Control*, vol. 49, no. 1, pp. 125–130, 2004.

[9] J. Richard, "Time-delay systems: an overview of some recent advances and open problems," *Automatica*, vol. 39, no. 10, pp. 1667–1694, 2003.

[10] S. Boyd, L. El Ghaoui, E. Feron, and V. Balakrishnan, *Linear Matrix Inequalities in System and Control Theory*. Philadelphia, PA: SIAM, 1994.

[11] J. Hespanha, P. Naghshtabrizi, and Y. Xu, "A Survey of Recent Results in Networked Control Systems," *Proceedings of the IEEE*, vol. 95, no. 1, pp. 138–162, 2007.

[12] E. Fridman, "Tutorial on Lyapunov-based methods for time-delay systems," *European Journal of Control*, vol. 20, no. 6, pp. 271–283, 2014.

[13] K. Gu, V. L. Kharitonov, and J. Chen, *Stability of Time-Delay Systems*. Boston: Birkhauser, 2003.

[14] J. Wertz, *Spacecraft Attitude Determination and Control*. Springer Science & Business Media, 1978.

[15] S. Bahrami, M. Namvar, and F. Aghili, "Attitude control of satellites with delay in attitude measurement," in *IEEE International Conference on Robotics and Automation (ICRA)*, 2013, pp. 947–952.

[16] B. B. Spratling and D. Mortari, "A survey on star identification algorithms," *Algorithms*, vol. 2, no. 1, pp. 93–107, 2009.

[17] D. Kingston and A. Beard, "Real-time Attitude and Position Estimation for Small UAVs using Low-cost Sensors," *Proc. of the AIAA Unmanned Unlimited Technical Conference, Workshop and Exhibit*, no. September, pp. 2004–6488, 2004.

[18] D. Jung and P. Tsiotras, "Inertial Attitude and Position Reference System Development for a Small UAV," *AIAA Infotech at aerospace*, pp. 1–15, 2007.

[19] J.-Y. Wen and K. Kreutz-Delgado, "The attitude control problem," *IEEE Transactions on Automatic Control*, vol. 36, no. 10, pp. 1148–1162, 1991.

[20] S. Bahrami and M. Namvar, "Rigid Body Attitude Control With Delayed Attitude Measurement," *IEEE Transactions on Control Systems Technology*, vol. 23, no. 5, pp. 1961–1969, 2015.

[21] A. A. Chunodkar and M. R. Akella, "Attitude stabilization with unknown bounded delay in feedback control implementation," *Journal of Guidance, Control, and Dynamics*, vol. 34, no. 2, pp. 533–542, 2011.

[22] F. Mazenc and M. Akella, "Quaternion-based stabilization of attitude dynamics subject to pointwise delay in the input," in *Proceedings of the American Control Conference*, 2014, pp. 4877–4882.

[23] F. Mazenc, S. Yang, and M. Akella, "Time-Delayed Gyro-Free Attitude Stabilization," in *American Control Conference, (ACC)*, 2015, pp. 3206–3211.

[24] M. D. Shuster, "A Survey of Attitude Representations," pp. 439–517, 1993.

[25] W. Hamilton, "Note respecting the researches of John T. Graves," *Transactions of the Irish Academy*, vol. 21, pp. 338–341, 1843.

[26] J. Stuelpnagel, "On the Parametrization of the Three-Dimensional Rotation Group," *SIAM Review*, vol. 6, no. 4, pp. 422–430, 1964.

[27] R. Bellman and K. Cooke, *Differential-difference equations*. Academic, New York, 1963.

[28] W. Zhang, M. S. Branicky, and S. M. Phillips, "Stability of Networked Control Systems," *IEEE Control Systems Magazine*, vol. 21, no. 1, pp. 84–99, 2001.

[29] H. Khalil, *Nonlinear Systems*. Prentice-Hall, Englewood Cliffs, 2002.

[30] N. Krasovskii, *Stability of Motion*. Stanford Univ. Press, 1963.

[31] E. Fridman and U. Shaked, "An improved Stabilization Method for Linear Time-Delay Systems," *IEEE Transactions on Automatic Control*, vol. 47, no. 11, pp. 1931–1937, 2002.

[32] F. Gouaisbaut, "Delay-dependent stability analysis of linear time delay systems," in *6th IFAC Workshop on Time Delay Systems*, 2006, pp. 54–59.

[33] Y. He, Q.-G. Wang, L. Xie, and C. Lin, "Further Improvement of Free-Weighting Matrices," *IEEE Transactions on Automatic Control*, vol. 52, no. 2, pp. 293–299, 2007.

[34] H. Shao, “New delay-dependent stability criteria for systems with interval delay,” *Automatica*, vol. 45, no. 3, pp. 744–749, 2009.

[35] J. Sun, G. P. Liu, J. Chen, and D. Rees, “Improved delay-range-dependent stability criteria for linear systems with time-varying delays,” *Automatica*, vol. 46, no. 2, pp. 466–470, 2010.

[36] L. Figueredo, J. Ishihara, G. Borges, and A. Bauchspiess, “New delay-and-delay-derivative-dependent stability criteria for systems with time-varying delay,” in *49th IEEE Conference on Decision and Control (CDC).* Ieee, dec 2010, pp. 1004–1009.

[37] ——, “A delay-fractioning approach to stability analysis of networked control systems with time-varying delay,” in *IEEE Conference on Decision and Control and European Control Conference*. Ieee, dec 2011, pp. 4048–4053.

[38] A. Seuret and F. Gouaisbaut, “Wirtinger-based integral inequality: Application to time-delay systems,” *Automatica*, vol. 49, no. 9, pp. 2860–2866, 2013.

[39] J. Vilela, L. Figueredo, J. Ishihara, and G. Borges, “An improved stability criterion of networked control systems with dynamic controllers in the feedback loop,” in *IEEE 53rd Annual Conference on Decision and Control (CDC).* Ieee, jun 2014, pp. 5278–5283.

[40] ——, “Robust stability of networked control systems with dynamic controllers in the feedback loop,” in *Indian Control Conference*, 2016, pp. 5278 – 5283.

[41] S. Friedberg, A. Insel, and L. Spence, *Linear Algebra*. Englewood Cliffs, NJ,: Prentice-Hall, 1979.

[42] P. Hughes, *Spacecraft Attitude Dynamics*, 1986.

[43] M. Spong, S. Hutchinson, and M. Vidyasagar, *Robot Modeling and Control*, 2006, vol. 141, no. 1.

[44] J. Kuipers, “Quaternions and Rotation Sequences,” pp. 127–143, 2000.

[45] C. Mayhew, R. Sanfelice, and A. Teel, “Quaternion-Based Hybrid Control for Robust Global Attitude Tracking,” *IEEE Transactions on Automatic Control*, vol. 56, no. 11, pp. 2555–2566, 2011.

[46] J. C. K. Chou, “Quaternion kinematics and dynamic differential equations,” *IEEE Trans. Robot. Autom.*, vol. 8, no. 1, pp. 53–64, 1992.

[47] B. Balachandran, T. Kalmar-Nagy, and D. Gilsinn, *Delay Differential Equations: Recent Advances and New Directions*. Springer-Verlag, 2009.

[48] P. Shcherbakov, “Alexander mikhailovitch lyapunov: On the centenary of his doctoral dissertation on stability of motion,” *Automatica*, vol. 28, no. 5, pp. 865–871, 1992.

[49] Y. Pyatnitskiy and V. Skorodinskiy, “Numerical methods of lyapunov function construction and their application to the absolute stability problem,” *Systems & Control Letters*, vol. 2, no. 2, pp. 130–135, 1982.

[50] Y. Nesterov and A. Nemirovsky, *Interior-point polynomial methods in convex programming*. Philadelphia: Studies in Applied Mathematics - SIAM, 1994.

[51] J. F. Sturm, "Using SeDuMi 1.02, A Matlab toolbox for optimization over symmetric cones," *Optimization Methods and Software*, vol. 11, no. 1-4, pp. 625–653, 1999.

[52] H. R. Tutuncu, C. K. Toh, and J. M. Todd, "Solving semidefinite-quadratic-linear programs using SDPT3," *Mathematical Programming*, vol. 95, no. 2, pp. 189–217, 2003.

[53] J. Loefberg, "YALMIP : a toolbox for modeling and optimization in MATLAB," *2004 IEEE International Conference on Computer Aided Control Systems Design*, pp. 284–289, 2004.

[54] X. Jiang and Q.-L. Han, "New stability criteria for linear systems with interval time-varying delay," *Automatica*, vol. 44, no. 10, pp. 2680–2685, oct 2008.

[55] D. Yue, E. Tian, and Y. Zhang, "A piecewise analysis method to stability analysis of linear continuous / discrete systems with time-varying delay," *International Journal of Robust and Nonlinear Control*, no. November 2008, pp. 1493–1518, 2009.

[56] E. Fridman, U. Shaked, and K. Liu, "New conditions for delay-derivative-dependent stability," *Automatica*, vol. 45, no. 11, pp. 2723–2727, nov 2009.

[57] L. Figueredo, J. Ishihara, G. Borges, and A. Bauchspiess, "Delay-Dependent Robust Hinf Output Tracking Control for Uncertain Networked Control Systems," in *Proceedings of the 18th IFAC World Congress*, Milan, 2011, pp. 3256–3261.

[58] H. Royden, *Real Analysis*. New York: Macmillan, 1963.

[59] P. G. Park and J. W. Ko, "Stability and robust stability for systems with a time-varying delay," *Automatica*, vol. 43, no. 10, pp. 1855–1858, 2007.

[60] A. Abdessameud, A. Tayebi, and I. Polushin, "Attitude synchronization of multiple rigid bodies with communication delays," *IEEE Transactions on Automatic Control*, vol. 57, no. 9, pp. 2405–2411, 2012.

[61] C. Aldana, E. Romero, E. Nuño, and L. Basañez, "Pose consensus in networks of heterogeneous robots with variable time delays," *International Journal of Robust and Nonlinear Control*, vol. 25, no. 14, pp. 2279–2298, 2014.

[62] E. Fresk and G. Nikolakopoulos, "Full Quaternion Based Attitude Control for a Quadrotor," in *European Control Conference*, 2013, pp. 3864–3869.

[63] W. Ren, "Distributed cooperative attitude synchronization and tracking for multiple rigid bodies," *IEEE Transactions on Control Systems Technology*, vol. 18, no. 2, pp. 383–392, 2010.

[64] R. Schlanbusch, A. Loria, R. Kristiansen, and P. Nicklasson, "PD+ based output feedback attitude control of rigid bodies," *IEEE Transactions on Automatic Control*, vol. 57, no. 8, pp. 2146–2152, 2012.

[65] D. Scharf, F. Hadaegh, and S. Ploen, “A survey of spacecraft formation flying guidance and control (part 1): guidance,” *Proceedings of the 2003 American Control Conference, 2003.*, vol. 2, no. Part I, pp. 1733–1739, 2003.

[66] ——, “A survey of spacecraft formation flying guidance and control. Part II: control,” *Proceedings of the 2004 American Control Conference*, vol. 4, no. Part 11, pp. 2976–2985, 2004.

[67] S.-J. Chung, U. Ahsun, and J.-J. Slotine, “Application of Synchronization to Formation Flying Spacecraft: Lagrangian Approach,” *Journal of Guidance Control and Dynamics*, vol. 32, no. 2, pp. 512–526, 2008.

[68] S. Li, H. Du, and P. Shi, “Distributed attitude control for multiple spacecraft with communication delays,” *IEEE Transactions on Aerospace and Electronic Systems*, vol. 50, no. 3, pp. 1765–1773, 2014.

[69] L. Figueredo, B. Adorno, J. Ishihara, and G. Borges, “Robust kinematic control of manipulator robots using dual quaternion representation,” in *IEEE International Conference on Robotics and Automation (ICRA)*, 2013, pp. 1949–1955.

[70] Y. Moon, P. Park, W. Kwon, and Y. Lee, “Delay-dependent robust stabilization of uncertain state-delayed systems,” *International Journal of Control*, vol. 74, no. 14, pp. 1447–1455, 2001.